DISCLAIMER:

This document does not meet the
current format guidelines of
the Graduate School at
The University of Texas at Austin.

It has been published for
informational use only.

The Thesis Committee for Michael Anthony Sandoval
Certifies that this is the approved version of the following thesis:

Targeted Nanoparticle Formulation for a Poorly Water Soluble

Gemcitabine Derivative and its *In Vivo* and *In Vitro* Anti-tumor Activity

APPROVED BY

SUPERVISING COMMITTEE:

Supervisor:

Zhengong Cui

Janet Walkow

Robert O. Williams III

Targeted Nanoparticle Formulation for a Poorly Water Soluble

Gemcitabine Derivative and its *In Vivo* and *In Vitro* Anti-tumor Activity

by

Michael Anthony Sandoval, B.S.; B.S.

Thesis

Presented to the Faculty of the Graduate School of

The University of Texas at Austin

in Partial Fulfillment

of the Requirements

for the Degree of

Master of Science in Pharmacy

The University of Texas at Austin

August 2012

Dedication

To my loving parents, who have always supported my educational and personal goals.

To my professional development mentors, whose vision and guidance provided personal growth and challenged me to be an innovator in teaching, research, and education.

To the College of Pharmacy faculty for their efforts and support to provide an enriching and thorough pharmaceutical education.

To all my Pharm.D students, who held me to the highest standards of teaching, knowledge, and compassion.

And finally, to my closest friends and loved one for their support, patience, and time they have sacrificed to make this all possible.

Acknowledgements

In joy, I would like to extend my deepest gratitude and sincerest appreciation to my closest friends and family, for their patience, support, and love, all of which made my experiences at The University of Texas at Austin productive and enjoyable. Most notably, I would like to thank present and former researchers in Dr. Cui's lab: Mr. Amit Kumar, Dr. Nijaporn Yanasarn, Dr. Dharmika Lansakara, Ms. Letty Rodriguez, Ms. Xinran Li, Dr. Melisande Holzer, Dr. Woongye Chung, and Dr. Rebecca De Angel. I would like to specifically highlight Dr. Brian R. Sloat's contribution towards my success in graduate school. He was kind, patient, and most of all willing to train/mentor me as well as everyone else in the lab. I would also like to acknowledge God, my lord and savior, who has always guided me through the walks of life, providing means for intellectual apprehension, courage to stand up for what is right, and the reason to love all whom I encounter. I am especially grateful for the other graduate students in the pharmacy program, for who they are and the enthusiasm they bring to the scientific community. I owe a special thanks to my supervisor, Dr. Zhengrong Cui, for his high expectations, and intellectual and personal guidance he provided throughout my graduate education. I would like to thank Dr. Janet Walkow, for her unprecedented business aptitude, as well as her admirable people skills and practical knowledge in translational research. She is really someone special and eager to make positive impacts on society. Moreover, her advice throughout my graduate education has always been kind and helpful. As a graduate student at UT, I had the privilege to sit, listen, and learn from the finest professors in the field – I would like to give my upmost gratitude and respect to Dr. Robert Williams, Dr. James McGinity, Dr. Salomon Stavchansky, Dr. Hugh Smyth, Dr.

Abstract

Targeted Nanoparticle Formulation for a Poorly Water Soluble Gemcitabine Derivative and its *In Vivo* and *In Vitro* Anti-tumor Activity

Michael Anthony Sandoval, M.S.Phr

The University of Texas at Austin, 2012

Supervisor: Zhengrong Cui

Cancer is a collection of over one hundred different types of diseases and is responsible for the leading cause of death in the United States. More strikingly, cancer mortality rates have remained relatively unchanged for the past several decades, indicating significant clinical demand for improved cancer therapy. Gemcitabine, known clinically as Gemzar®, is used to treat a variety of human cancers, however, clinical efficacy is modest due to it's brief blood circulation, rapid clearance, manifestation of tumor-drug resistance, and lack of drug specificity. This thesis sought to develop a solid lipid nanoparticle-based platform to passively and actively target a gemcitabine lipophilic derivative, 4-(N)-stearoyl gemcitabine, into tumor cells over-expressing epidermal growth factor receptor (EGFR) after intravenous injection. Considering gemcitabine is hydrophilic and the core of the nanoparticle is solid (hydrophobic), we lipophilized gemcitabine by conjugating a stearoyl group to its N-terminus to form 4-(N)-stearoyl gemcitabine. Second, we incorporated stearoyl gemcitabine into lecithin-based nanoparticles. The nanoparticle formulation was prepared from lecithin/glyceryl

monostearate-in-water emulsions. Third, we grafted the gemcitabine nanoparticles with polyethylene glycol chains with reactive end groups that are capable of conjugating with a targeting moiety on the surface to actively target tumors that over-express EGFR. Taken together, the overall objective of the research presented in this thesis is to develop, characterize, and evaluate the anti-tumor performance *in vitro* as well as in mice against both human and mouse tumor models.

.

Table of Contents

List of Tables

List of Figures

Chapter 1: General Introduction

1.1   Motivation: Statistics and Significance

Nearly 1.6 million cases of cancer will be diagnosed in year 2012, and will claim an estimated 577,190 lives in the United States [1]. As a result, cancer ranks as the second leading cause of death after heart disease, accounting for nearly one of every four deaths. Globally, the World Health Organization estimates an astonishing 7.6 million deaths from cancer to lead as the number one cause of death in 2008. Economically, the National Institute of Health projected the overall cost for cancer in the United States was $226.8 billion: $103.8 billion for direct medical costs and $123 billion for indirect mortality costs [1]. Interestingly, for the past several decades the scientific community has made exceptional progress towards the deeper understanding in cancer biology and advancing therapeutic options, however this has not translated into even distantly comparable advances in the clinic. If mortality rates of other chronic diseases (i.e. heart, cerebrovascular disease, and influenza) are compared to that of cancer from 1991 to 2006, its shown that while heart disease and other major chronic diseases decreased substantially during this period, the mortality rates of cancer remained relatively constant (~16% decrease) [1]. Taken together, proportional and additional research is needed to gain a better understanding of cancer and identify new therapeutic options to fight this disease.

1.2   Cancer and Chemotherapy

Cancer is a collection of over one hundred different types of diseases and is responsible to consume as the second leading cause of death in the United States. The mechanism by which cancer develops and progresses is not completely understood, as

there are several distinct pathways this can happen. However, its widely accepted that cancer is thought to develop from a cell in which the normal mechanism for control of growth and proliferation is abnormally altered [2]. A large body of research has accumulated demonstrating the concept of cancer development is a multi-stage process that is genetically regulated in three stages. The first stage "initiation," requires cell exposure to carcinogenic substances that produce genetic damage, and if not mended, results in irreversible cellular mutations and the potential to develop into influential populations of cancer cells [2]. Substances that may act like carcinogens can be chemicals, physical, and/or biological agents. In the second stage, known as "promotion," carcinogens stimulate the newly initiated cancerous environment to grow and flourish. Additionally, age, gender, diet, growth factors, and chronic inflammation may act together or in sequence to promote the development of cancer. Scientific literature states that several years (~10-20 years) can pass before any clinically relevant symptoms manifest [1-3]. Torring et al. conducted a population-based study that investigated the relationship between diagnostic interval and mortality in 268 colorectal cancer patients. They found that in patients that present clinical symptoms of cancer, the risk of dying within three years decreased with diagnostic intervals up to five weeks   and   then increased (p = 0.002). Moreover, the American Cancer Society believes there is evidence to suggest that one-third of the involved cancer deaths in 2012 is directly correlated to physical inactivity and obesity. Meaning, innovative chemoprevention strategies can potentially aim to improve lifestyle and diet, thereby increasing the time at which cancer is detected, however more research needs to be conducted for further conclusions and recommendations. The third stage of cancer development is known as "progression," which involves further genetic mutations leading to increase cellular proliferation, invasion, and development of metastases [2].

It has been reported that approximately 85% of cancers develop solid tumors [4], and depending on the tumor biology, more than half of deaths result. A solid tumor may arise from four tissue types: epithelial, connective, lymphoid, and nerve tissues; and are classified as either benign or malignant. By definition, benign tumors are non-cancerous, localized, and rarely metastasize [2]. In contrast, malignant tumors are genetically unstable and have the ability to invade contiguous tissues and metastasize to the surroundings. The primary modality in the approach to cancer treatment is surgery for most localized, solid tumors. However, because most cancer patients have metastatic disease at time of diagnosis, localized therapies are often obsolete, failing to produce a cure. Therefore, the goals of systemic therapy using highly cytotoxic drugs, referred to as chemotherapy, are intended to treat primary solid tumors and any metastatic disease.

The remnants of cancer therapy using chemotherapy can be traced back to the late 1940's when Goodman and Gilman first administered nitrogen mustard to patients with lymphoma [3]. The fundamental medical objective of chemotherapy is to destroy and prevent cancer cells from multiplying and metastasizing. In general, chemotherapeutic drugs, with the exception of immunotherapeutics (not covered in this thesis) are efficacious by exerting their effects primarily to the mammalian cell cycle [5]. All tumor cells, as well as normal cells in the body, undergo the process of cell division and renewal, all of which involves the five-phase cell cycle: G0, G1, S, G2, and M. The G0 phase ("resting phase") is the starting point of the cell cycle in which no division occurs. The actively reproducing phases (G1, S, G2, and M) are associated with ready division synthesis, pre-mitosis, and mitosis, respectively [5]. Depending on which phase(s) is altered or interfered, chemotherapeutic drugs are categorized into two groups: cell cycle specific and cell cycle non-specific [3,5]. Cell cycle specific drugs have the ability to

3

exert its affect on a particular phase of the cell cycle and not on the resting phase. Whereas, cell cycle non-specific drugs can attack cells at any phase of the cycle [5-6].

1.3 Gemcitabine as a Chemotherapeutic Drug

Gemcitabine is an anti-metabolite indicated to treat a variety of human cancers including breast, ovarian, and non small cell lung cancers, yet, gemcitabine has been clinically adopted as the first-line treatment for patients diagnosed with locally advanced or metastatic pancreatic cancer [7]. Gemcitabine is known commercially as Gemzar® upon FDA approval in 2004, and originally marketed and distributed by Eli Lilly & Company. Due to Gemzar's® recent patent expiration, the commercial launch of generic gemcitabine has been licensed to Teva Pharmaceuticals. According to IMS Health, the annual U.S net sales of Gemzar® were nearly $785 million. Since then, net sales have dropped ~72% to 91 million due to generic competition in most major markets.

Chemically, gemcitabine (2′, 2′-difluorodeoxycytidine, dFdC), has a molecular weight of 263.2 g/mol and is water-soluble (2.23^{01} g/L). Its structure, like many drugs in the anti-metabolite class, is closely related to the analogue of deoxycytidine, which fluoride replace the hydrogen atoms on the 2' carbons of the deoxycytidine. Literature reports that gemcitabine acts on the G1, M, and G2 cell cycle phase by replacing deoxycytidine during DNA replication, thus interrupting cell division, inhibiting DNA synthesis, and inducing programmed cell death [7-9].

Gemcitabine is considered a pro-drug, thus, in order for gemcitabine to exert its therapeutic action, the molecule must first traverse the cell membrane and be "activated" [7]. However, since gemcitabine is water-soluble and cannot pass through the cell membrane via passive diffusion, specialized transport systems, known as nucleoside transporters (i.e human equilibrative nucleoside transporter-1), are required for both

cellular entry and exit. Upon cell entry, gemcitabine is phosphorylated by deoxycytidine kinase (dCK) into gemcitabine monophosphate. It is then further phosphorylated into gemcitabine diphosphate and gemcitabine triphosphate [7]. The triphosphate derivative is then intercalated into DNA by DNA-polymerase alpha to inhibit DNA synthesis and induce programmed cell death. In addition, the diphosphate derivative acts as ribonucleotide reductase inhibitor that increases gemcitabine's DNA incorporation.

1.4   Gemcitabine and its Clinical Limitations

Patients with advanced pancreatic adenocarcinoma are considered incurable with a median survival of less than one year [10-11]. The gold standard treatment is a single agent, gemcitabine. Despite its favorable *in vitro* toxicity profiles, the therapeutic efficacy of gemcitabine as a single agent is not clinically efficacious due its rapid *in vivo* metabolism (i.e short half-life of 32-84 minutes for short infusions in humans), pre-clinical studies revealing patient tolerability is highly dose dependent, and induction of tumor-drug resistance [12-13]. For example, its reported that about ninety percent of the active gemcitabine triphosphate is rapidly eliminated *in vivo* due to the deamination to an inactive metabolite 2`, 2`-difluorodeoxyuridine (dFdU) by cytidine deaminase [14]. By synthesizing an amino acid ester prodrug of gemcitabine, Bergman et al. demonstrated gemcitabine's *in vivo* sensitivity to deamination by cytidine deaminase was significantly improved. Gemcitabine is water-soluble and must be intracellularly activated, thus membrane transporters are needed to enter tumor cells as mentioned previously in this chapter. Immordino et al. synthesized a series of increasingly lipophilic gemcitabine derivatives by linking the 4-amino group with valeroyl, heptanoyl, lauroyl, and stearyol linear acyl fatty acid groups. They report that the lipophilic gemcitabine derivatives (90% recovered) degraded much slower in plasma than gemcitabine (40% recovered) after 8

hours. Furthermore, when gemcitabine or the lipophilic derivative of gemcitabine (i.e stearoyl gemcitabine) was intravenously administered to mice and their pharmacokinetic parameters were evaluated, the terminal half-life of gemcitabine was increased by 3.5 times to that of unmodified gemcitabine (0.54 h vs. 1.86 h, respectively) [15-16]. It may seem when the metabolic problems of gemcitabine are addressed and circumvented, the anti-tumor activity would improve as well. Surprisingly, when Zhu et al. evaluated the *in vivo* anti-tumor activity of a stearoyl gemcitabe solution in a B16-F10 tumor model after intravenous injection, no significant differences were observed between stearoyl gemcitabine, unmodified gemcitabine, and normal saline.

1.5   Cancer Nanotechnology

During the development and growth of solid tumors, a process known as "angiogenesis" is induced to accommodate tumor dependency for nutrients and oxygen to grow beyond 1-2 mm in size [2]. Unlike blood vessels in normal tissue, tumor vessels become irregular in shape, dilated, and leaky with large fenestrations [17]. In addition, tumor blood vessels develop wide lumens and have impaired lymphatic drainage, which drives the extensive leakage of blood into the tumor tissue. As a result, the structural defects provide potential to propel macromolecules or nanoparticles to extravasate through gaps in the tumor vasculature and accumulate due to the slow venous return in tumor tissues and poor lymphatic drainage [17]. Exploiting this tumor biological phenomenon is known as the Enhanced Permeation and Retention (EPR) effect.

An increasing emergence of nanotechnology has made a significant impact for cancer therapy by enhancing therapeutic effectiveness, reducing adverse side effects and improving drug pharmacokinetics [18]. In regards to size, the National Nanotechnology Initiative defines nano-scaled technology in the dimensions of 1 to 1000 nanometers. As

previously mentioned, nanoparticles with prolonged circulation time have the ability to accumulate at the tumor site via the EPR effect. For example, a 10- to 50-fold increase in drug accumulation was achieved using nanoparticles over nanoparticle-free drug after intravenous injection [19]. This observed phenomenon is referred to as "Passive targeting," making nanoparticle-based therapeutics a promising delivery system for intravenous cancer therapy. It's important to note that the extent and rate of tumor drug accumulation using nanoparticles is largely influenced by particle size, stability, shape, surface characteristics, as well as *in vivo* blood circulation time. For example, nanoparticles are commonly engineered with poly-ethylene glycol (PEG) to reduce the uptake by the reticuloendothelial system and increase blood circulation time versus non-PEG counterparts [17, 20-21].

Presently, there are several FDA approved nanoparticle-based drug products, as well as several in various stages of clinical trials [22]. To name a few, doxorubicin was formulated into liposomes, commercially known as Doxil®, for the treatment of patients with ovarian cancer; and paclitaxel-bound protein nanoparticles, known as Abraxane ®, for the treatment of metastatic breast cancer. The FDA approved Doxil® and Abraxane® in 1999 and 2005, respectively [22]. However, there are currently no FDA approved products that incorporate gemcitabine into nanoparticles.

There are several research groups attempting to optimize the *in vivo* properties of gemcitabine using nanoparticle delivery systems [15-16,23-24]. For example, gemcitabine has been covalently coupled with 1,1`,2-tris-nor-squaenic acid to formulate 4-(N)-Tris-nor-squalenoyl-gemcitabine (SQdFdC NA). Following intravenous treatment in murine metastatic leukemia L1210 wt bearing mice, the SQdFdC Na caused significant increase in mouse survival time as compared to gemcitabine alone [24]. After synthesis of stearoyl gemcitabine and incorporation into liposomes, Immordino et al. observed that

the *in vivo* anti-tumor activity and pharmacokinetic properties were significantly enhanced versus liposome-free stearoyl gemcitabine.

1.6 Cancer Drug Targeting: The Epidermal Growth Factor Receptor

Prior to FDA approval of any cancer drug, the main objective is to provide evidence of clinical effectiveness through significant survival return, beneficial effects to cancer-related symptoms and improved patient quality of life [25]. Ultimately, the beneficial effects of cancer treatment should outweigh any potential associated toxic or adverse clinical endpoints. Simply put, the performance of any drug is measured by its ability to achieve therapeutic benefit without damaging healthy, living cells. As previously mentioned in this chapter, normal and tumor cells both involve the cell cycle and undergo cell proliferation as a biological innate characteristic. It is well known that traditional chemotherapeutic drugs tend to exhibit deleterious effects on normal cells as well, particularly those with speedy turnover such as bone marrow cells, red blood cells, mucous membrane cells, hair follicle cells, and reproductive cells [2,17]. These cells are highly vulnerable, causing common clinically toxic effects like bone marrow depression, low white blood count (i.e. prone to infections), anemia, fatigue, vomiting, hair-loss, diarrhea, and fertility changes, to name a few. These foreseen and undesirable side effects are mainly due to the lack of drug specificity of the chemotherapeutics and encourage most chemotherapeutics to be used near their maximum tolerated dose. In addition, many of the chemotherapeutic drugs are low molecular weight molecules and are excreted easily by the body [26]. This remains one of the major limitations in cancer treatment. Therefore, the development of tumor-specific cytotoxic effects is highly sought after. A large body of research has accumulated demonstrating efforts to increase tumor-drug specificity can be achieved by means of "active targeting" [27].

Over 100 years ago, Paul Ehrlich cleverly referenced the term, "magic bullet" after screening and connecting Salvarsan as the first selective and host friendly treatment option for Treponema pallidum, the causative agent for syphilis [17]. Prior to the discovery of salvarsan, targeted therapy for syphilis has not been achieved and highly toxic trivalent arsenic compounds were used. Since then, the term, "active targeted therapy," has been used to describe the concept of overcoming therapeutic limitations poised by intravenously (parental) administered drugs. In cancer therapy, chemotherapeutics can be tumor targeted though a variety of means such as physical, biological, or molecular systems by taking advantage of tumor associated receptors including the epidermal growth factor receptor (EGFR) [27].

Epidermal growth factor (EGF) is a ligand to the EGFR, a 170 kD endogenous cell surface glycoprotein that, when stimulated, acts through protein-tyrosine kinase activity to stimulate several normal cellular functions including cell proliferation, survival, adhesion, migration, and differentiation. In addition to EGF, more than ten ligands have been identified to exhibit strong receptor-ligand affinity towards EGFR [27-28]. Epidermal growth factor receptor is expressed in a variety of normal cell types and there are many reports showing that EGFR is overexpressed in several tumor cells (10-1000 times greater than normal cell expression of 1×10^4 receptors per cell), including those cell types where gemcitabine hydrochloride is indicated for usage [28-29]. For example, it has been discovered that EGFR is over-expressed in 30-50% of pancreatic cancer cells, 80-100% of human head and neck cancer cells, and 14-91% of human breast cancer cells [29]. Multiple EGFR targeting agents have been developed for cancer therapy, and the clinical efficacy are those EGFR targeting agents have been promising. For example, EGF and antibodies against EGFR had been conjugated onto liposomes and targeted to EGFR over-expressing tumor cells [30-31]. Similarly, Arya et al. (2011)

reported that conjugation of anti-HER2, an antibody against human EGFR-2, onto a gemcitabine-chitosan nanoparticle enhanced the anti-proliferative activity of the nanparticles against HER2-expressing Mia PaCa-2 cells and PANC-1 tumor cells in culture.

1.7 References

1. American Cancer Society (2012). Cancer Facts & Figures 2012. Atlanta: American Cancer Society.

2. Rubin, R. and D. Strayer (2008). Rubin's Patholoty: Clinicopathologic Foundations of Medicine. Philadelphia, Lippincott Williams & Wilkins.

3. DiPiro, J. T., R. L. Talbert, et al. (2008). Pharmacotherapy: A Pathophysiologic Approach. New York, McGraw-Hill Medical.

4. Jain, R. K. (1996). "Delivery of molecular medicine to solid tumors." Science 271(5252): 1079-1080.

5. Collins, K., T. Jacks, et al. (1997). "The cell cycle and cancer." Proc Natl Acad Sci U S A 94(7): 2776-2778.

6. Priestman, T. (2008). Cancer therapy in clinical practice. London, Springer-Verlag.

7. Abbruzzese, J. L., R. Grunewald, et al. (1991). "A phase I clinical, plasma, and cellular pharmacology study of gemcitabine." J Clin Oncol 9(3): 491-498.

8. Reid, J. M., W. Qu, et al. (2004). "Phase I trial and pharmacokinetics of gemcitabine in children with advanced solid tumors." J Clin Oncol 22(12): 2445-2451.

9. Huang, P., S. Chubb, et al. (1991). "Action of 2',2'-difluorodeoxycytidine on DNA synthesis." Cancer Res 51(22): 6110-6117.

10. Philip, P. A. (2010). "Novel targets for pancreatic cancer therapy." Surg Oncol Clin N Am 19(2): 419-429.

11. Lillemoe, K. D. (1995). "Current management of pancreatic carcinoma." Ann Surg 221(2): 133-148.

12. Castelli, F., M. G. Sarpietro, et al. (2007). "Interaction of lipophilic gemcitabine prodrugs with biomembrane models studied by Langmuir-Blodgett technique." J Colloid Interface Sci 313(1): 363-368.

13. Barton-Burke, M. (1999). "Gemcitabine: a pharmacologic and clinical overview." Cancer Nurs 22(2): 176-183.

14. Bouffard, D. Y., J. Laliberte, et al. (1993). "Kinetic studies on 2',2'-difluorodeoxycytidine (Gemcitabine) with purified human deoxycytidine kinase and cytidine deaminase." Biochem Pharmacol **45**(9): 1857-1861.

15. Brusa, P., M. L. Immordino, et al. (2007). "Antitumor activity and pharmacokinetics of liposomes containing lipophilic gemcitabine prodrugs." Anticancer Res **27**(1A): 195-199.

16. Immordino, M. L., P. Brusa, et al. (2004). "Preparation, characterization, cytotoxicity and pharmacokinetics of liposomes containing lipophilic gemcitabine prodrugs." J Control Release **100**(3): 331-346.

17. Sinko, P. J. and A. N. Martin (2006). Martin's physical pharmacy and pharmaceutical sciences: physical chemical and biopharmaceutical principles in the pharmaceutical sciences. . Philadelphia, Lippincott Williams & Wilkins.

18. Zhang, L., F. X. Gu, et al. (2008). "Nanoparticles in medicine: therapeutic applications and developments." Clin Pharmacol Ther **83**(5): 761-769.

19. Cuenca, A. G., H. Jiang, et al. (2006). "Emerging implications of nanotechnology on cancer diagnostics and therapeutics." Cancer **107**(3): 459-466.

20. Owens, D. E., 3rd and N. A. Peppas (2006). "Opsonization, biodistribution, and pharmacokinetics of polymeric nanoparticles." Int J Pharm **307**(1): 93-102.

21. Allen, C., N. Dos Santos, et al. (2002). "Controlling the physical behavior and biological performance of liposome formulations through use of surface grafted poly(ethylene glycol)." Biosci Rep **22**(2): 225-250.

22. Wang, A. Z., R. Langer, et al. (2012). "Nanoparticle delivery of cancer drugs." Annu Rev Med **63**: 185-198.

23. Stella, B., S. Arpicco, et al. (2007). "Encapsulation of gemcitabine lipophilic derivatives into polycyanoacrylate nanospheres and nanocapsules." Int J Pharm **344**(1-2): 71-77.

24. Arias, J. L., L. H. Reddy, et al. (2008). "Magnetoresponsive squalenoyl gemcitabine composite nanoparticles for cancer active targeting." Langmuir **24**(14): 7512-7519.

25. O'Shaughnessy, J. A., R. E. Wittes, et al. (1991). "Commentary concerning demonstration of safety and efficacy of investigational anticancer agents in clinical trials." J Clin Oncol **9**(12): 2225-2232.

26. Bharali, D. J., M. Khalil, et al. (2009). "Nanoparticles and cancer therapy: a concise review with emphasis on dendrimers." Int J Nanomedicine **4**: 1-7.

27. Byrne, J. D., T. Betancourt, et al. (2008). "Active targeting schemes for nanoparticle systems in cancer therapeutics." Adv Drug Deliv Rev **60**(15): 1615-1626.

28. LeMaistre, C. F., C. Meneghetti, et al. (1994). "Targeting the EGF receptor in breast cancer treatment." Breast Cancer Res Treat **32**(1): 97-103.

29. Klijn, J. G., P. M. Berns, et al. (1992). "The clinical significance of epidermal growth factor receptor (EGF-R) in human breast cancer: a review on 5232 patients." Endocr Rev **13**(1): 3-17.

30. Baselga, J. (2000). "Monoclonal antibodies directed at growth factor receptors." Ann Oncol **11 Suppl 3**: 187-190.

31. Ranson, M., L. A. Hammond, et al. (2002). "ZD1839, a selective oral epidermal growth factor receptor-tyrosine kinase inhibitor, is well tolerated and active in patients with solid, malignant tumors: results of a phase I trial." J Clin Oncol **20**(9): 2240-2250.

Chapter 2: In Vivo and In Vitro Anti-tumor Activities of a Gemcitabine Derivative Carried by Nanoparticles

Contributing authors:

Brian R. Sloat, Dong Li, Woon-Gye Chung, Dharmika Lansakara-P, Philip Proteau, Kaoru Kiguchi, John J. DiGiovanni, and Zhengrong Cui.

2.1   Abstract

Gemcitabine (Gemzar®) is the first line treatment for pancreatic cancer and often used in combination therapy for non-small cell lung, ovarian, and metastatic breast cancers. Although extremely toxic to a variety of tumor cells in culture, the clinical outcome of gemcitabine treatment still needs improvement. In the present study, a new gemcitabine nanoparticle formulation was developed by incorporating a previously reported stearic acid amide derivative of gemcitabine into nanoparticles prepared from lecithin/glyceryl monostearate-in-water emulsions. The stearoyl gemcitabine nanoparticles were cytotoxic to tumor cells in culture, although it took a longer time for the gemcitabine in the nanoparticles to kill tumor cells than for free gemcitabine. In mice with pre-established model mouse or human tumors, the stearoyl gemcitabine nanoparticles were significantly more effective than free gemcitabine in controlling the tumor growth. PEGylation of the gemcitabine nanoparticles with polyethylene glycol (2000) prolonged the circulation of the nanoparticles in blood and increased the accumulation of the nanoparticles in tumor tissues (>6-fold), but the PEGylated and un-PEGylated gemcitabine nanoparticles showed similar anti-tumor activity in mice. Nevertheless, the nanoparticle formulation was critical for the stearoyl gemcitabine to

show a strong anti-tumor activity. It is concluded that for the gemcitabine derivate-containing nanoparticles, cytotoxicity data in culture may not be used to predict their in vivo anti-tumor activity, and this novel gemcitabine nanoparticle formulation has the potential to improve the clinical outcome of gemcitabine treatment.

2.2   Introduction

Gemcitabine (2′, 2′-difluorodeoxycytidine, dFdC) is the active ingredient in Gemzar® (Eli Lilly & Co., Indianapolis, IN), which is the first line treatment for pancreatic cancer [1]. The therapeutic efficacy of Gemzar® as a single agent is modest, and thus, Gemzar® is often used in combination therapy for non-small cell lung cancer, ovarian cancer, and metastatic breast cancer. Although extremely cytotoxic to tumor cells in culture, the clinical efficacy from gemcitabine (Gemzar®) treatment requires further improvement [2,3].

Gemcitabine is a prodrug, and its mechanism of action is based solely on intracellular phosphorylation into its active triphosphate derivative [4]. About ninety percent of gemcitabine triphosphate (dFdCTP) is rapidly eliminated, mainly due to deamination to 2′, 2′-difluorodeoxyuridine (dFdU), a gemcitabine derivative with minimal anti-tumor activity [5]. The rapid metabolism of gemcitabine explains its short half-life (32-84 min for short infusions in humans) [6,7,8] and is thought to be responsible for its modest clinical activity [6]. Consequently, alternative methods were explored to improve the gemcitabine formulation such as enhancing the lipophilicity of gemcitabine by conjugating long fatty acid chains onto it. It was shown that a fatty acid ester derivative of gemcitabine (CP-4126, gemcitabine-5′-elaidic acid ester) exhibited a better anti-tumor activity than its parent compound when given orally or intraperitoneally to mice [9], but an intravenous formulation of the CP-4126 was not reported. It was also

15

shown that incorporation of a gemcitabine fatty acid amide derivative (4-(N)-stearoyl-gemcitabine, GemC18) into liposomes offered advantages including hindered metabolic deactivation and improved anti-tumor activity in mouse models [10,5]. Recently, nanoparticles have gained attention as a delivery system for anticancer drugs including gemcitabine [11-15]. For example, gemcitabine had been covalently coupled with 1,1′,2-tris-nor-squalenic acid to formulate 4-(N)-Tris-nor-squalenoyl-gemcitabine (SQdFdC NA) [11]. Following intravenous treatment of murine metastatic leukemia L1210 wt bearing mice, the SQdFdC NA caused a significant increase in mouse survival time compared to gemcitabine alone [11]. However, an alternative and efficacious gemcitabine formulation other than Gemzar® remains unavailable on the market.

Previously, our group reported the preparation of solid lipid nanoparticles of 180-200 nm from lecithin/glyceryl monostearate (GMS)-in-water emulsions [16-18]. Lecithins are components of cell membranes. They are included in intramuscular and intravenous injectables [19]. GMS is used in a variety of food, pharmaceutical, and cosmetic applications and is GRAS (generally regarded as safe) listed [20]. In the present study, the feasibility of using the solid lipid nanoparticles as a delivery system for gemcitabine was evaluated. In order to incorporate the hydrophilic gemcitabine into the lipophilic matrix of the nanoparticles, the previously reported 4-(N)-stearoyl gemcitabine was adopted to increase the lipophilicity of the gemcitabine [5]. Tween 20 was one of the components of the nanoparticles [17]. Although Tween 20 has short polyethylene glycol (PEG) chains, the chains may be too short to prevent or minimize the uptake of the nanoparticles by the reticuloendothelial system (RES) after intravenous injection. Therefore, the gemcitabine nanoparticles were PEGylated using a longer PEG (molecular weight, 2000), and the anti-tumor activities of the PEGylated and un-PEGylated gemcitabine nanoparticles were evaluated in vitro and in vivo.

16

2.3 Materials and Methods

2.3.1 Chemicals and Cell-lines

Acetone, dioxane, mannitol, ethyl acetate (EtOAc), ethylchloride, dichloromethane (CH_2Cl_2), anhydrous dimethylformamide (DMF), hexane, ammonium chloride (NH_4Cl), trifluoroacetic acid (TFA), human plasma, isopropanol, 3-(4,5-dimethylthiazol-2-yl)-2,5-diphenyltetrazolium bromide (MTT), Sepharose® 4B, sodium sulfate (Na_2SO_4), sodium carbonate (Na_2CO_3), stearic acid, sodium chloride (NaCl), 1-hydroxy-7-aza-benzotriazole (HOAt), methanol, sodium dodecyl sulfate (SDS), and 1-ethyl-3-(3-dimethylaminopropyl) carbodiimide (EDCI) were from Sigma-Aldrich (St. Louis, MO). Gemcitabine hydrochloride (gemcitabine HCl) was from U.S. Pharmacopeia (Rockville, MD). Soy lecithin was from Alfa Aesar (Ward Hill, MA). GMS was from Gattefosse Corp (Paramus, NJ). Mouse lung (TC-1, ATCC # CRL-2785) and human pancreatic (BxPC-3, ATCC # CRL-1687) cancer cell lines were from American Type Culture Collection (ATCC, Manassas, VA). TC-1 cells were grown in RPMI1640 medium (Invitrogen, Carlsbad, CA). BxPC-3 cells were grown in DMEM medium (Invitrogen). All media were supplemented with 10% fetal bovine serum (FBS, Invitrogen), 100 U/mL of penicillin (Invitrogen), and 100 µg/mL of streptomycin (Invitrogen).

2.3.2 Synthesis of 4-(N)-Stearoyl Gemcitabine (synthesis performed by Dong Li & Dharmika S.P. Lansakara-P et al.)

The 4-(N)-stearoyl-gemcitabine was prepared as previously described with slight modifications [5,20]. Briefly, 3′,5′-O-bis(tert-butoxycarbonyl) gemcitabine was synthesized following a literature protocol [20]. This Boc-protected gemcitabine (179 mg, 0.39 mmol), stearic acid (121 mg, 0.42 mmol), and HOAt (57 mg, 0.42 mmol) were

17

dissolved in 4 mL of freshly distilled CH_2Cl_2. After the solution was cooled in an ice-water bath, EDCI (89 mg, 0.46 mmol) was added. The reaction mixture was stirred under argon for 30 h. The mixture was diluted with 10 mL of water and extracted with EtOAc/hexane mixture (2:1). The combined organic phases were washed with saturated NH_4Cl and NaCl, dried over anhydrous Na_2SO_4, and concentrated. The crude product was purified by silica chromatography (3:7 EtOAc/hexane). The purified Boc-protected-N-stearoyl gemcitabine (230 mg, 0.32 mmol) was dissolved in 4 mL of freshly distilled CH_2Cl_2, and 1 mL of TFA was added. The solution was stirred at room temperature for 2 h. The solvent and excess TFA were removed in vacuo to provide the desired product, which was confirmed using 1H NMR and MS data [5].

2.3.3   Incorporation of 4-(N)-Stearoyl Gemcitabine Into Nanoparticles

Nanoparticles were prepared as previously described [17]. Briefly, 3.5 mg of soy lecithin and 0.5 mg of GMS were weighed into a 7 mL glass vial. One mL of de-ionized and filtered (0.22 μm) water was added into the lecithin/GMS mixture, which was then maintained on a 70-75°C hot plate while stirring until a homogenous slurry was formed. Tween 20 was added drop-wise to a final concentration of 1% (v/v). The resultant emulsions were allowed to cool to room temperature while stirring to form nanoparticles.

To incorporate GemC18 into the nanoparticles to form stearoyl gemcitabine nanoparticles (GemC18-NPs), a predetermined amount of GemC18 was added into the lecithin and GMS mixture before the addition of water. The remaining steps were identical to the preparation of the gemcitabine-free nanoparticles. The size and zeta potential of the nanoparticles were measured using a Malvern Zetasizer Nano ZS (Westborough, MA). To monitor the short-term stability of the GemC18-NPs, the

18

nanoparticles were suspended in water and left at ambient condition for 20 days. Their particle size was measured at pre-determined time points.

PEGylated GemC18-NPs (PEG-GemC18-NPs) were prepared by including 1,2-distearyol-sn-glycero-3-phosphoethanolamine-N-[amino(polyethyleneglycol)-2000] (DSPE-PEG(2000), 11.6%, w/w of total lipids and Tween 20) (Avanti Polar Lipids, Alabaster, AL) in the GemC18, lecithin, and GMS mixture during the nanoparticle preparation.

To determine the stability of the GemC18-NPs and the PEG-GemC18-NPs in simulated biological medium, the nanoparticles were diluted into normal saline or in normal saline with 10% of FBS, and their sizes were measured immediately (0 min) and after 30 min of incubation at 37°C.

To fluorescently label the nanoparticles, 1,2-dioleoyl-sn-glycero-3-phosphoethanolamine-N-(carboxyfluorescein) (ammonium salt) (DOPE-fluorescein, 1.9 mg, Avanti Polar Lipids) was included in the lecithin, GMS, and GemC18 mixture during the nanoparticle preparation.

To determine the solubility of the GemC18 in Tween 20 (1%), 1 mg of the GemC18 in tetrohydrofuran (THF) was placed into a glass vial. A pilot study showed that the solubility of the GemC18 in 1% Tween 20 was less than 1 mg/mL. After the evaporation of the THF, 1 mL of Tween 20 (1%) was added, and the mixture was treated following the procedure identical to the preparation of the GemC18-NPs. The mixture was spun down (18,000 × g), and the concentration of the GemC18 in the supernatant was determined using high-performance liquid chromatography (HPLC).

2.3.4 Transmission Electron Microscopy (TEM)

The nanoparticles were examined using a transmission electron microscope (Philips CM12 TEM/STEM) following a previously reported method [17]. Briefly, a carbon-coated 200-mesh copper specimen grid was glow-discharged for 1.5 min. Nanoparticles in suspension were deposited on the grid and then stained with uranyl acetate before observation under TEM.

2.3.5 Gel Permeation Chromatography (GPC)

To separate un-incorporated GemC18 from nanoparticles, GPC was performed using a 6 mm × 30 cm Sepharose® 4B column, which was equilibrated using phosphate buffered saline (PBS, pH 7.4). Samples (100 μL) were applied into the column and eluted with PBS. Elution fractions of 250 μL were collected, and their absorbances at 269 nm and 248 nm were measured using a BioTek Synergy™ HT Multi-Mode Microplate Reader (Winooski, VT).

2.3.6 *In Vitro* Release of GemC18 From GemC18-NPs and PEG-GemC18-NPs

GemC18-NPs or PEG-GemC18-NPs in PBS (100 μg of GemC18) were placed into a 1 mL cellulose ester dialysis tube (MWC 50,000) from Spectrum Chemicals & Laboratory Products (New Brunswick, NJ). The dialysis tube was then placed into a plastic conical tube containing 13 mL of PBS with 0.05% (w/v) of SDS and incubated in a 37°C shaker incubator. At predetermined time points, 200 μL of the release medium was withdrawn and replaced with 200 μL of fresh release medium. As a control, the release of GemC18 from GemC18-in-Tween 20 micelles (100 μg/mL of GemC18 in 1% of Tween 20 in water) was also measured. The concentration of the GemC18 was determined by measuring the absorbance at 248 nm or using HPLC.

2.3.7   HPLC

Agilent or Shimadzu HPLC with an Agilent C18 column (5 μm, 4.6 × 250 mm; Santa Clara, CA) was used to determine the concentration of GemC18. The mobile phase was methanol and water (93%:7%). The flow rate was 1 mL/min. The detection wavelength was 248 nm [5].

2.3.8   Uptake of Nanoparticles by Tumor Cells in Culture

To microscopically examine the uptake of the nanoparticles, TC-1 cells (2×10^4) were seeded on poly-D-lysine-coated glass cover slips for 24 h. Cells were incubated with fluorescein-labeled GemC18-NPs (Fluorescein-GemC18-NPs) and maintained at 4°C or 37°C for 6 h. Cells were then washed with PBS, fixed in 3% paraformaldehyde for 20 min, and washed three additional times prior to mounting on slides with Fluoromount G® (Southern Biotech, Birmingham, AL). Bright-field and fluorescent images were obtained using a Zeiss AutoImager Z1 microscope (Carl Zeiss, Thornwood, NY) with a Zeiss 20 × objective [17].

Moreover, the uptakes of the PEGylated and un-PEGylated GemC18-NPs by TC-1 cells were compared as previously described [18]. Briefly, TC-1 cells (2.5×10^5 cells/well) (n = 4) were seeded in a 24-well plate and incubated overnight at 37°C, 5% CO_2. The cells (in 600 μL medium) were then incubated with 100 μL of fluorescein-labeled PEGylated or un-PEGylated GemC18-NPs at 37°C, 5% CO_2 or at 4°C for 6 h. The initial fluorescence intensities of the PEGylated and un-PEGylated nanoparticles were confirmed to be identical. At 4°C, the internalization of the nanoparticles was inhibited, and thus, a comparison of the data at 4°C and 37°C can provide information about the internalization of the nanoparticles. After the incubation, the cells were washed 3 times with PBS (10 mM, pH 7.4) and lysed with a lysis buffer (0.5% Triton X-100).

The fluorescence intensity was measured using a BioTek Synergy™ HT Multi-Detection Microplate Reader.

2.3.9 *In Vitro* Cytotoxicity Assay

Cells were seeded into 96-well plates (5,000 cells per well) and incubated at 37°C, 5% CO_2 overnight. Various amounts of gemcitabine HCl or GemC18-NPs in PBS were added into the wells, and the cells were then incubated for an additional 24 or 48 h. As a control, cells were treated with fresh medium. The number of cells alive was determined using an MTT assay. The fraction of killed or affected cells (Fa) and the fraction of viable or unaffected cells (Fu) at each concentration were calculated and plotted as the log (Fa/Fu) against the log (Dose). The IC_{50} was the dose at Log (Fa/Fu) = 0 [21]. This experiment was repeated at least once. The IC_{50} values of the GemC18-in-Tween 20 and GemC18 alone were determined similarly.

2.3.10 *In Vivo* Tumor Treatment Studies

National Institutes of Health guidelines for animal use and care were followed. The animal protocol was approved by the Institutional Animal Care and Use Committee at the University of Texas at Austin. Female C57BL/6 (18-20 g) and Nu/Nu mice (6-8 weeks) were from Charles River Laboratories (Wilmington, MA). To establish tumors in mice, TC-1 or BxPC-3 tumor cells (5×10^5/mouse) were subcutaneously (s.c.) injected in the right flank of C57BL/6 or athymic mice, respectively. The hair, if any, at the injection site was carefully trimmed one day before the injection. GemC18-NPs or PEG-GemC18-NPs in sterile mannitol solution (5%, w/v) were injected via the tail vein. As controls, tumor-bearing mice were injected with sterile mannitol solution (5%) or gemcitabine HCl dissolved in mannitol solution. To make sure that the same molar amount of gemcitabine

was injected, the doses of the gemcitabine HCl and GemC18 were 0.566 mg and 1 mg per mouse, respectively [22,23]. To evaluate the anti-tumor activity of the nanoparticles when injected peritumorally, PEG-GemC18-NPs or GemC18-NPs (0.25 mg of GemC18 in 50 μL) were injected three times per week for a total of 5 times peritumorally around TC-1 tumors, starting when the tumors reached 5 mm in diameter. Control mice received sterile mannitol. To evaluate the anti-tumor activity of the GemC18-in-Tween 20 micelles, GemC18 was saturated into 1% of Tween 20. The micelles were then i.v. injected into TC-1 tumor-bearing mice (150 μg/mouse) twice a week for 5 times. Control mice received an equivalent dose of PEG-GemC18-NPs or sterile mannitol. Tumor size was measured and calculated based on the following equation: tumor volume (mm3) = [length × width × width]/2. The experiment was repeated up to 3 times to confirm the antitumor activity of the GemC18-NPs.

2.3.11 *In Vivo* and *Ex Vivo* Fluorescence Imaging

BxPC-3 tumors were established in nude mice by s.c. injection of 5.0×10^5 cells. When the tumor size reached 10-12 mm, fluorescein-labeled, PEGylated or un-PEGylated GemC18-NPs were injected intravenously via the tail vein into the mice (n = 3). Twenty-four h after the injection, mice in each group were imaged using an In Vivo Imaging System (IVIS Spectrum Series, Caliper Life Sciences, Hopkiton, MA). Region of interest (ROI) values were recorded using Living Image® (ver. 4.0). Fluorescence intensity (total counts) was determined in a fixed, circular ROI. Relative fluorescence intensity was calculated by subtracting the fluorescence intensity counts in the ROI in the grayscale images from that of the ROI in the fluorescence images. After the in vivo imaging, mice were euthanized. Blood (500 μL), heart, lung, liver, spleen, and

kidney were harvested and imaged immediately. The total blood volume of a mouse (20 g) was assumed to be 1.5 mL [24].

To determine the half-life ($t_{1/2}$) of the PEGylated and un-PEGylated GemC18-NPs in the blood circulation, tumor-free C57BL/6 mice were injected with fluorescein-labeled PEG-GemC18-NPs or fluorescein-GemC18-NPs and then euthanized 5 min, 1 h, 3 h, 6 h, 12 h, or 24 h later. Blood samples (500 μL/mouse) were collected immediately, placed into a multi-well plate, and imaged using the IVIS Spectrum. Fluorescence intensity for each blood sample was determined, and data were analyzed using the PK Solver® and two-compartmental model to determine the $t_{1/2}$ at the elimination phase [25].

2.3.12 Statistics

Statistical analyses were completed by performing ANOVA followed by Fisher's protected least significant difference (LSD) procedure. A p value of ≤ 0.05 (two-tail) was considered significant.

2.4   Results and Discussion

2.4.1   Preparation and Characterization of Stearoyl Gemcitabine-incorporated Solid Lipid Nanoparticles

The nanoparticles were prepared from lecithin/GMS-in-water emulsions, and thus, had a lipophilic core [17,18]. Gemcitabine is water-soluble. To increase its lipophilicity, a previously reported stearic acid amide derivative of gemcitabine, stearoyl gemcitabine (GemC18), was adopted and synthesized, which was then incorporated into the nanoparticles by taking advantage of its lipophilic stearoyl group. The nanoparticles were prepared with lecithin, GMS, and Tween 20, which can potentially form micelles.

24

For example, the critical micelle concentration of Tween 20 was reported to be approximately .01 % (v/w) at 20°C [30]. Because the GemC18 molecules can be potentially incorporated into micelles that may be present in the nanoparticle preparation, GPC was carried out to examine whether the GemC18 in the nanoparticles can be separated from the GemC18 in micelles prepared with Tween 20. Nanoparticles and micelles were prepared with a final concentration of 100 μg/mL GemC18 and then applied into GPC columns. As shown in Fig. 2.1A, the nanoparticles eluted mainly in fraction 7, whereas the micelles eluted mainly in fraction 9, demonstrating that the Sepharose 4B column can be used to separate GemC18 molecules that were not incorporated into the nanoparticles, if any, from the GemC18-incorporated nanoparticles. At 0.1 mg/mL of GemC18, it appeared that 100% of the GemC18 was incorporated into the nanoparticles (Fig. 2.1A). When the GemC18 concentration was increased to 5 mg/mL in the nanoparticle preparation, all the GemC18 molecules (100%) were still incorporated into the nanoparticles as well because a micelle peak in fraction 9 was not detected (Fig. 2.1B). However, when more than 5 mg/mL of GemC18 was used, and if the final concentration of the Tween 20 was kept at 1%, emulsions can no longer be formed, and the preparation simply remained as a turbid slurry even after an extended period of stirring at increased temperature. Therefore, the GemC18-NPs prepared with 5 mg/mL of GemC18 were used for further studies. The GemC18-NPs were spherical (Fig. 2.1C) and were stable when stored as an aqueous suspension in ambient conditions during a 20-day short-term storage period (data not shown).

Similar to the GemC18-NPs, PEGylated GemC18-NPs were prepared with 5 mg/mL of GemC18, and it appeared that all of the GemC18 was also incorporated into the nanoparticles due to the lack of a micelle peak on the gel permeation chromatograph of the PEGylated GemC18-NPs (Fig. 2.1D). The particle size and zeta potential of the

PEGylated and un-PEGylated GemC18-NPs are shown in Fig. 2.1E. As expected, PEGylation of the GemC18-NPs slightly increased its particle size (Fig. 2.1E). The zeta potentials of both the PEGylated and un-PEGylated GemC18-NPs were not within the range of −30 to +30 mV, which was considered to be unstable for colloid suspensions [26]. Shown in Fig. 1Fare the dynamic light scattering spectra of the GemC18-NPs, PEGylated and un-PEGylated, overlaid with that of the GemC18-in-Tween 20 micelles (i.e., the peak around 8 nm). The dynamic light scattering spectra of the PEGylated and un-PEGylated GemC18-NPs also did not reveal the presence of a significant amount of micelles in the nanoparticle preparations. There are two possible reasons for the lack of a significant amount of micelles in the nanoparticle preparation: 1) the Tween 20 was added in drop-wise; 2) the Tween 20 needed to act as an emulsifier for the formation of the emulsions.

In an *in vitro* release study, GemC18 in Tween 20 micelles rapidly diffused out of the dialysis tube, in which the GemC18 micelles were placed (i.e., $36.8 \pm 3.8\%$ in 30 min) (Fig. 2.1G), indicating that the diffusion of the GemC18 molecules through the dialysis membrane was not rate-limiting. However, when the GemC18-NPs were placed into an identical dialysis tube, only about 4% of the GemC18 was diffused in the release medium within 4 h (Fig. 2.1G) and less than 15% with 24 h (data not shown). Finally, the release curve of the GemC18 from the PEGylated GemC18-NPs was not significantly different from the release curve of the GemC18 from the un-PEGylated GemC18-NPs (Fig. 2.1G).

Data in Fig. 2.1H (data not shown) showed that the hydrolysis of the gemcitabine from the GemC18-NPs was slow as well. After 72 h in PBS or mouse serum, more than 80% of the gemcitabine was still in the GemC18 form (Fig. 2.1H). The rate of the hydrolysis of the gemcitabine from the GemC18-NPs seemed to be higher in human

serum than in mouse serum (Fig. 2.1H), likely due to interspecies variations in plasma amidase activity.

Finally, after 30 min of incubation in normal saline with fetal bovine serum (FBS) (10%, v/v) at 37°C, the size of the PEG-GemC18-NPs did not change significantly (p = 0.1) (Fig. 2.1I). However, the size of the un-PEGylated GemC18-NPs increased by 40.3 ± 6.9% (p = 0.006) (Fig. 2.1I). The sizes of the PEGylated and un-PEGylated GemC18-NPs did not change after 30 min of incubation at 37°C in normal saline (i.e., without FBS) (data not shown). It is suspected that when the un-PEGylated GemC18-NPs were incubated in the presence of FBS, significant binding of proteins to the nanoparticles may have happened, or the nanoparticles may have aggregated in the presence of the FBS. Similar serum protein binding and/or particle aggregation are expected when the un-PEGylated GemC18-NPs are injected intravenously into mice.

2.4.2   Uptake of Nanoparticles by Tumor Cells in Culture

To examine the uptake of the GemC18-NPs by tumor cells, fluorescein-labeled GemC18-NPs were incubated with mouse TC-1 tumor cells for 6 h at 37°C or 4°C. Strong fluorescence was observed when the cells were incubated with GemC18-NPs at 37°C, but not when incubated at 4°C (Fig. 2.2A), suggesting that the internalization (or uptake) of the nanoparticles by the cells in culture was likely mediated by endocytosis. At 4°C, endocytosis is arrested. The weaker fluorescence detected at 4°C was likely from particles bound on the surface of the cells. As expected, data in Fig. 2.2B showed that PEGylation of the GemC18-NPs significantly limited the uptake of nanoparticles by the TC-1 tumor cells in culture, but as it will be shown later, the PEGylation helps prolong the circulation of the nanoparticles in blood.

2.4.3 Evaluation of the Cytotoxicity of the GemC18-NPs and PEGylated GemC18-NPs in Tumor Cells in Culture

Prior to in vivo evaluation of the nanoparticles in mice, the cytotoxicity of the stearoyl gemcitabine nanoparticles to tumor cells in culture was evaluated. The gemcitabine nanoparticles were cytotoxic to both TC-1 and BxPC-3 tumor cells (Fig. 2.3A). The IC_{50} values of the gemcitabine HCl were significantly lower than those of the GemC18-NPs and PEG-GemC18-NPs (Fig. 2.3A), indicating that in cell culture, the stearoyl gemcitabine nanoparticles were less toxic than the free gemcitabine HCl. The IC_{50} values of the GemC18-NPs and the PEG-GemC18-NPs were not different (p = 0.13 in TC-1 cells, 0.129 in BxPC-3 cells). Data in Fig. 2.3B showed that when TC-1 tumor cells were incubated with the GemC18-NPs for 48 h, the percent of the dead TC-1 cells reached a level similar to that when the TC-1 cells were incubated with the gemcitabine HCl for 24 h, indicating that it simply took a longer time for the GemC18-NPs to kill tumor cells, which may be explained by the slow release of the gemcitabine or the GemC18 from the GemC18-NPs (Figs. 2.1G and H). Free gemcitabine molecules can enter cells in culture via nucleoside transporters [27]. Possible routes for the gemcitabine in GemC18-NPs or PEG-GemC18-NPs to enter the cells may include: i) cells take up the nanoparticles, and the gemcitabine is then hydrolyzed from the nanoparticles intracellularly; ii) the gemcitabine molecules is released by hydrolysis from nanoparticles and then transported inside the tumor cells by the nucleoside transporters. It remains unknown to what extent each route was responsible for the uptake of the gemcitabine in the nanoparticles by cells in culture. Finally, in TC-1 cells, the IC_{50} value of GemC18 (in trace amount of dimethyl sulfoxide) was 2.3-fold less than that of the GemC18-NPs (data not shown).

2.4.4 Biodistribution of the GemC18-NPs and PEG-GemC18-NPs in Tumor-bearing Mice

Imaging and biodistribution of the nanoparticles were completed using fluorescein-labeled GemC18-NPs in athymic mice with pre-established human BxPC-3 tumors. *In vivo* imaging showed that PEGylation of the GemC18-NPs with PEG(2000) significantly increased the accumulation of the nanoparticles in the tumors (6.3-fold, p = 0.0006) (Figs. 2.4A and B). Ex vivo imaging data shown in Fig. 2.4C indicated that PEGylation of the GemC18-NPs significantly increased the blood circulation of the nanoparticles and decreased the accumulation of the nanoparticles in the RES such as liver and spleen. For example, 24 h after injection, the amount of PEGylated GemC18-NPs remaining in the blood was 5.3-fold higher than the GemC18-NPs (Fig. 2.4C). In fact, the half-life ($t_{1/2}$) of the PEG-GemC18-NPs at the elimination phase in healthy C57BL/6 mice was determined to be 24.3 ± 3.8 h (with a mean residence time (MRT) of 23.4 ± 0.5 h), but it was only 10.0 ± 0.7 h (MRT, 6.3 ± 2.0 h) for the un-PEGylated GemC18-NPs. The prolonged circulation of the PEGylated GemC18-NPs in blood was likely responsible for the enhanced accumulation of the PEG-GemC18-NPs in tumors (Figs. 2.4A and B) by the enhanced permeability and retention effect [28]. It is expected that the biodistribution and the pharmacokinetics of the GemC18 were similar to that of the nanoparticles they were incorporated into.

2.4.5 Evaluation of the Anti-tumor Activity of the GemC18-NPs in Mice with Pre-grafted Tumors

The anti-tumor activity of the stearoyl gemcitabine nanoparticles was evaluated in mice with pre-established TC-1 or BxPC-3 tumors. As shown in Figs. 2.5A and B (data not shown), the GemC18-NPs were effective in controlling the growth of mouse TC-1 tumors. TC-1 tumors grew aggressively in C57BL/6 mice when treated with sterile

mannitol (Fig. 2.5A). Two doses (i.v. on days 4 and 13) of GemC18-NPs in mice with TC-1 tumors (3.5 mm) led to a significant delay of the tumor growth (Fig. 2.5A). The same molar dose of the gemcitabine HCl (i.v. on days 4 and 13) significantly delayed the growth of the TC-1 tumors as well (Fig. 2.5A), but the GemC18-NPs were more effective than the gemcitabine HCl. Moreover, 21 days after tumor cell injection, the mean weights of tumors in mice that received sterile mannitol, gemcitabine HCl, or GemC18-NPs were 1.13 ± 0.28 g, 0.11 ± 0.03 g, and 0.03 ± 0.03 g, respectively, and they were significantly different from one another ($p < 0.01$). H&E staining showed that there were more intercellular spaces in tumors in mice that received the GemC18-NPs, and the size of the cells and their nuclei in tumors in mice that received the GemC18-NPs was significantly larger (Fig. 2.5C, data not shown). Ki67 proliferation marker indicated that there was much less cell proliferation in tumors in mice that received the GemC18-NPs. Moreover, angiogenesis marker CD31, which indicated the presence of endothelial cells in blood vessels, showed that there were significantly less blood vessels in the tumors in mice that received the GemC18-NPs (62.9 ± 17.0 per 0.25 mm2) or gemcitabine HCl (46.2 ± 10.7 per 0.25 mm2) than in tumors in mice that received the sterile mannitol (86.4 ± 27.8 per 0.25 mm2) ($p = 0.02$, Control vs. Gemcitabine; $p = 0.03$, Control vs. GemC18-NPs). Also, the average length of the lumen of the blood vessels in tumors in mice that received the GemC18-NPs (12.7 ± 19.1 μm) or the gemcitabine HCl (10.7 ± 15.7 μm) were significantly smaller than in mice that received the sterile mannitol (26.6 ± 44.4 μm) ($p = 0.005$, Control vs. Gemcitabine; $p = 0.01$, Control vs. GemC18-NPs). Finally, caspase 3 staining showed that more cells in tumors in mice that received the GemC18-NPs (14.1 ± 5.2 per 0.25 mm2) or gemcitabine HCl (12.1 ± 3.3 per 0.25 mm2) were caspase 3 positive than in mice that received the sterile mannitol (6.1 ± 2.6 per 0.25 mm2) ($p = 0.0001$, Control vs. Gemcitabine; $p = 0.003$, Control vs. GemC18-NPs). Taken together,

treatment with the GemC18-NPs inhibited tumor cell proliferation and angiogenesis, but promoted more tumor cells to undergo apoptosis, which may explain the increased anti-tumor activity of the GemC18-NPs (Figs. 2.5A&B, not shown).

The *in vivo* anti-tumor activity of the GemC18-NPs was also evaluated in athymic mice with pre-established human BxPC-3 tumors, and the GemC18-NPs were also more effective than gemcitabine HCl in controlling the growth of BxPC-3 tumors (Fig. 2.5A). Two doses of the GemC18-NPs (i.v. on days 6 and 19) completely inhibited the growth of the BxPC-3 tumors, whereas the same molar dose of gemcitabine HCl did not significantly affect the growth of the BxPC-3 tumors ($p = 0.18$ on day 24, Control vs. Gemcitabine) (Fig. 2.5A). Treatment with gemcitabine HCl or GemC18-NPs both helped mice maintain their weight. However, 3 weeks after the tumor injection, mice that received the sterile mannitol were significantly lighter than mice that received the gemcitabine HCl or GemC18-NPs ($p = 0.0007$, ANOVA) (Fig. 6B).

Finally, to evaluate the extent to which the anti-tumor activity of the GemC18-NPs may be attributed to the GemC18-free blank nanoparticles alone, another study using BxPC-3 tumors in nude mice was carried out. As shown in Fig. 2.5C, the GemC18-free nanoparticles alone did not significantly affect the tumor growth, whereas the GemC18-NPs significantly inhibited the growth of the BxPC-3 tumors. Therefore, the anti-tumor activity of the GemC18-NPs was not simply from the blank nanoparticles.

2.4.6 Comparison of the *In Vivo* Anti-tumor Activities of the PEGylated and un-PEGylated Gemcitabine Nanoparticles

Treatment of TC-1 tumor-bearing mice (i.v., a single dose) with the GemC18-NPs or the PEG-GemC18-NPs was initiated when tumors reached an average diameter of 4.5 mm. Because the PEGylation of the GemC18-NPs significantly increased the

accumulation of the nanoparticles into tumors after i.v. injection, it was expected that the PEG-GemC18-NPs would have a stronger anti-tumor activity than the GemC18-NPs. Unfortunately, the PEG-GemC18-NPs and the GemC18-NPs did not show significantly different anti-tumor activities (p = 0.38 on day 12 after injection) (Fig. 2.6A). Twelve days after the injection of the GemC18-NPs, 50% (3/6) of mice in both groups became tumor free, and one mouse that received the PEG-GemC18-NPs had to be euthanized due to its large tumor. In the BxPC-3 tumor model, the GemC18-NPs and the PEGylated GemC18-NPs were not different in their abilities to inhibit the tumor growth as well (Fig.2.6B). In culture, the IC_{50} values of the PEG-GemC18-NPs and GemC18-NPs in TC-1 and BxPC-3 cells were not significantly different (Fig. 2.3A). Therefore, it appeared that although PEGylation of the GemC18-NPs increased the accumulation of the nanoparticles into tumor tissues (Fig. 2.4B), it did not further improve the anti-tumor activity of the nanoparticles. Of course, the data from the *in vivo* or *ex vivo* imaging were representations of the distribution of the fluorescein associated with the nanoparticles, not the gemcitabine per se. It was assumed that the biodistribution of the fluorescein was similar to that of the gemcitabine because both of them were conjugated to a lipophilic molecule and then incorporated into the nanoparticles. Future experiments will be carried out to quantify the gemcitabine directly. Surprisingly, even when the PEGylated and un-PEGylated GemC18-NPs were injected peritumorally, they showed similar anti-tumor activities as well (Fig. 2.6C). It was expected that same amount of the PEG-GemC18-NPs or the GemC18-NPs accumulated into the tumor tissues after peritumoral injection. Therefore, it seemed that it was not the amount of the GemC18-NPs accumulated in the tumor tissues that determined the resultant anti-tumor activity. The lack of difference in the anti-tumor activities from the PEGylated and un-PEGylated GemC18-NPs was unlikely due to the dose of the GemC18 (i.e., too much GemC18 was dosed) because

32

both nanoparticles did not cause total tumor regression at the dose used. At present, it is speculated that the slow release of the GemC18 from the PEGylated or un-PEGylated GemC18-NPs (Fig. 2.1G) may be related to the similar anti-tumor activity from them after either intravenous injection or peritumoral injection (Fig. 2.6).

2.4.7 The PEGylated GemC18-NPs Were More Effective than the GemC18-in-Tween 20 Micelles in Controlling Tumor Growth

Data in Figures 2.4, 2.6, and 2.6 showed that the GemC18-NPs, PEGylated or un-PEGylated, were more effective than gemcitabine HCl in controlling the growth of experimental model tumors in mice. However, it remains unknown whether the enhanced anti-tumor activity from the GemC18-NPs was simply due to the GemC18 molecules. To understand the importance of incorporating the GemC18 into the solid lipid nanoparticles, the anti-tumor activity of the PEGylated GemC18-NPs was compared with that of the GemC18-in-Tween 20 micelles. The solubility of GemC18 in 1% of Tween 20 was estimated to be 726 ± 112 μg/mL (n =8). As shown in Figure 8, the PEG-GemC18-NPs were significantly more effective than same dose of the GemC18-in-Tween 20 micelles in inhibiting the growth of pre-established TC-1 tumors. In fact, although the GemC18-in-Tween 20 micelles slightly delayed the TC-1 tumor growth in the beginning, the mean size of the tumors in mice that received the GemC18-in-Tween 20 micelles was not significantly different from that in the untreated mice in the end (data not shown). The IC_{50} value of the GemC18-in-Tween 20 in TC-1 cells in culture was determined to be 125.7 ± 15.8 nM (after 48 h of co-incubation), indicating that the GemC18 in the Tween 20 micelles was still cytotoxic. Again, it is speculated that the slow release of the GemC18 from the GemC18-NPs, as observed in Fig. 1G, was important for the strong anti-tumor activity of the GemC18-NPs. The GemC18-in-Tween 20 was less effective

than the PEG-GemC18-NPs, possibly related to the fast release of the GemC18 from the GemC18-in-Tween 20 micelles (Fig. 2.1G). A comparison of the anti-tumor activities of an extended-release and an immediate-release gemcitabine or GemC18 formulations should help confirm this speculation.

Taken together, data in Figures 2.5, 2.6, 2.7, and 2.8 demonstrated that the GemC18-NPs, PEGylated or un-PEGylated, were more effective than gemcitabine HCl or GemC18-in-Tween 20 micelles in controlling tumor growth *in vivo*. Apparently, and the lower cytotoxic activity against the TC-1 tumor cells in culture as shown in Figure 2.3A may not be used to predict the in vivo antitumor activity of the stearoyl gemcitabine nanoparticles. The *in vivo* tumor treatment studies with the nanoparticles were carried out because data in Fig. 3B showed that it simply took the GemC18-NPs a longer incubation time to kill as many cells as the gemcitabine HCl did, which was likely due to the slow release of the gemcitabine or GemC18 from the nanoparticles as shown in Fig. 2.1G. The slow release may be beneficial because it can potentially slow down the clearance of the gemcitabine from blood circulation. In addition, it is speculated that the following mechanisms have also contributed to the enhancement of *in vivo* anti-tumor activity by formulating the gemcitabine in the GemC18-NPs or PEG-GemC18-NPs: i) compared to free gemcitabine HCl, the nanoparticles extended the circulation time of the gemcitabine in mice; ii) the stearoyl group protected the deamination of the gemcitabine; and iii) the nanoparticles increased the concentration of the gemcitabine in tumor tissues. Although the PEGylated GemC18-NPs showed similar anti-tumor activity as the GemC18-NPs (Fig. 2.6), the PEGylated GemC18-NPs will be used in future studies due to their ability to decrease the accumulation of the nanoparticles into the RES.

The advantages of using nanoparticles engineered from lecithin/GMS-in-water emulsions may include, but are not limited to the following. Firstly, lecithin, GMS, and

Tween 20 were all used previously in parenterals. Lecithin is a complex mixture of phosphatides consisting of phosphatidylcholine, phosphatidylethanolamine, phosphatidylserine, phosphatidylinositol and other substances such as triglycerides and fatty acids. It is GRAS listed and accepted in the FDA Inactive Ingredients Guide for parenterals [19]. Tween 20 is a polyoxyethylene (20) derivative of sorbitan monolaurate. It is GRAS listed and included in the FDA Inactive Ingredients Guide for parenterals [19]. GMS is used in a variety of pharmaceutical applications and is GRAS listed as well [19]. Therefore, it is expected that the nanoparticles have a favorable safety profile. In fact, data from preliminary toxicity studies are promising. For example, the GemC18-NPs did not induce detectable acute or subacute liver toxicity when injected intravenously into mice (Fig. 2.7). Previously, it was shown that the nanoparticles, even with cytotoxic docetaxel incorporated inside, did not cause any significant red blood cell lysis or platelet aggregation [18]. Moreover, in a related long-term study (1.5 years), the pathological and histological parameters of mice that received three doses of the nanoparticles by subcutaneous injection were compared to that of untreated mice, and an examination by a board-certified veterinary pathologist did not reveal any significant difference between those two groups of mice (Sloat and Cui, unpublished data). Secondly, the nanoparticles were solidified from warm oil-in-water emulsion droplets, and the emulsions were prepared by mechanical stirring at an increased temperature. In other words, both mechanical energy and heat provided the energy needed for the formulation of the emulsions. Toxic organic solvents are not needed during the preparation of the emulsions, and thus, there is not a need to remove organic solvents. Thirdly, the gemcitabine nanoparticle formulation is versatile in that it may be readily modified in multiple ways such as the incorporation of another lipophilic active compound into the core of the gemcitabine nanoparticles to further enhance their anti-tumor activity or the conjugation

of ligands onto the surface of the nanoparticles to target the nanoparticles to tumor cells that over-express a specific receptor.

2.5 Conclusions

In the present study, a new nanoparticle-based gemcitabine formulation that showed enhanced anti-tumor activity in mice with pre-established model tumors was reported. When fully developed, this new gemcitabine formulation can potentially improve the clinical outcome of gemcitabine therapy. Moreover, it was shown that *in vitro* cytotoxicity data from the stearoyl gemcitabine nanoparticles couldn't be used to predict their *in vivo* anti-tumor activity. PEGylation of the nanoparticles significantly prolonged their blood circulation time and increased the accumulation of the nanoparticles into tumor tissues, but did not further enhance the anti-tumor activity.

2.6 References

1. Burris, H.A., 3rd, et al., Improvements in survival and clinical benefit with gemcitabine as first-line therapy for patients with advanced pancreas cancer: a randomized trial. J Clin Oncol, 1997. **15**(6): p. 2403-13.

2. Philip, P.A., Novel targets for pancreatic cancer therapy. Surg Oncol Clin N Am, 2010. **19**(2): p. 419-29.

3. Kleeff, J., et al., Pancreatic cancer: from bench to 5-year survival. Pancreas, 2006. **33**(2): p. 111-8.

4. Bergman, A.M., H.M. Pinedo, and G.J. Peters, Determinants of resistance to 2',2'-difluorodeoxycytidine (gemcitabine). Drug Resist Updat, 2002. **5**(1): p. 19-33.

5. Immordino, M.L., et al., Preparation, characterization, cytotoxicity and pharmacokinetics of liposomes containing lipophilic gemcitabine prodrugs. J Control Release, 2004. **100**(3): p. 331-46.

6. Pappas, P., et al., Coadministration of oxaliplatin does not influence the pharmacokinetics of gemcitabine. Anticancer Drugs, 2006. **17**(10): p. 1185-91.

7. Reid, J.M., et al., Phase I trial and pharmacokinetics of gemcitabine in children with advanced solid tumors. J Clin Oncol, 2004. **22**(12): p. 2445-51.

8. Abbruzzese, J.L., et al., A phase I clinical, plasma, and cellular pharmacology study of gemcitabine. J Clin Oncol, 1991. **9**(3): p. 491-8.

9. Bergman, A.M., et al., Antiproliferative activity, mechanism of action and oral antitumor activity of CP-4126, a fatty acid derivative of gemcitabine, in in vitro and in vivo tumor models. Invest New Drugs, 2010.

10. Brusa, P., et al., Antitumor activity and pharmacokinetics of liposomes containing lipophilic gemcitabine prodrugs. Anticancer Res, 2007. **27**(1A): p. 195-9.

11. Arias, J.L., L.H. Reddy, and P. Couvreur, Polymeric nanoparticulate system augmented the anticancer therapeutic efficacy of gemcitabine. J Drug Target, 2009. **17**(8): p. 586-98.

12. Wang, C.X., et al., Antitumor effects of polysorbate-80 coated gemcitabine polybutylcyanoacrylate nanoparticles in vitro and its pharmacodynamics in vivo on C6 glioma cells of a brain tumor model. Brain Res, 2009. **1261**: p. 91-9.

13. Gang, J., et al., Magnetic poly epsilon-caprolactone nanoparticles containing Fe3O4 and gemcitabine enhance anti-tumor effect in pancreatic cancer xenograft mouse model. J Drug Target, 2007. **15**(6): p. 445-53.

14. Stella, B., et al., Encapsulation of gemcitabine lipophilic derivatives into polycyanoacrylate nanospheres and nanocapsules. Int J Pharm, 2007. **344**(1-2): p. 71-7.

15. Reddy, L.H., et al., A new nanomedicine of gemcitabine displays enhanced anticancer activity in sensitive and resistant leukemia types. J Control Release, 2007. **124**(1-2): p. 20-7.

16. Arias, J.L., L.H. Reddy, and P. Couvreur, Magnetoresponsive squalenoyl gemcitabine composite nanoparticles for cancer active targeting. Langmuir, 2008. **24**(14): p. 7512-9.

17. Sloat, B.R., et al., Strong antibody responses induced by protein antigens conjugated onto the surface of lecithin-based nanoparticles. J Control Release, 2010. **141**(1): p. 93-100.

18.   Yanasarn, N., B.R. Sloat, and Z. Cui, Nanoparticles engineered from lecithin-in-water emulsions as a potential delivery system for docetaxel. Int J Pharm, 2009. **379**(1): p. 174-80.

19.   Cui, Z., F. Qiu, and B.R. Sloat, Lecithin-based cationic nanoparticles as a potential DNA delivery system. Int J Pharm, 2006. **313**(1-2): p. 206-13.

20.   Wade A, W.P.J., Handbook of Pharmaceutical Excipients (2nd Ed), 1994: p. 392-399.

21.   Guo Zw, Z. and J.M. Gallo, Selective Protection of 2',2'-Difluorodeoxycytidine (Gemcitabine). J Org Chem, 1999. **64**(22): p. 8319-8322.

22.   Chou, T.C. and P. Talalay, Quantitative analysis of dose-effect relationships: the combined effects of multiple drugs or enzyme inhibitors. Adv Enzyme Regul, 1984. **22**: p. 27-55.

23.   Le, U.M., et al., Tumor chemo-immunotherapy using gemcitabine and a synthetic dsRNA. Cancer Biol Ther, 2008. **7**(3): p. 440-7.

24.   Pratesi, G., et al., Therapeutic synergism of gemcitabine and CpG-oligodeoxynucleotides in an orthotopic human pancreatic carcinoma xenograft. Cancer Res, 2005. **65**(14): p. 6388-93.

25.   Milas, L., et al., CpG oligodeoxynucleotide enhances tumor response to radiation. Cancer Res, 2004. **64**(15): p. 5074-7.

26.   Davies, B. and T. Morris, Physiological parameters in laboratory animals and humans. Pharm Res, 1993. **10**(7): p. 1093-5.

27.   Zhang, Y., et al., PKSolver: An add-in program for pharmacokinetic and pharmacodynamic data analysis in Microsoft Excel. Comput Methods Programs Biomed, 2010. **99**(3): p. 306-14.

28.   Garcia-Manteiga, J., et al., Nucleoside transporter profiles in human pancreatic cancer cells: role of hCNT1 in 2',2'-difluorodeoxycytidine- induced cytotoxicity. Clin Cancer Res, 2003. **9**(13): p. 5000-8.

29.   Romberg, B., W.E. Hennink, and G. Storm, Sheddable coatings for long-circulating nanoparticles. Pharm Res, 2008. **25**(1): p. 55-71.

Chapter 3: EGFR-targeted Stearoyl Gemcitabine Nanoparticles Show Enhanced Anti-tumor Activity

Contributing authors:

Brian R. Sloat, Dharmika Lansakara-P, Amit Kumar, Bertha Rodriguez, Kaoru Kiguchi, John J. DiGiovanni, and Zhengrong Cui.

3.1   Abstract

Previously, it was shown that a novel 4-(N)-stearoyl gemcitabine nanoparticle formulation was more effective than gemcitabine hydrochloride in controlling the growth of model mouse or human tumors pre-established in mice. In the present study, the feasibility of targeting the stearoyl gemcitabine nanoparticles (GemC18-NPs) into tumor cells that over-express epidermal growth factor receptor (EGFR) to more effectively control tumor growth was evaluated. EGFR is over-expressed in a variety of tumor cells, and EGF is a known natural ligand of EGFR. Recombinant murine EGF was conjugated onto the GemC18-NPs. The ability of the EGF to target the GemC18-NPs to human breast adenocarcinoma cells that expressed different levels of EGFR was evaluated in vitro and in vivo. In culture, the extent to which the EGF-conjugated GemC18-NPs were taken up by tumor cells was correlated to the EGFR density on the tumor cells, whereas the uptake of untargeted GemC18-NPs exhibited no difference among those same cell lines. The relative cytotoxicity of the EGF-conjugated GemC18-NPs to tumor cells in culture was correlated to EGFR expression as well. *In vivo*, EGFR-over-expressing MDA-MB-468 tumors in mice treated with the EGF-conjugated GemC18-NPs grew significantly slower than in mice treated with untargeted GemC18-NPs, likely due to that the EGF-GemC18-NPs were more anti-proliferative, anti-angiogenic, and pro-apoptotic.

Fluorescence intensity data from *ex vivo* imaging showed that the EGF on the nanoparticles helped increase the accumulation of the GemC18-NPs into MDA-MB-468 tumors pre-established in mice by more than 2-fold as compared to the un-targeted GemC18-NPs. In conclusion, active targeting of the GemC18-NPs into EGFR-over-expressed tumors can further enhance their anti-tumor activity.

3.2   Introduction

Gemzar®, gemcitabine hydrochloride for injection, is approved for the treatment of pancreatic, breast, lung, and ovarian cancers [1]. Although extremely toxic to tumor cells in culture, there continues to be a need to improve the clinical outcomes of Gemzar® therapy, and there are reports showing that formulating gemcitabine into nanoparticles may be an effective approach to address this need [2-10]. Previously, we reported a novel gemcitabine nanoparticle formulation and demonstrated that the nanoparticles were more effective than gemcitabine hydrochloride (HCl) in controlling the growth of model mouse or human tumors in mice, clearly indicating that the in vivo efficacy of gemcitabine can be improved using nanoparticles [8]. The nanoparticle delivery system for gemcitabine was prepared from lecithin/glycerol monostearate (GMS)-in-water emulsions. Gemcitabine is highly water soluble; and thus, in order to incorporate it into the solid lipid nanoparticles, gemcitabine was lipophilized by conjugating a stearoyl group to its N-terminus to form 4-(N)-stearoyl gemcitabine (GemC18) [5]. The enhanced anti-tumor activity from the stearoyl gemcitabine nanoparticles (GemC18-NPs) was not simply due to the GemC18 because the same dose of GemC18 in Tween 20 micelles did not show any significant anti-tumor activity [8].

In the present study, the feasibility of further improving the anti-tumor activity of the stearoyl gemcitabine nanoparticles by actively targeting them into tumors was evaluated. It was hypothesized that conjugation of epidermal growth factor (EGF) as a ligand to EGF receptor (EGFR) on the surface of the stearoyl gemcitabine nanoparticles will increase the delivery of the nanoparticles into tumor (cells), and thus improve the resultant anti-tumor activity. Among the earliest growth factors characterized and sequenced, EGFR (a 170 kD endogenous cell surface glycoprotein) has been inherently tied with normal cellular function including cell proliferation, survival, adhesion, migration, and differentiation. More than ten ligands, including EGF, have been shown to exhibit strong receptor-ligand affinity towards EGFR [11]. Although EGFR is expressed in a variety of normal cell types at $\sim 1 \times 10^4$ per cell, there are numerous studies reporting the over-expression of EGFR in various tumor cells (i.e., 10–1000-fold greater than in normal cells) [12]. For example, it has been discovered that EGFR is over-expressed in 80–100% of human head and neck cancer cells, 14–91% of human breast cancer cells, and 30–50% of human pancreatic cancer cells [13]. Multiple EGFR targeting agents have been developed for cancer therapy (e.g., anti-EGFR MAb 225, ZD1839 (Iressa))[14] and [15], and the clinical efficacy of those EGFR targeting agents have been promising [16]. In the present study, the over-expressed EGFR was exploited as a target to more specifically deliver the GemC18-NPs into tumor cells by conjugating EGF onto the surface of the nanoparticles. Previously, EGF and antibodies against EGFR had been conjugated onto liposomes to successfully target them to EGFR-over-expressing tumor cells [17-19]. For example, it was shown that treatment of nude mice with EGFR-over-expressing A549 human non-small cell lung cancer cells with gemcitabine-incorporated liposomes surface-conjugated with monoclonal antibodies against EGFR more effectively inhibited the tumor growth than un-targeted liposomes [19]. Similarly, Arya et al. (2011)

reported that conjugation of anti-HER2, an antibody against human EGFR-2, onto gemcitabine–chitosan nanoparticles enhanced the anti-proliferative activity of the nanoparticles against HER2-expressing Mia PaCa-2 cells and PANC-1 tumor cells in culture [20].

3.3 Materials and Methods

3.3.1 Materials and Cell-lines

Gemcitabine HCl was from U.S. Pharmacopeia (Rockville, MD). Soy lecithin was from Alfa Aesar (Ward Hill, MA). Geleol™ (Glycerol-monostearate, GMS) was from Gattefosse Corp. (Paramus, NJ). The 1, 2-distearoyl-sn-glycero-3-phosphoethanolamine-N-[maleimide (polyethylene glycol)-2000] (DSPE-PEG(2000)-maleimide) and 1,2-dioleoyl-sn-glycero-3-phosphoethanolamine-N-(carboxyfluorescein) (ammonium salt) (DOPE-fluorescein) were from Avanti Polar Lipids, Inc. (Alabaster, AL). Ovalbumin (OVA), 3-(4, 5-dimethylthiazol-2-yl)-2, 5-diphenyltetrazolium bromide (MTT), poly-D-lysine hydrobromide, 2-iminothiolane hydrochloride (Traut's Reagent), and Tween 20 were from Sigma-Aldrich (St. Louis, MO). CBQCA Protein Quantification Kit, cell culture medium, fetal bovine serum (FBS), and antibiotics were from Invitrogen (Carlsbad, CA). Sephadex™ G-25 column (PD-10) was from GE Biosciences (Piscataway, NJ). Recombinant murine EGF was from Peprotech Inc. (Rocky Hills, NJ). Human breast adenocarcinoma cell lines, MDA-MB-468 (HTB-132), MDA-MB-231 (HTB-26), and MCF-7 (HTB-22) were from the American Type Culture Collection (ATCC, Rockville, MD). It was reported that those cells express 1×10^6, 2×10^5, and 1×10^4 EGFR per cell, respectively [21] and [22], and our RT-PCR data confirmed the differential expression as well (Rodriguez and Cui, unpublished data). All tumor cells

were grown in Dulbecco's modification of Eagle's medium (DMEM) supplemented with 10% FBS, 100 U/mL of penicillin, and 100 μg/mL of streptomycin.

3.3.2 Preparation and Characterization of EGFR-targeted Stearoyl Gemcitabine Nanoparticles

Recombinant murine EGF was conjugated onto nanoparticles by forming a stable thioether group. GemC18 and GemC18-containing nanoparticles (GemC18-NPs) were prepared as previously described [23]. Briefly, 3.5 mg of soy lecithin, 0.5 mg of GMS, 5 mg of GemC18, and 0.875 mg of DSPE-PEG (2000)-maleimide were placed into a 7 mL glass vial. One milliliter of water was added into the mixture, which was then maintained at 70–75 °C while stirring until the formation of homogeneous slurry. Tween 20 was added in a step-wise manner to achieve a final concentration of 1% (v/v). The resultant emulsions were allowed to stay at room temperature while stirring to form nanoparticles. To thiolate EGF, EGF was diluted into phosphate buffer saline (PBS, 0.1 M, pH 8.0) with ethylenediaminetetraacetic acid (EDTA, 5 mM), followed by the addition of Traut's reagent (2 mg/mL) and a 1 h incubation at room temperature. Thiolated EGF was purified/desalted using a Sephadex™ G-25 column and mixed with pre-prepared GemC18-NPs. The mixture was incubated overnight in a nitrogen-enriched atmosphere. Un-conjugated EGF was removed using a Sepharose® 4B column. The purified EGF-conjugated GemC18-NPs are named EGF-GemC18-NPs. As a control, OVA was conjugated onto the GemC18-NPs using the same procedure to prepare OVA-GemC18-NPs. To fluorescently label the nanoparticles, DOPE-fluorescein (0.95 mg) was included in the lipid mixture during the nanoparticle preparation. The concentration of the EGF and OVA in the nanoparticle preparations was determined using the CBQCA Protein Quantitation Kit following the manufacturer's instruction(s). The concentration of

the GemC18 in the final nanoparticle preparations was determined using Agilent high performance liquid chromatography (HPLC) with an Agilent ZORBAX Eclipse Plus C18 column (4.6 × 150 mm, 5 μm; Santa Clara, CA) after the nanoparticles were dissolved into tetrahydrofuran. The mobile phase was methanol (100%). The flow rate was 1 mL/min. The detection wavelength was 248 nm[5] and [8].

The particle size and zeta potential of the nanoparticles were determined using a Malvern Zetasizer® Nano ZS (Westborough, MA). The nanoparticles in suspension were stored in ambient condition for 20 days, and their particle sizes were measured every five days.

3.3.3 *In Vitro* Cellular Uptake Assay

MDA-MB-468, MDA-MB-231, or MCF-7 cells were seeded in 12-well plate (2×10^5 cells/well) (n = 6) and incubated at 37 °C, 5% CO_2 for 24 h. Cells were then incubated with fluorescein-labeled EGF-GemC18-NPs or fluorescein-labeled OVA-GemC18-NPs (50 μL) for 6 h at 37 °C, 5% CO_2, washed three times with PBS, and re-suspended in a cell lysis buffer (20 mM Tris, 100 mM NaCl, 1 mM EDTA, 0.5% Triton X-100). The 6 h incubation time was chosen based on data from previous studies [8] and [24]. The fluorescence intensity of the samples in a black bottom plate (Corning, NY) was measured at 492/518 nm using a BioTek Synergy®Multi-Mode Microplate Reader (Winooski, CT). To confirm that the uptake was mediated by the EGF-EGFR interaction, the cells were incubated with free EGF (0.1 mg/mL) for 1 h prior to the addition of the nanoparticles. Data are reported as the absolute fluorescence intensity values or the % of uptake, which was calculated using the following formula: % uptake = (fluorescence intensity value in the cell lysates)/(total fluorescence intensity value of the nanoparticles added into the cell culture).

3.3.4   Fluorescence Microscopy for the Detection of the Uptake of Nanoparticles

MDA-MB-468 or MCF-7 cells (2×10^5) were seeded on poly-D-lysine-coated glass cover slips and incubated in 6-well plates at 37 °C, 5% CO_2 for 24 h. After complete adherence, cells and cover slips were incubated with fluorescein-labeled EGF-GemC18-NPs or fluorescein-labeled OVA-GemC18-NPs for 6 h at 37 °C and 5% CO_2, washed three times with PBS, and fixed with paraformaldehyde (3% in PBS) for 20 min at room temperature. The cover slips were washed with PBS an additional three times and mounted onto ethanol-cleaned glass slides using Vectashield H-1200 with 4′,6-diamidino-2-phenylindole (DAPI) (Vector laboratories, Burlingame, CA). Cells were examined using an Olympus BX60 microscope (Center Valley, PA).

3.3.5   Flow Cytometry

MDA-MB-468, MDA-MB-231, and MCF-7 cells (1×10^6/well) were incubated with fluorescein-labeled EGF-GemC18-NPs or fluorescein-labeled OVA-GemC18-NPs for 6 h at 37 °C, 5% CO_2. Cells were washed three times with PBS, re-suspended in PBS, and analyzed using a BD FACSCalibur Flow Cytometer (San Jose, CA). Data was analyzed using the FlowJo Flow Cytometry Analysis software (Tree Star Inc., Ashland, OR).

3.3.6   *In Vitro* Cytotoxicity Assay

Cells (5000/well) were seeded in a 96-well plate and incubated overnight at 37 °C, 5% CO_2. Cells were then incubated in the presence of various concentrations of

EGF-GemC18-NPs, OVA-GemC18-NPs, or sterile PBS for 48 h. Cell viability was determined using an MTT assay following the manufacturer's instructions. OD570 nm and OD630 nm values were measured using a BioTek Synergy™ HT Multi-Mode Microplate Reader. To understand whether the cells underwent apoptosis after treatment with the GemC18-NPs, MDA-MB-468 cells (5×10^4) were incubated with EGF-GemC18-NPs or OVA-GemC18-NPs for 48 h, washed, stained using a Guava Nexin kit that contains annexin V and 7-amino actinomycin D (7-AAD) according to the manufacturer's protocol, and analyzed using a Guava Easycyte 8HT Flow Cytometry System (Millipore, Hayward, CA).

3.3.7 Evaluation of the *In Vivo* Anti-tumor Activity of the EGF-GemC18-NPs

National Institutes of Health guidelines for animal use and care were followed. Animal protocol was approved by the Institutional Animal Care and Use Committee at the University of Texas at Austin. Female athymic Nu/Nu mice (18–20 g) were from Charles River Laboratories (Wilmington, MA). MDA-MB-468 tumor cells (1×10^7 cells/mouse) were mixed with BD Matrigel™ (50:50, v/v) and subcutaneously injected in the right flank of the mice on day 0. On day 11, mice (n = 7, 5 for control) were randomized and injected intravenously (i.v.) via the tail vein with 200 μL of EGF-GemC18-NPs or OVA-GemC18-NPs in sterile mannitol (5%, w/v) or sterile mannitol alone as a negative control. Injection was repeated on days 17, 28, and 37. The dose of the GemC18 was about 860 μg per mouse per injection. Tumor growth and mouse survival was monitored. Tumor size was calculated based on the following equation: tumor diameter (mm) = (length × width)/2.

3.3.8 *Ex Vivo* Imaging Using IVIS® Spectrum

The biodistribution of EGF-GemC18-NPs and OVA-GemC18-NPs were evaluated in Nu/Nu mice with pre-established MDA-MB-468 tumors using an

IVIS® Spectrum from Caliper (Hopkinton, MA). When the tumor size reached 8–10 mm, fluorescein-labeled EGF-GemC18-NPs or fluorescein-labeled OVA-GemC18-NPs were injected intravenously via the tail vein into mice (n = 3). As a control, mice were injected with sterile mannitol (5%, w/v). Mice were euthanized 24 h later to collect tumor, heart, lung, liver, spleen, and kidney. Samples were imaged immediately on non-fluorescent black Strathmore Artagain paper (Neenah, WI). Region of interest (ROI) values were recorded using Living Image® software (ver. 4.0). Fluorescence intensity (total counts) was determined in a fixed, circular ROI and reported after normalizing to the weight of the tumors or organs.

To determine the half-lives of the EGF-GemC18-NPs and OVA-GemC18-NPs, healthy, tumor-free C57BL/6 mice were injected intravenously with fluorescein-labeled EGF-GemC18-NPs or fluorescein-labeled OVA-GemC18-NPs and euthanized 5 min, 3 h, 6 h, 12 h, or 24 h later to collect blood samples (500 μL/mouse), which were placed into a multi-well plate and imaged using the IVIS® Spectrum to determine the fluorescence intensity. Pharmacokinetic data were analyzed based on the fluorescence intensity values using the PK-Solver assuming a two-compartmental model [25].

3.3.9   Histology

Nu/Nu mice (n = 3) with pre-established MDA-MB-468 tumors were dosed (i.v.) with sterile mannitol, OVA-GemC18-NPs, or EGF-GemC18-NPs 20, 30, 40, and 53 days after the tumor cell injection. On day 54, mice were injected intraperitoneally with 5-bromo-2′-deoxyuridine (BrdU, 100 μg/g body weight) in sterile PBS and euthanized 30 min later. Tumor tissues were collected, fixed in formalin, embedded, sectioned, and stained at the University of Texas MD Anderson Cancer Center Science Park Research Division (Smithville, TX) with antibodies against BrdU, CD31, and caspase 3 as markers

of cell proliferation, angiogenesis, and apoptosis, respectively. Slides were examined under a bright-field microscope. In addition, a slide was also stained with anti-EGFR-Alexa fluor 488 (Millipore, diluted 1/500) and DAPI, and then examined using a Leica TCS SP5 X Supercontinuum confocal microscope (Buffalo Grove, IL).

3.3.10 Statistical Analysis

Statistical analyses were completed by performing analysis of variance (ANOVA) followed by Fisher's protected least significant procedure. Mouse survival curves were analyzed using the Mantel–Cox log-rank method (GraphPad Prism®). A p-value of ≤ 0.05 was considered significant.

3.4 Results and Discussion

3.4.1 Preparation and Characterization of EGF-GemC18-NPs and OVA-GemC18-NPs

The EGFR-targeted GemC18-NPs were prepared by conjugating murine EGF onto pre-prepared GemC18-NPs. It was shown that murine EGF and human EGF bind to human EGFR with similar affinity at pH 7.4, and they have similar biological activity, but murine EGF is preferred due to the absence of lysine residues, which minimizes cross reaction [26] and [27]. As a control, OVA was also conjugated onto the GemC18-NPs to generate OVA-GemC18-NPs. OVA was used as a control to EGF because the isoelectric point (pI) of OVA is similar to that of the murine EGF (pI = 4.6) [28] and [29], and there is no report showing that OVA is a ligand to EGFR. Data that will be presented later also demonstrated that OVA did not affect the EGF-EGFR interaction.

The particle size, polydispersity index, and zeta potential of the EGF-GemC18-NPs and OVA-GemC18-NPs are shown in Table 1. Also shown in Table 1 are the final

concentrations of GemC18 and EGF (or OVA) in the EGF-GemC18-NPs and OVA-GemC18-NPs. Statistical analyses did not reveal any significant difference between the EGF-GemC18-NPs and OVA-GemC18-NPs in those parameters, except the EGF or OVA protein concentration, which was likely due to the difference in the molecular weights of OVA and murine EGF. In a short 20-day stability study, when the nanoparticles were stored in ambient condition in an aqueous suspension, the particle size of both EGF-GemC18-NPs and OVA-GemC18-NPs did not change (data not shown).

3.4.2 *In Vitro* Uptake of the EGF-GemC18-NPs by Tumor Cells Expressing Different Levels of EGFR

Three human breast adenocarcinoma cell lines, MDA-MB-468, MDA-MB-231, and MCF-7, were used in the *in vitro* uptake studies because they express different levels of EGFR per cell (1×10^6, 2×10^5 and 1×10^4, respectively) [21] and [22]. As shown in Fig. 3.1A, after 6 h of incubation, the cellular uptakes of the OVA-GemC18-NPs by the three different cell lines were not different (p = 0.71, ANOVA). However, the extent of the uptake of the EGF-GemC18-NPs by the same cell lines was dependent on the number of EGFR per cell (Fig. 3.1A). In other words, the MDA-MB-468 tumor cells took up more EGF-GemC18-NPs than the MDA-MB-231 cells, and the MDA-MB-231 cells took up more EGF-GemC18-NPs than the MCF-7 cells (Fig. 3.1A). Data in Fig. 1B showed that pre-incubation of the MDA-MB-468 cells with free EGF for 1 h significantly inhibited the cellular uptake of the EGF-GemC18-NPs, but not the OVA-GemC18-NPs, by the MDA-MB-468 cells, demonstrating that the uptake of EGF-GemC18-NPs was mediated by the EGF–EGFR interaction. This is in agreement with Blessing et al., who reported that the competition of free EGF with EGF-containing plasmid DNA-

49

polyethylenimine complexes resulted in decreased transfer of the plasmid into EGFR-over-expressing cells [30].

Flow cytometry and fluorescence microscopy were also employed to confirm that the uptake of the EGF-GemC18-NPs, but not the OVA-GemC18-NPs, was dependent on the density of the EGFR on tumor cells. As shown by the right-shifting of the fluorescein-positive peak in Fig. 3.2A, the uptake of the EGF-GemC18-NPs by the MDA-MB-468 cells was much more extensive than that of the OVA-GemC18-NPs, but it was only slightly different in the MDA-MB-231 and MCF-7 cells. Moreover, as indicated by the green fluorescence intensity in the micrographs in Fig. 3.2B, after 6 h of incubation, the uptake of the EGF-GemC18-NPs by the MDA-MB-468 cells was significantly greater than the uptake of the OVA-GemC18-NPs. However, the uptake of both nanoparticles by the MCF-7 cells was weak (Fig. 3.2B). The microscopic and flow cytometric data also showed that there is a slight increase in the uptake of the EGF-GemC18-NPs over the OVA-GemC18-NPs by MCF-7 cells (Fig. 3.2), which was expected because the MCF-7 cells express EGFR at a level of 1×10^4 per cell [21]. Taken together, data in Fig. 3.1 and Fig. 3.2 showed that the murine EGF conjugated onto the GemC18-NPs helped facilitate the uptake of nanoparticles by EGFR-expressing tumor cells through the EGF-EGFR interaction.

3.4.3   Correlation of the *In Vitro* Cytotoxicity of the EGF-GemC18-NPs with the Density of the EGFR on Tumor Cells

The cytotoxicities of the EGF-GemC18-NPs and OVA-GemC18-NPs in MDA-MB-468, MDA-MB-231, and MCF-7 cells were evaluated and compared. As expected, in all three cell lines, the EGF-GemC18-NPs were more cytotoxic than the OVA-GemC18-NPs (Fig. 3.3A). Moreover, it appeared that the extent to which the EGF-

GemC18-NPs were more cytotoxic than the OVA-GemC18-NPs was dependent on the density of the EGFR on the cells (Fig. 3.3A). In other words, the difference in the cytotoxicities between the EGF-GemC18-NPs and the OVA-GemC18-NPs was much greater in the MDA-MB-468 cells than in the MDA-MB-231 cells; and it was greater in the MDA-MB-231 cells than in the MCF-7 cells (Fig. 3.3A). Finally, data in Fig. 3.3B showed that the tumors cells treated with the GemC18-NPs underwent apoptosis as well. The cytotoxicity data are in agreement with the cell uptake data shown in Fig. 3.1 and Fig. 3.2. It is likely that the high density of EGFR on the surface of the MDA-MB-468 cells allowed the cells to take up more EGF-GemC18-NPs. The more EGF-GemC18-NPs that are internalized into the cells, the more cytotoxicity is expected.

3.4.4   The EGFR-targeting GemC18-NPs More Effectively Controlled the Growth of Pre-established EGFR-over-expressing Tumors in Mice

To investigate whether the EGF-GemC18-NPs are more cytotoxic than the OVA-GemC18-NPs to EGFR-over-expressing tumors *in vivo*, their ability to control tumor growth *in vivo* was evaluated and compared in mice with pre-established MDA-MB-468 tumors. As shown in Fig. 3.4A, tumors in mice that were treated with the EGF-GemC18-NPs grew significantly slower than in mice that were treated with the OVA-GemC18-NPs. From day 45 to day 50, the mean diameter of tumors in mice treated with the EGF-GemC18-NPs was significantly smaller than in mice treated with the OVA-GemC18-NPs ($p < 0.05$) (Fig. 3.4A). Statistical comparison of the size of tumors in mice treated with EGF-GemC18-NPs and that in mice treated with OVA-GemC18-NPs beyond day 50 was not carried out due to the death of mice in both groups around day 50. In fact, it seemed that the 4 doses of OVA-GemC18-NPs simply inhibited the growth of the MDA-MB-468 tumors for about 40 days. When the treatment was stopped — last dose on day 37, the

tumors started to grow again (Fig. 3.4A). In contrast, when the treatment with the EGF-GemC18-NPs was terminated, the mean diameter of the tumors continued to decrease (Fig. 3.4A). Mice that were treated with the EGF-GemC18-NPs also survived longer than those treated with the OVA-GemC18-NPs (Fig. 3.4B). The median survival time for mice that were treated with the EGF-GemC18-NPs was 160 days, only 69 days for mice treated with the OVA-GemC18-NPs. A comparison of the survival curves of the EGF-GemC18-NPs and OVA-GemC18-NPs revealed a p value of 0.053, which would have been smaller (i.e., 0.023) if one of the mice that were treated with the OVA-GemC18-NPs did not accidently pass away during the i.v. injection of the nanoparticles on day 37. Nonetheless, data in Fig. 3.4 showed that the EGF-conjugated GemC18-NPs were more effective than the control GemC18-NPs in controlling the growth of EGFR-over-expressing tumors *in vivo*. It is worth mentioning that gemcitabine HCl at the molar equivalent dose (28.3 mg/kg) caused serious toxicity to nude mice with MDA-MB-468 tumors because mice that were treated with gemcitabine HCl did not survive as long as mice that were injected with sterile mannitol (Fig. 3.7).

For immunohistology analysis, another mouse study was carried out by treating MDA-MB-468 tumor-bearing mice with sterile mannitol, OVA-GemC18-NPs, or EGF-GemC18-NPs 20, 30, 40, and 53 days after tumor cell injection. Similar to what was shown in Fig. 3.4A, tumors in mice that were treated with the EGF-GemC18-NPs grew significantly slower than in mice that were treated with the OVA-GemC18-NPs (Fig. 3.4C). Tumors were harvested on day 54 for analysis. Anti-BrdU staining showed that cell proliferation was less extensive in tumors in mice that were treated with the GemC18-NPs (Fig. 3.5A). More importantly, BrdU positive staining was significantly less extensive in tumors in mice that were treated with the EGF-GemC18-NPs than in tumors in mice that were treated with the OVA-GemC18-NPs (Figs. 3.5A, B). Anti-

CD31 staining, a marker of endothelial cells, revealed extensive vascularization in tumors in mice that were treated with sterile mannitol and to a less extent in tumors in mice that were treated with OVA-GemC18-NPs (Fig. 3.5A). However, CD31 positive staining was very rare in tumors in mice that were treated with EGF-GemC18-NPs (Fig. 3.5A). Finally, caspase3 positive staining, an apoptosis marker, was extensive in tumors in mice that were treated with the EGF-GemC18-NPs, but significantly less extensive in tumors in mice that were treated with OVA-GemC18-NPs or sterile mannitol (Figs. 3.5A, C). Data in Fig. 3.5D (data not shown) showed that almost all the tumor cells were EGFR positive, because almost all cell nuclei (DAPI positive) were surrounded by EGFR positive staining. Therefore, it is likely that the caspase 3 positive cells in Fig. 3.5A were EGFR positive. Taken together, it appeared that, compared to the OVA-GemC18-NPs, the EGFR-targeted EGF-GemC18-NPs were more anti-proliferative, anti-angiogenic, and pro-apoptotic, which may explain why the EGF-GemC18-NPs were more effective than the OVA-GemC18-NPs in controlling the growth of the MDA-MB-468 tumors as shown in Fig. 3.4.

3.4.5   The EGF on the EGF-GemC18-NPs Increased the Accumulation of the Nanoparticles in Tumors in Mice

To evaluate the biodistribution of the EGF-GemC18-NPs and OVA-GemC18-NPs in mice, fluorescein-labeled nanoparticles were injected (i.v.) into nude mice with pre-established MDA-MB-468 tumors with an average diameter of 7–10 mm. Twenty four hours later, mice were euthanized to harvest tumor, lung, liver, spleen, kidney, and heart, and the fluorescence intensity in them were determined using an IVIS® Spectrum. It was reported that the fluorescence intensity determined in ex vivo imaging is an accurate reflection of fluorescence-labeled nanoparticles accumulated inside organs due

to the deep penetration in the near-infrared region and negligible auto-fluorescence in ex vivo organs [31]. Shown in Fig. 3.6A are the fluorescence images of different organs and tumor tissues. The values of the fluorescence intensity, after normalization to tumor or organ weights, are shown in Fig. 3.6B. The fluorescence intensity in tumors in mice that were treated with the EGF-GemC18-NPs was more than 2-fold greater than that in tumors in mice that were treated with the OVA-GemC18-NPs (p = 0.0003), clearly demonstrating that the EGF on the EGF-GemC18-NPs enhanced the accumulation of the EGF-GemC18-NPs into EGFR-over-expressing tumors. It is noticed that the fluorescence intensity in the livers in mice that were injected with the EGF-GemC18-NPs tended to be higher than that in mice that were injected with the OVA-GemC18-NPs (Fig. 3.6A), which may be explained by the fact that the EGFR expression is slightly higher in cells in the liver and kidney (i.e., 1×10^5 EGFR/cell). Due to the variations in the size (or weight) of the organs from different mice, the fluorescence intensity values reported in Fig. 3.6B were normalized by organ weight. Interestingly, the fluorescence intensity values in livers after normalizing to weight were no longer significantly different in mice that were injected with EGF-GemC18-NPs or OVA-GemC18-NPs (Fig. 3.6B).

Shown in Fig. 3.6C are the kinetics of the fluorescence intensity in the blood samples in healthy C57BL/6 mice injected with fluorescein-labeled EGF-GemC18-NPs or fluorescein-labeled OVA-GemC18-NPs, and there appears to be no difference between those two nanoparticle formulations. In fact, the half-lives of the EGF-GemC18-NPs and the OVA-GemC18-NPs at the elimination phase were not different (5.9 ± 2 h vs. 6.2 ± 1.5 h, respectively, p = 0.86). The half-lives of the EGF-GemC18-NPs and the OVA-GemC18-NPs have the potential to be significantly increased, because the original GemC18-NPs exhibited a half-life of around 24 h at the elimination phase [8]. Conjugation of the EGF or the OVA to the terminal of the PEG chains on the GemC18-

NPs was likely responsible for the shorter half-life observed. It is known that the ability of the PEG to extend the blood circulation time of a drug carrier is related to parameters such as the amount and the molecular weight of the PEG [32]. Therefore, future research efforts are underway to examine the feasibility of extending the half-life of the EGF-GemC18-NPs by increasing the amount of PEG(2000) in the formulation or using longer PEG molecules. The inclusion of certain percent of PEG(2000) that lacks the maleimide group, and thus does not allow the conjugation of the EGF protein, is expected to help as well.

As aforementioned, Gemzar® is commonly used as a single agent or in combination with additional anti-cancer drugs to treat pancreatic, breast, and lung cancers. Although relatively efficacious, there is still room to improve the anti-tumor activity of the gemcitabine HCl for injection. Data from several previous studies showed that formulating gemcitabine or its derivatives into nanoparticles (e.g., liposomes, polymeric nanoparticles, solid lipid nanoparticles) could potentially improve the resultant anti-tumor activity in vivo [2-10]. Previously, our group reported that change of the gemcitabineformulation from the gemcitabine HCl solution to a stearoyl gemcitabine in solid lipid nanoparticles significantly improved the resultant anti-tumor activity [8], and the data in the present study clearly demonstrated that further surface modification of the nanoparticles by conjugating EGF as a ligand to actively target the GemC18-NPs to tumor cells significantly increased the anti-tumor activity of the GemC18-NPs against the EGFR-over-expressing MDA-MB-468 tumors in mice (Fig. 3.4), very likely due to the EGF's ability to increase the accumulation of the EGF-GemC18-NPs into the MDA-MB-468 tumors *in vivo* (Fig. 3.6). It remains unknown to what extent the EGF on the GemC18-NPs also increased the uptake or internalization of the GemC18-NPs by the tumor cells in tumor tissues. Data from a previous study showed

that anti-HER2 antibody targeting of long-circulating lipidic nanoparticles increased the cellular uptake of the nanoparticles by the tumor cells in animal models, although they did not increase tumor localization (accumulation) [33]. Nonetheless, it is clear that the in vivo anti-tumor efficacy of the gemcitabine can be improved by formulating it into a tumor-targeting nanoparticle formulation.

The nanoparticles used in the present study were prepared from lecithin/GMS-in-water emulsions. Lecithin is a complex mixture of phosphatidylcholine, phosphatidylethanolamine, phosphatidylserine, phosphatidylinositol and other substances such as triglycerides and fatty acids. It is generally regarded as safe (GRAS) and accepted in the FDA Inactive Ingredients Guide for parenterals [34]. GMS is used in a variety of pharmaceutical applications and is GRAS listed as well [34]. Tween 20 was used in the nanoparticle preparation as an emulsifier. Tween 20 is also GRAS listed and included in the FDA Inactive Ingredients Guide for parenterals [34]. Therefore, it is expected that the nanoparticles have a favorable toxicity profile, and data from our preliminary toxicity studies are promising. For example, it was previously shown that the GemC18-NPs did not induce detectable acute or sub-acute liver toxicity when injected intravenously into mice [8]. Similar nanoparticles did not cause any significant red blood cell lysis or platelet aggregation [24]. Moreover, in a 1.5-year study, the pathological and histological parameters of mice that received three doses of similar nanoparticles by subcutaneous injection were evaluated, and an examination by a board-certified veterinary pathologist did not reveal any significant difference between the treated and untreated mice (Sloat and Cui, unpublished data). Therefore, the possibility exists for the translation of these GemC18-NPs and/or the EGF-GemC18-NPs from bench to clinic as a novel and more efficacious gemcitabine formulation. Similar alternative GemC18 nanoparticle

56

formulations may also be developed to improve the clinical outcome of gemcitabine therapy.

The EGFR was chosen as the target to actively deliver the GemC18-NPs into tumors in the present study. The majority of the normal cells express EGFR at 1×10^4 per cell, but EGFR is over-expressed in a variety of cancer cells [35]. In case targeting EGFR is not feasible, alternative targets including transferrin receptors, folate receptors, or vascular cell adhesion molecule-1 (VCAM-1) may be utilized [36-38]. Other tumor-specific ligands may be identified using phage display as well.

3.5   Conclusions

It was previously shown that formulating a stearoyl gemcitabine derivative into nanoparticles significantly improved the resultant anti-tumor activity. Data in the present study showed that the anti-tumor activity of stearoyl gemcitabine nanoparticles can be further improved by actively targeting them into tumors.

3.6 References

1.   Barton-Burke, M., *Gemcitabine: a pharmacologic and clinical overview*. Cancer Nurs, 1999. **22**(2): p. 176-83.

2.   Arias, J.L., L.H. Reddy, and P. Couvreur, *Polymeric nanoparticulate system augmented the anticancer therapeutic efficacy of gemcitabine*. J Drug Target, 2009. **17**(8): p. 586-98.

3.   Arias, J.L., L.H. Reddy, and P. Couvreur, *Superior preclinical efficacy of gemcitabine developed as chitosan nanoparticulate system*. Biomacromolecules, 2011. **12**(1): p. 97-104.

4.   Celano, M., et al., *Cytotoxic effects of gemcitabine-loaded liposomes in human anaplastic thyroid carcinoma cells*. BMC Cancer, 2004. **4**: p. 63.

5.   Immordino, M.L., et al., *Preparation, characterization, cytotoxicity and pharmacokinetics of liposomes containing lipophilic gemcitabine prodrugs*. J Control Release, 2004. **100**(3): p. 331-46.

6.   Jantscheff, P., et al., *Anti-metastatic effects of liposomal gemcitabine in a human orthotopic LNCaP prostate cancer xenograft model*. Clin Exp Metastasis, 2009. **26**(8): p. 981-92.

7.   Paolino, D., et al., *Gemcitabine-loaded PEGylated unilamellar liposomes vs GEMZAR: biodistribution, pharmacokinetic features and in vivo antitumor activity*. J Control Release, 2010. **144**(2): p. 144-50.

8.   Sloat, B.R., et al., *In vitro and in vivo anti-tumor activities of a gemcitabine derivative carried by nanoparticles*. Int J Pharm, 2011.

9.   Stella, B., et al., *Encapsulation of gemcitabine lipophilic derivatives into polycyanoacrylate nanospheres and nanocapsules*. Int J Pharm, 2007. **344**(1-2): p. 71-7.

10.   Wang, C.X., et al., *Antitumor effects of polysorbate-80 coated gemcitabine polybutylcyanoacrylate nanoparticles in vitro and its pharmacodynamics in vivo on C6 glioma cells of a brain tumor model*. Brain Res, 2009. **1261**: p. 91-9.

11.   Byrne, J.D., T. Betancourt, and L. Brannon-Peppas, *Active targeting schemes for nanoparticle systems in cancer therapeutics*. Adv Drug Deliv Rev, 2008. **60**(15): p. 1615-26.

12.   LeMaistre, C.F., et al., *Targeting the EGF receptor in breast cancer treatment*. Breast Cancer Res Treat, 1994. **32**(1): p. 97-103.

13.   Klijn, J.G., et al., *The clinical significance of epidermal growth factor receptor (EGF-R) in human breast cancer: a review on 5232 patients*. Endocr Rev, 1992. **13**(1): p. 3-17.

14.   Baselga, J., *Monoclonal antibodies directed at growth factor receptors*. Ann Oncol, 2000. **11 Suppl 3**: p. 187-90.

15.   Ranson, M., et al., *ZD1839, a selective oral epidermal growth factor receptor-tyrosine kinase inhibitor, is well tolerated and active in patients with solid, malignant tumors: results of a phase I trial*. J Clin Oncol, 2002. **20**(9): p. 2240-50.

16.   Ciardiello, F. and G. Tortora, *Epidermal growth factor receptor (EGFR) as a target in cancer therapy: understanding the role of receptor expression and other molecular determinants that could influence the response to anti-EGFR drugs*. Eur J Cancer, 2003. **39**(10): p. 1348-54.

17.   Kullberg, E.B., M. Nestor, and L. Gedda, *Tumor-cell targeted epiderimal growth factor liposomes loaded with boronated acridine: uptake and processing*. Pharm Res, 2003. **20**(2): p. 229-36.

18.   Mamot, C., et al., *Epidermal growth factor receptor (EGFR)-targeted immunoliposomes mediate specific and efficient drug delivery to EGFR- and EGFRvIII-overexpressing tumor cells*. Cancer Res, 2003. **63**(12): p. 3154-61.

19.   Kim, I.Y., et al., *Antitumor activity of EGFR targeted pH-sensitive immunoliposomes encapsulating gemcitabine in A549 xenograft nude mice*. J Control Release, 2009. **140**(1): p. 55-60.

20.   Arya, G., et al., *Enhanced antiproliferative activity of Herceptin (HER2)-conjugated gemcitabine-loaded chitosan nanoparticle in pancreatic cancer therapy*. Nanomedicine, 2011.

21.   Reilly, R.M., et al., *111In-labeled EGF is selectively radiotoxic to human breast cancer cells overexpressing EGFR*. J Nucl Med, 2000. **41**(3): p. 429-38.

22.   Walker, R.A. and S.J. Dearing, *Expression of epidermal growth factor receptor mRNA and protein in primary breast carcinomas*. Breast Cancer Res Treat, 1999. **53**(2): p. 167-76.

23.   Sloat, B.R., et al., *Strong antibody responses induced by protein antigens conjugated onto the surface of lecithin-based nanoparticles*. J Control Release, 2010. **141**(1): p. 93-100.

24.   Yanasarn, N., B.R. Sloat, and Z. Cui, *Nanoparticles engineered from lecithin-in-water emulsions as a potential delivery system for docetaxel*. Int J Pharm, 2009. **379**(1): p. 174-80.

25.   Zhang, Y., et al., *PKSolver: An add-in program for pharmacokinetic and pharmacodynamic data analysis in Microsoft Excel*. Comput Methods Programs Biomed, 2010. **99**(3): p. 306-14.

26.   French, A.R., et al., *Intracellular trafficking of epidermal growth factor family ligands is directly influenced by the pH sensitivity of the receptor/ligand interaction*. J Biol Chem, 1995. **270**(9): p. 4334-40.

27.   Spitzer, E., et al., *Binding properties of biotinylated epidermal growth factor to its receptor on cultured cells and tissue sections*. J Cell Biochem, 1989. **41**(2): p. 47-56.

28.   Carpenter, G. and S. Cohen, *Epidermal growth factor*. Annu Rev Biochem, 1979. **48**: p. 193-216.

29.   Kurihara, K., et al., *Incorporation of impurity to a tetragonal lysozyme crystal*. Journal of Crystal Growth, 1999. **196**(2-4): p. 285-290.

30.   Blessing, T., et al., *Different strategies for formation of pegylated EGF-conjugated PEI/DNA complexes for targeted gene delivery*. Bioconjug Chem, 2001. **12**(4): p. 529-37.

31.   Gao, J., et al., *Ultrasmall near-infrared non-cadmium quantum dots for in vivo tumor imaging*. Small, 2010. **6**(2): p. 256-61.

32.   Francis, G.E., et al., *Polyethylene glycol modification: relevance of improved methodology to tumour targeting*. J Drug Target, 1996. **3**(5): p. 321-40.

33.   Kirpotin, D.B., et al., *Antibody targeting of long-circulating lipidic nanoparticles does not increase tumor localization but does increase internalization in animal models*. Cancer Res, 2006. **66**(13): p. 6732-40.

34.   Wade A, W.P.J., Handbook of Pharmaceutical Excipients (2nd Ed), 1994: p. 392-399.

35.   Herbst, R.S. and D.M. Shin, *Monoclonal antibodies to target epidermal growth factor receptor-positive tumors: a new paradigm for cancer therapy*. Cancer, 2002. **94**(5): p. 1593-611.

36.   Singh, M., *Transferrin As A targeting ligand for liposomes and anticancer drugs*. Curr Pharm Des, 1999. **5**(6): p. 443-51.

37.   Zhang, Y. and J. Zhang, *Surface modification of monodisperse magnetite nanoparticles for improved intracellular uptake to breast cancer cells*. J Colloid Interface Sci, 2005. **283**(2): p. 352-7.

38.   Dienst, A., et al., *Specific occlusion of murine and human tumor vasculature by VCAM-1-targeted recombinant fusion proteins*. J Natl Cancer Inst, 2005. **97**(10): p. 733-47.

Chapter 4: Anti-tumor Efficacy of Oral 4-(N)-Stearoyl Gemcitabine Nanoparticles

4.1 Abstract

Previously, we reported the development of novel gemcitabine nanoparticles (GemC18-NPs) by incorporating 4-(N)-stearoyl gemcitabine into solid lipid nanoparticles. When administered intravenously, the GemC18-NPs were more effective than gemcitabine alone in controlling the growth of various human and mouse tumors in mouse models. In the present study, we evaluated the antitumor activity of the GemC18-NPs when given orally. GemC18-NPs were prepared from lecithin/glyceryl monostearate-in-water emulsions, as previously described. The stability of the GemC18-NPs in simulated gastric and intestinal fluid was evaluated and found to be relatively stable in both environments. Gemcitabine plasma pharmacokinetic parameters (e.g., Tmax, Cmax, $t_{1/2}$, AUC) were determined using healthy mice after intravenous or oral administration. The antitumor activity of the GemC18-NPs against model mouse lung tumors (TC-1) in mice was evaluated after the nanoparticles were given orally or intravenously. Oral GemC18-NPs significantly inhibited TC-1 tumor growth, whereas oral dosing with GemC18-in-vegetable oil (nanoparticle-free) did not. Tumor-bearing mice that were treated with oral GemC18-NPs also survived longer than with oral GemC18-in-vegatable oil (mean survival time, 51 d vs. 31 d). In addition, the oral GemC18-in-vegetable oil seemed to be toxic to mice. The relative oral bioavailability of GemC18 given as GemC18-NPs was ~70%. Taken together, the oral stearoyl gemcitabine nanoparticles showed strong antitumor activity.

4.2   Introduction

Gemcitabine (Gemzar®) is a chemotherapeutic drug indicated for use in a variety of cancers including, ovarian, breast, non-small lung, and pancreatic cancer. Currently, gemcitabine is formulated and FDA approved for intravenous infusions of 1,000 – 1,250 mg/m^2 on days 1 and 8 of a 21 d cycle, or days 1, 8, and 15 for a 28 d cycle [1-3].

Due to the aggressive biologic nature of some cancers, such as pancreatic cancer with a median 5-year survival rate less than 4%, improving the patient's quality of life is becoming an increasing central consideration to improve overall therapy. A research study by Liu et al. found that ~90% of 103 metastatic cancer patients indicated a preference for orally administered chemotherapy, of which relating to convenience (57%), avoiding difficulties in intravenous access lines (55%), and preference for a controlled, personalized therapy environment (33%) [3-4]. Simply put, most patients would prefer an orally formulated therapeutic. From a financial perspective, hospital administration costs further propagate the desire to formulate oral chemotherapeutics. Traditionally, medical costs for cancer therapy include: hospitalization, physician fees, salaries of nurses and technical support personnel, intravenous infusion equipment supply costs, administration supply product fees, and overhead charges (capital equipment, regulatory compliance costs, and liability insurance costs) [5]. The National Institute of Health estimated an overall cost for cancer in the United States to be ~$226.8 billion. Furthermore, between 1991 and 1996, a sharp decline (57%) in Medicare reimbursement for cancer therapy was observed.

Even though economic incentives as well as patient preference provide enough rationale to orally formulate FDA approved chemotherapeutics, undesirable pharmacokinetics is a major hurdle that needs to be overcome. Studies have confirmed that the majority of currently available chemotherapeutics are not suitable applicants for

oral delivery due to low and highly variable oral bioavailability, including gemcitabine [6-8]. For example, in a clinical study by Veltkamp et al. evaluating gemcitabine toxicity, tolerability, pharmacokietincs, and anti-tumor activity in patients with advanced or metastatic cancer, found that systemic exposure was low with an estimated bioavailability of 10% due to first-pass liver metabolism [7]. Hence, oral administration of gemcitabine may be an unrealistic alternative to intravenous treatments of the drug due to its extensive first-pass liver metabolism and conversion into an inactive gemcitabine metabolite, 2′,2′-difluorodeoxyuridine (dFdU).

There have been recent efforts to decrease the deamination or conversion of the active gemcitabine molecule (dFdC) into it's inactive metabolite (dFdU) by covalently attaching long chain fatty acids to the 4-amino group (i.e. 4-(N)-stearoyl gemcitabine, as previously discussed), or through coupling acyclic isoprenoid chains of squalene (SQdFdC NA) [7]. It was shown that a fatty acid ester derivative of gemcitabine (CP-4126) exhibited better anti-tumor activity than its parent compound when given orally in human non-small cell lung cancer tumors in mice [9-10]. However, one of the three dosing regimens investigated at 10 mg/kg CP-4126 daily caused severe toxicity and forced the study to terminate. Further, dosing regimens of 15 mg/kg or 20 mg/kg CP-4126 at five times every three days, showed either favorable toxicity profiles with no anti-tumor activity or significant anti-tumor activity with non-favorable toxicity, respectively [9]. Alternatively, Couvreur et al. assessed anti-tumor activity in leukemic F344 Fischer rats after oral administration of gemcitabine or SQdFdC NA. They show that the rats receiving SQdFdC NA survived statistically longer gemcitabine alone, however tumor size regression was not reported [10].

Previously, we reported the development of 4-(N)-stearoyl gemcitabine solid lipid nanoparticles (GemC18-NPs) and demonstrated significant anti-tumor performance and

63

prolonged mouse survival in both human and mouse tumor model versus gemcitabine-alone or GemC18-in-Tween 20 micelles [11]. Due to our favorable results and the increasing attention to formulate oral chemotherapeutics, we were driven to evaluate the *in vivo* anti-tumor activity of the GemC18-NP when given orally.

4.3 Materials and Methods

4.3.1 Chemicals and Cell-lines

Mannitol, methanol (HPLC-grade), ethyl acetate (EtOAc), dichloromethane (DCM), potassium phosphate monobasic, sodium chloride, sodium hydroxide, Tween 20, and Tween 80 were from Sigma-Aldrich (St. Louis, MO). Gemcitabine hydrochloride (gemcitabine HCl) was from U.S. Pharmacopeia (Rockville, MD). Soy lecithin was from Alfa Aesar (Ward Hill, MA). Glycerol monostearate (GMS) was from Gattefosse Corp (Paramus, NJ). Mouse lung (TC-1, ATCC # CRL-2785) cancer cell lines were from American Type Culture Collection (ATCC, Manassas, VA). TC-1 cells were grown in RPMI1640 medium (Invitrogen, Carlsbad, CA). All media were supplemented with 10% fetal bovine serum (FBS, Invitrogen), 100 U/mL of penicillin (Invitrogen), and 100 µg/mL of streptomycin (Invitrogen).

4.3.2 Preparation of 4-(N)-Stearoyl Gemcitabine Nanoparticles

GemC18-NPs were prepared as previously described in Sloat and Sandoval et al, 2011. Briefly, 3.5 mg soy lecithin, 0.5 mg of glycerol monostearate, 1,2-distearyol-sn-glycero-3-phosphoethanolamine-N-[amino (polyethyleneglycol)-2000] (DSPE-PEG(2000), 11.6% (w/w) of total lipids and Tween 20) (Avanti Polar Lipids, Alabaster, AL), and 5 mg of GemC18 were placed into a 7 mL scintillation glass vial. One mL of de-ionized (Millipore Milli-Q; Billerica, MA) and filtered (0.22 µm) water was added

into the mixture, which was then maintained on a 70-75 ℃ hot plate while stirring, with occasional water-bath sonication (Bransonic Ultrasonic Cleaner, Danbury, CT), until the formation of homogenous slurry. Tween 20 was added in a step-wise manner to a final concentration of 1% (v/v). The resultant emulsions were allowed to cool to room temperature while stirring to form nanoparticles. As control, GemC18-free nanoparticles (Blank NPs) were prepared as described above without the addition GemC18. GemC18-alone was also dissolved into vegetable oil (GemC18-in-oil, ConAgra Foods; Omaha, NE). The size and zeta potential of the nanoparticles were measured using a Malvern Zetasizer Nano ZS (Westborough, MA).

Prior to animal studies, the GemC18-NPs were prepared with 5% mannitol (w/v) to adjust for tonicity for intravenous injection.

4.3.3   Stability of 4-(N)-Stearoyl Gemcitabine Nanoparticles

To evaluate the gastrointestinal stability of the GemC18-NPs similar to what they may experience when orally administered, non-fed Simulated Gastric Fluid (SGF) and Simulated Intestinal Fluid (SIF) was prepared as follows. SGF (pH 1.2) was prepared by dissolving 2 g of NaCl into 7 mL HCl and adding 991 mL deionized and filtered (0.22 μm) water. The SIF (pH 6.8) was prepared by adding 6.8 g of KH_2PO_4 and 896 mg NaOH into 1000 mL deionized and filtered (0.22 μm) water. The GemC18-NPs were incubated with SGF or SIF in 37°C for 0, 1, 2, 4, and 6 h. As control, the nanoparticles were incubated in PBS (pH 7.4) as well. At pre-determined time points, particle size was measured using a Malvern Zetasizer Nano ZS.

4.3.4 *In vitro* Release in Simulated Gastric Fluid (SGF) and Simulated Intestinal Fluid (SIF)

GemC18-NPs and GemC18-in-Tween 20 micelles in SGF or SIF were placed into a 1 mL cellulose ester dialysis tube (MWC 50,000) from Spectrum Chemicals & Laboratory Products (New Brunswick, NJ). The dialysis tube was then placed into a plastic conical tube containing 13 mL of SGF or SIF with 0.05% Tween 80 and incubated in a 37ºC shaker incubator. At predetermined time points (0, 0.5, 1, 1.5, 2, 3, 4, or 6 h), 200 μL of the release medium was withdrawn, and 200 μL of fresh release medium was added back. The concentration of the GemC18 was estimated by measuring the absorbance at 248 nm (BioTek Synergy™ HT Multi-Mode Microplate Reader (Winooski, VT) as previously described [11].

4.3.5 *In Vivo* Anti-tumor Efficacy Study

Animal protocol was approved by the IACUC at the University of Texas at Austin. Female C57BL/6 mice (18-20g, 6-8 weeks, n = 5) were subcutaneously (s.c) injected with mouse TC-1 lung cancer cells (ATCC # CRL-2785, 5 x 10^5 cells/mouse) in the right flank. Mouse hair was carefully trimmed at the injection site 1 day prior to the injection. Treatment with GemC18-NPs, GemC18-in-oil, Blank NPs, and sterile mannitol (5% w/v) were started on day 11, and mice were orally gavaged daily until the endpoint (i.e., death, tumor size greater than 15 mm, tumor ulceration, weight loss of more than 20%, or severe signs of pains and distress). As a positive control, a group of mice were injected via the tail vein with the GemC18-NPs, twice a week until the endpoint. The dose of GemC18 was 250 μg per mouse per dose for all formulations. Tumor size was measured 2-3 times a week, and tumor diameter was calculated as: diameter (mm) = [length + width]/2. Mouse survival time was also recorded.

An additional animal study was performed to evaluate and compare orally administered GemC18-NPs, gemcitabine hydrocholoride (GemHCl), and GemC18-free vegetable oil. Female C57Bl/6 mice with TC-1 tumors were used as described above. The mice were dosed with 150 μg of GemC18 per mouse per dose as well as equal molar doses of GemHCl (85 μg per mouse per dose).

4.3.6   Plasma Pharmacokinetics

To evaluate the pharmacokinetic parameters of GemC18-NPs when given orally or intravenously, mice were dosed with 1 mg of GemC18-NPs (0.56 mg gemcitabine). At pre-determined time points (0.25, 0.5, 1, 2, 4, 8, 12, 24, or 48 h), mice were euthanized and blood was collected into heparin-coated tubes and centrifuged (8000 rcf) for 10 min to isolate plasma. Samples were stored in a −80 °C until analysis. At time of analysis, a hydrolysis method was used to detect the concentration of GemC18 in plasma [12]. Briefly, to 75 μL of plasma, 25 μL of uracil 1-β-D-arabinofuranoside solution (AraU, 10 μg/mL) was added as an internal standard, followed by the addition of 100 μL of 2 N NaOH. This mixture was then vortexed and incubated at 40 °C for 1 h. Following incubation, 800 μL of acetonitrile and 75 μL of 1.4 M H_3PO_4 was added, followed by centrifugation at 13,000 rpm for 10 min. The supernatant was then collected and dried under vacuum. Lastly, the residue was re-dissolved in 100 μL of 2.5 mM PBS (pH 7.4) and centrifuged (13,000 rpm 10 min) to collect the supernatant, which was then analyzed using an Agilent HPLC with Agilent C18 column (5 μm, 4.6 mm × 250 mm; Santa Clara, CA) to measure gemcitabine concentration. The mobile phase was 5 mM sodium acetate (pH 6.0) and methanol (95/5, v/v), and the detection wavelength was 266 nm. Drug concentration value was derived after the gemcitabine concentration was converted to

stearoyl gemcitabine concentration. Data was analyzed using the PK Solver® and two-compartmental model to determine the $t_{1/2}$ at the elimination phase [11].

4.3.7   Statistical Analysis

Statistical analyses were completed by performing analysis of variance, followed by Fisher's protected least significant difference procedure. Mouse survival curves were compared using the Mantel-Cox log-rank method using Prism® from GraphPad Software, Inc. (La Jolla, CA). A p value of ≤ 0.05 (two-tail) was considered significant.

4.4   Results and Discussion

The GemC18-NPs were prepared as previously described [11]. Considering that the intended application of these stearoyl gemcitabine nanoparticles is for oral administration, it's critical to study the effect on particle size in similar environments present in the gastrointestinal tract. When the GemC18-NPs were incubated in the presence of intestinal pH (SIF, pH 6.8) and PBS (pH 7.4), particle size did not change over a 6 h period (Fig. 4.1). In simulated gastric fluid (pH 1.2), the nanoparticles appeared to aggregate (~15%) after 1 h incubation and particle size did not change thereafter ($p > 0.5$, Fig. 4.1). Previous studies by Tobio et al. and Garca-Fuentes et al. showed the presence of increasing PEG or Poloxamer 188 on the surface of nanoparticles stabilized and hindered aggregation of the particle in gastric fluid. The GemC18-NPs were engineered with 11.6% w/w polyethylene glycol(2000), therefore we postulate that increasing the amount of PEG could retard particle growth in SGF. Its noteworthy to mention that in a previous study by Sloat and Sandoval et al. demonstrated that the GemC18-NPs were stable in simulated biological medium (10% FBS in 0.9% saline) suggesting that the GemC18-NPs may not extensively aggregate *in vivo*. In a release

study (Fig. 4.2), drug release from the nanoparticles in SGF was slow over 2 h (~16.8%), whereas the release of GemC18-in Tween 20 micelles was rapid. When the nanoparticles were incubated in the SIF release medium, about 15% of GemC18 was released from the nanoparticles over 6 h. Therefore, we concluded that the observed particle growth in SGF did not significantly influence drug release. This is of particular importance because an ideal delivery system intended for oral administration, drug release from the carrier should withstand acidic pH changes to not only protect the drug from degradation, but to facilitate transport and release in the small intestines [6,13-14].

Treatment of tumor-bearing mice with orally gavaged GemC18-NPs resulted in a significant delay in the growth of the TC-1 tumors, as compared to the untreated group (Fig 4.3A). Mice that received treatment with GemC18-in-oil (nanoparticle-free) exhibited similar anti-tumor activity in comparison with GemC18-NPs up to day 25; however, the mice in this group did not survive as long as those receiving the nanoparticles (p = 0.0031, Log-rank (Mantel-Cox) Test) (Fig. 4.4B). Similar anti-tumor activity of the GemC18-NPs given intravenously via mouse-tail vein to those reported earlier [11]. During treatment with GemC18-in-oil, mice exhibited significant weight loss, severe signs of pain and distress (arched backs, hair loss, and sedentary activity), and were euthanized preemptively. In another study (data not shown), we evaluated if orally gavaged vegetable oil had any deleterious effects on mice toxicity or survival. As expected, mice that received identical volumes of vegetable oil did not exhibit any adverse or similar reactions, indicating that the observed results in Fig 4A and B was not due to the solvent per se. No detectible anti-tumor activity or toxicity was observed in mice orally gavaged with Blank-NPs. The GemC18-NPs were prepared with excipients (lecithin, GMS, and Tween 20) that are considered Generally Regarded As Safe (GRAS) and accepted in the FDA inactive ingredients guide for parenterals [15]. Previous studies

shown that the GemC18-NPs did not induce any measurable signs of liver toxicity when injected intravenously into mice [11]. It was also shown by Yanasarn et al. that the nanoparticles, incorporated with docetaxel, did not cause any significant red blood cell lysis or platelet aggregation [16]. Furthermore, in a long-term study (1.5 years), the pathological and histological parameters of mice that received three doses of the nanoparticles by subcutaneous injection were compared to that of untreated mice, and an examination by a board-certified veterinary pathologist did not reveal any significant difference between those two groups of mice (Sloat and Cui, unpublished data). Taken together, we believe that the nanoparticles used to formulate stearoyl gemcitabine are safe and biocompatible.

To study the *in vivo* pharmacokinetics of the stearoyl gemcitabine nanoparticles, we administered GemC18-NP by tail vein intravenous injection or oral gavage to healthy BALB/c mice at a single dose of 1 mg. As Fig. 4.4A shows, gemcitabine from the GemC18-NPs, when given i.v, appeared to follow a two-compartment model with a distribution half-life ($T_{50}\alpha$) of 0.09 h, an elimination half-life ($T_{50}\beta$) of 13.02 h and an Area Under Curve ($AUC_{0\to\infty}$) of 196.47 mcg/mL*h. In parallel, mice that received the GemC18-NP by the oral route (Fig. 4.4B) presented a $T_{50}\alpha$ or 1.39 h, $T_{50}\beta$ of 6.84 h, the highest observed concentration (Cmax) of 17.56 mcg/mL, time to reach maximum concentration (Tmax) of 2.02 h, and $AUC_{0\to\infty}$ of 112.31 mcg/mL*h. Additional pharmacokinetic parameters can be found in Table 2. When we compared the relevant pharmacokinetic data of the oral versus intravenous administered GemC18-NPs, the relative oral bioavailability was determined to be around 70%. The observed and improved bioavailability of gemcitabine when given as GemC18-NPs is highly desirable, as in previously published pharmacokinetic literature, an observed bioavailbility of gemcitabine was found to be only ~10% [7,17].

70

4.5   Conclusions

We observed that the stearoyl gemcitabine nanoparticle formulation when given orally displayed encouraging anti-tumor activity, did not appear toxic to mice, and favorable pharmacokinetics. To date, there is currently no FDA approved gemcitabine formulations for the oral route. In future studies, we will evaluate the organ biodistribution of the GemC18-NPs in mice after oral and intravenous injection. Furthermore, we would like to produce a dose-response curve and further understand possible mechanisms for the observed anti-tumor activity.

4.6   References

1. Abbruzzese, J. L., R. Grunewald, et al. (1991). "A phase I clinical, plasma, and cellular pharmacology study of gemcitabine." J Clin Oncol **9**(3): 491-498.

2. Mini, E., S. Nobili, et al. (2006). "Cellular pharmacology of gemcitabine." Ann Oncol **17 Suppl 5**: v7-12.

3. Ramesh, H. (2010). "Management of pancreatic cancer: current status and future directions." Indian J Surg **72**(4): 285-289.

4. Liu, G., E. Franssen, et al. (1997). "Patient preferences for oral versus intravenous palliative chemotherapy." J Clin Oncol **15**(1): 110-115.

5. DeMario, M. D. and M. J. Ratain (1998). "Oral chemotherapy: rationale and future directions." J Clin Oncol **16**(7): 2557-2567.

6. Schellens, J. H., M. M. Malingre, et al. (2000). "Modulation of oral bioavailability of anticancer drugs: from mouse to man." Eur J Pharm Sci **12**(2): 103-110.

7. Veltkamp, S. A., R. S. Jansen, et al. (2008). "Oral administration of gemcitabine in patients with refractory tumors: a clinical and pharmacologic study." Clin Cancer Res **14**(11): 3477-3486.

8. Veltkamp, S. A., D. Pluim, et al. (2008). "New insights into the pharmacology and cytotoxicity of gemcitabine and 2',2'-difluorodeoxyuridine." <u>Mol Cancer Ther</u> **7**(8): 2415-2425.

9. Bergman, A. M., A. D. Adema, et al. (2011). "Antiproliferative activity, mechanism of action and oral antitumor activity of CP-4126, a fatty acid derivative of gemcitabine, in in vitro and in vivo tumor models." <u>Invest New Drugs</u> **29**(3): 456-466.

10. Couvreur, P., B. Stella, et al. (2006). "Squalenoyl nanomedicines as potential therapeutics." <u>Nano Lett</u> **6**(11): 2544-2548.

11. Sloat, B. R., M. A. Sandoval, et al. (2011). "In vitro and in vivo anti-tumor activities of a gemcitabine derivative carried by nanoparticles." <u>Int J Pharm</u> **409**(1-2): 278-288.

12. Zhu, S., P. D. Lansakara, et al. (2012). "Lysosomal Delivery of a Lipophilic Gemcitabine Prodrug Using Novel Acid-Sensitive Micelles Improved Its Antitumor Activity." <u>Bioconjug Chem</u>.

13. Bardelmeijer, H. A., O. van Tellingen, et al. (2000). "The oral route for the administration of cytotoxic drugs: strategies to increase the efficiency and consistency of drug delivery." <u>Invest New Drugs</u> **18**(3): 231-241.

14. Sparreboom, A., M. J. de Jonge, et al. (2002). "The use of oral cytotoxic and cytostatic drugs in cancer treatment." <u>Eur J Cancer</u> **38**(1): 18-22.

15. Wade A, W. P. J. (1994). <u>Handbook of Pharmaceutical Excipients (2nd Ed)</u>: 392-399.

16. Yanasarn, N., B. R. Sloat, et al. (2009). "Nanoparticles engineered from lecithin-in-water emulsions as a potential delivery system for docetaxel." <u>Int J Pharm</u> **379**(1): 174-180.

17. Veltkamp, S. A., D. Pluim, et al. (2008). "Extensive metabolism and hepatic accumulation of gemcitabine after multiple oral and intravenous administration in mice." <u>Drug Metab Dispos</u> **36**(8): 1606-1615.

Tables and Figures

Table 1: Characterization of nanoparticles. Data shown are mean ± S.D (n ≥ 3).

	Size (nm)	Polydispersity index	Zeta potential (mV)	[GemC18] (mg/mL)	[EGF or OVA] (mM)
EGF-GemC18-NPs	215±8	0.24±0.06	−26.0±0.5	4.4±0.2	462±39
OVA-GemC18-NPs	219±3	0.32±0.08	−28.4±0.5	4.2±0.1	120±42

Table 2: Pharmacokinetic Parameters Post Administration of GemC18-NP in Mice.

Intravenous Injection			Oral Gavage		
Parameter	**Unit**	**Observed**	**Parameter**	**Unit**	**Observed**
k10	1/h	2.21	Tmax	h	2.02
k12	1/h	5.62	Cmax	µg/ml	17.56
k21	1/h	0.19	t1/2Alpha	h	1.39
t1/2Alpha	h	0.09	t1/2Beta	h	6.84
t1/2Beta	h	13.02	t1/2Ka	h	1.29
C0	µg/ml	434.34	AUC0-t	µg/ml*h	109.22
V	(mg)/(µg/ml)	0.002	AUC0-inf	µg/ml*h	112.31
CL	(mg)/(µg/ml)/h	0.004	AUMC	µg/ml*h^2	659.78
V2	(mg)/(µg/ml)	0.06	MRT	h	5.87
CL2	(mg)/(µg/ml)/h	0.01	V/F	(mg)/(µg/ml)	0.02
AUC0-t	µg/ml*h	156.66	CL/F	(mg)/(µg/ml)/h	0.0146677
AUC0-inf	µg/ml*h	196.47	V2/F	(mg)/(µg/ml)	0.01
AUMC	µg/ml*h^2	2690.01	CL2/F	(mg)/(µg/ml)/h	0.00015
MRT	h	13.69			

Figure 2.1:   Preparation and characterization of GemC18-NPs. (A) In GPC, GemC18-free-NPs and GemC18-NPs eluted about two fractions earlier than GemC18 in Tween 20 micelles (□)..The concentration of the GemC18 in the micelles and GemC18-NPs was 100 μg/mL. (B) Gel permeation chromatographs of GemC18-NPs prepared with 0, 0.1, 0.5, 1, 2.5, and 5 mg/mL of GemC18. In A and B, gemcitabine was measured at 248 nm. (C) TEM micrograph of the GemC18-NPs (with 5 mg/mL of GemC18). (D) Chromatographs of GemC18-NPs (•) and PEGylated GemC18-NPs (Δ) prepared with 5 mg/mL of GemC18. (E) The size and zeta potential of the GemC18-NPs and the PEG-GemC18-NPs. (F) The dynamic light scattering spectra of the GemC18-in-Tween 20 micelles (left), GemC18-NPs, and PEG-GemC18-NPs (far right) overlaid. (G) The release of the GemC18 from the GemC18-NPs (•) or PEG-GemC18-NPs (Δ). (I) The size of the GemC18-NPs and PEG-GemC18-NPs after 30 min of incubation at 37 °C in FBS in normal saline. Except in C and F, all data presented were the mean from at least 3 independent determinations. Standard deviations were not included in some figures for clarity.
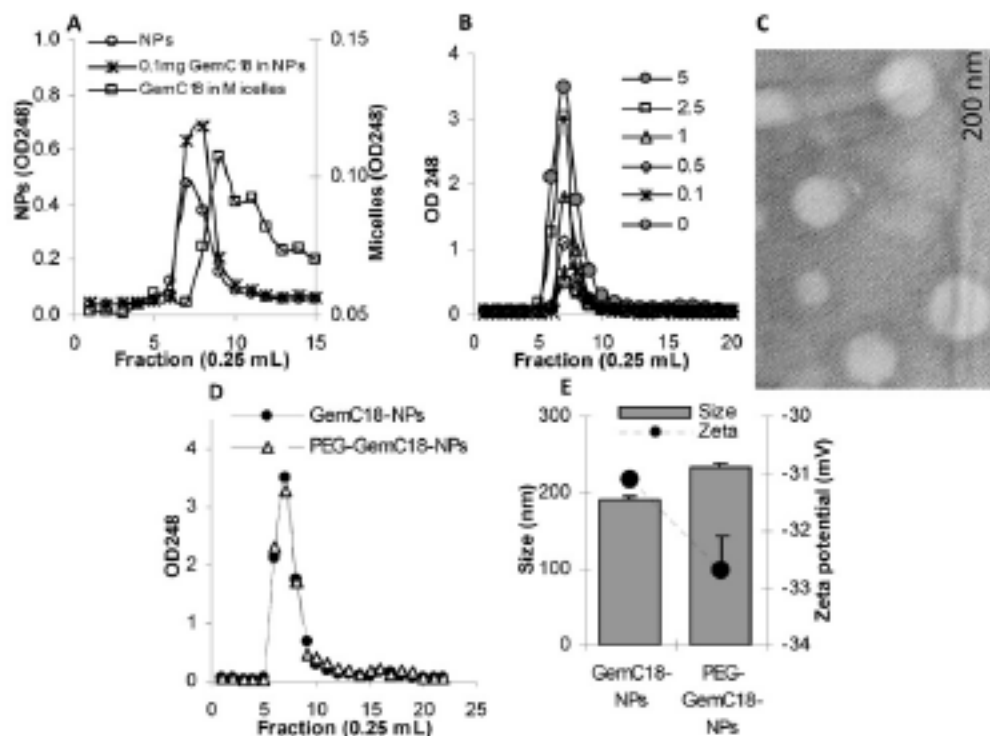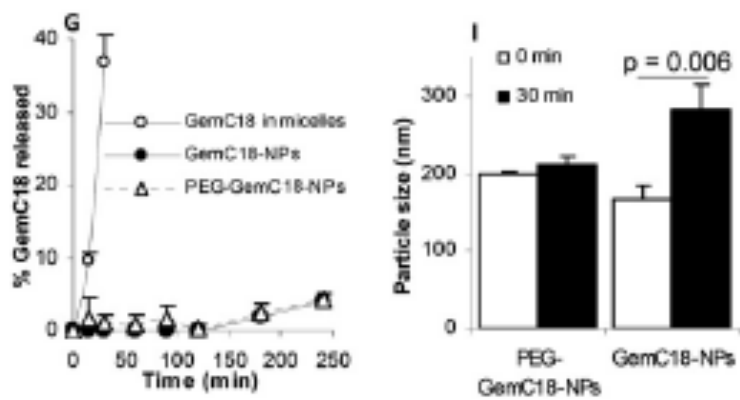
Figure 1: continued (p.75).

Figure 2.2:   The uptake of GemC18-NPs by TC-1 tumor cells in culture. (A) Fluorescence micrographs. Cells were incubated with fluorescein-labeled GemC18-NPs for 6 h at 37 °C or 4 °C and observed under a bright-field microscope (left panel) or a fluorescence microscope (right panel). Photos were taken at 20× magnification. (B) Comparison of the uptakes of PEGylated and un-PEGylated GemC18-NPs. *p < 0.001, PEG-GemC18-NPs vs. GemC18-NPs at 37 °C.
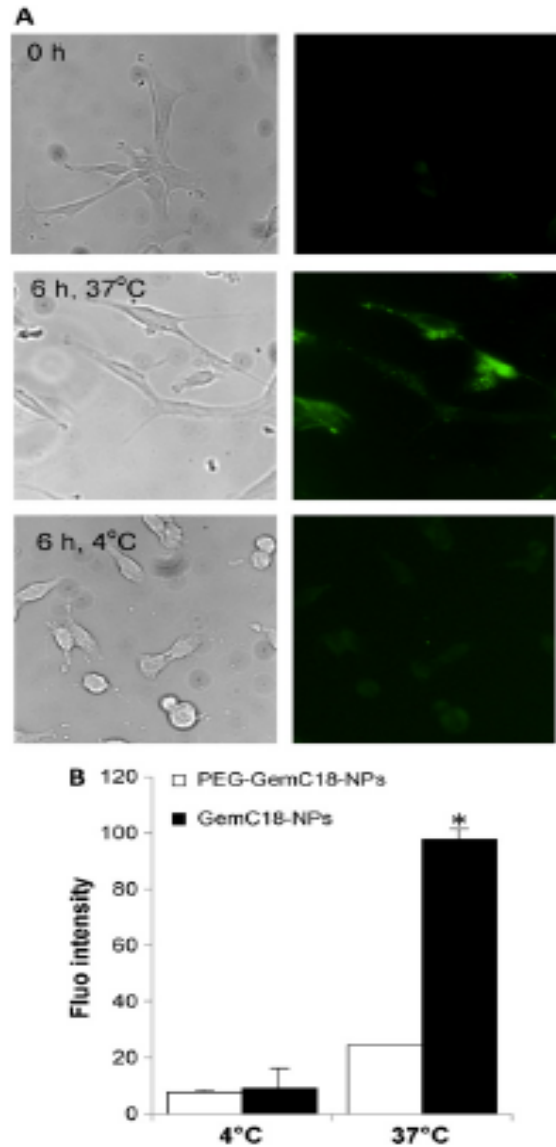
Figure 2.3:   GemC18-NPs were cytotoxic to tumor cells in culture. (A) The IC_{50} values of gemcitabine, GemC18-NPs, and PEG-GemC18-NPs in TC-1 and BxPC-3 cells. Cells were incubated with gemcitabine HCl or nanoparticles for 48 h. *For both cell lines, $p < 0.05$, Gemcitabine vs. GemC18-NPs. (B) It took the GemC18-NPs a longer time than thegemcitabine HCl to kill tumor cells. TC-1 cells were incubated with gemcitabine HCl or GemC18-NPs at 28.7 nM for 24 or 48 h, and the % of surviving cells was determined. Data are mean ± S.D. (n = 3–4).
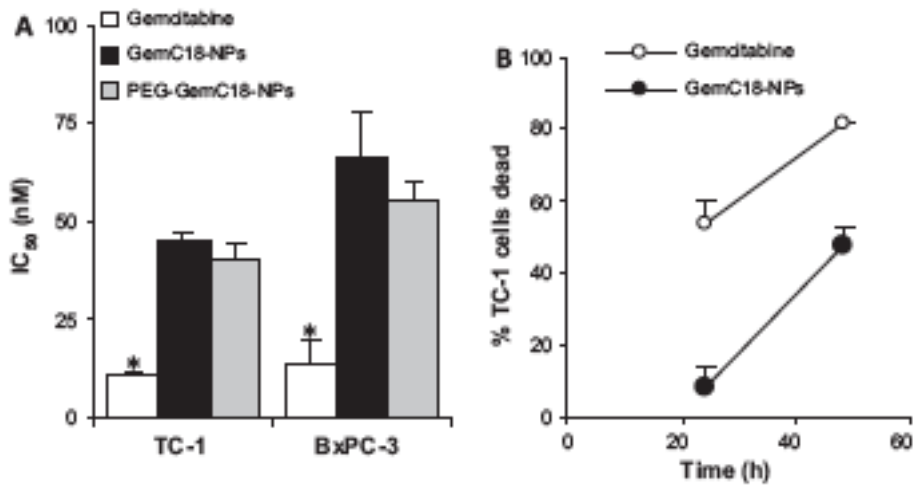
Figure 2.4:   *In vivo* and *ex vivo* imaging of GemC18-NPs and PEG-GemC18-NPs. (A) IVIS images of athymic mice 24 h after injection of fluorescein-labeled GemC18-NPs or PEG-GemC18-NPs. (B) Relative fluorescence intensity values in BxPC-3 tumors (circular ROI in A). ap = 0.0006, GemC18-NPs vs. PEG-GemC18-NPs. (C) Tissue distribution of fluorescein-labeled GemC18-NPs and PEG-GemC18-NPs 24 h after injection. b. GemC18-NPs vs. PEG-GemC18-NPs, p = 0.003, 0.021, and 0.002 for blood, liver, and spleen, respectively.
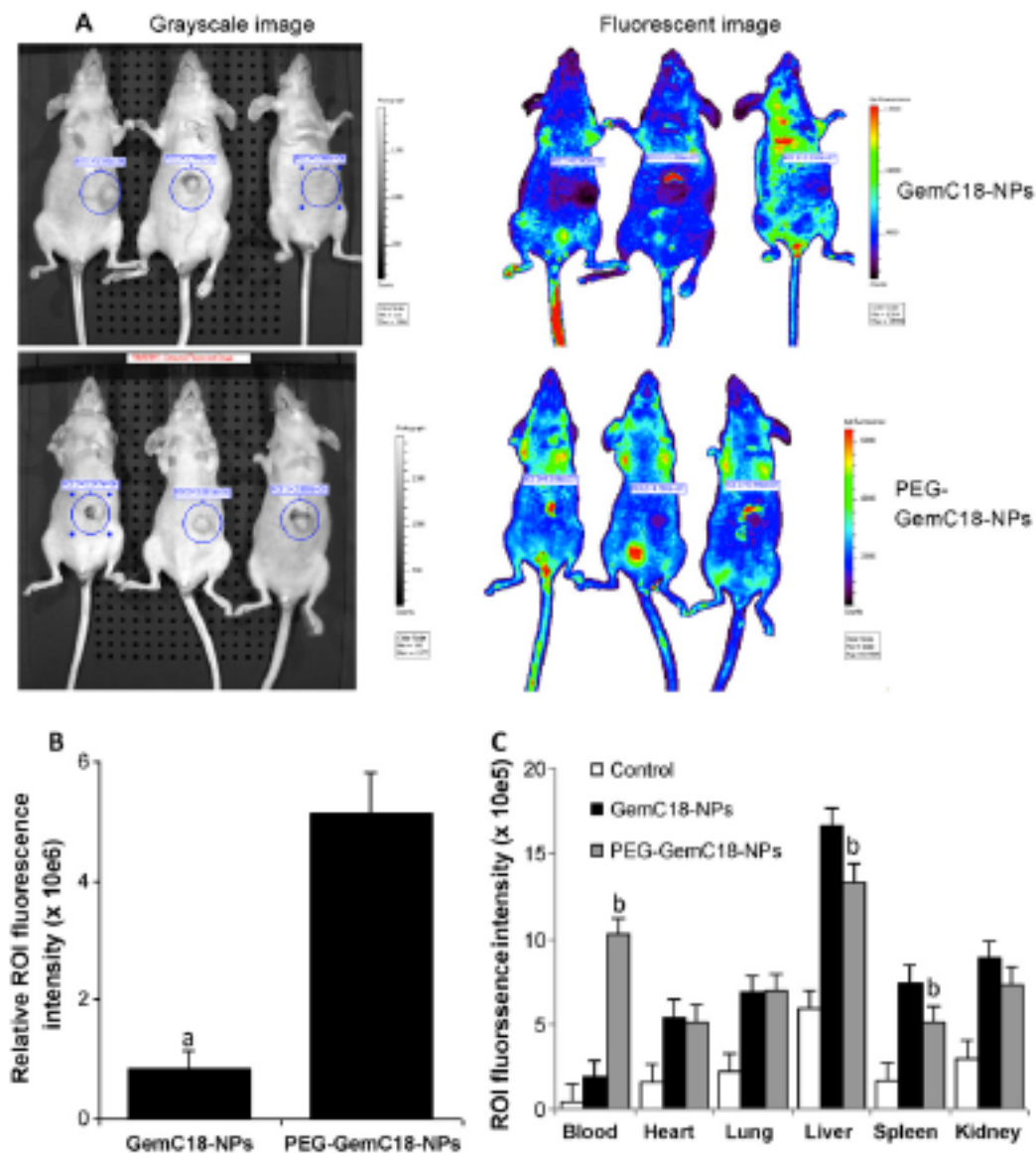
Figure 2.5: *In vivo* anti-tumor activity of GemC18-NPs against BxPC-3 tumors in athymic mice. (A) BxPC-3 tumor growth curves. Tumor cells were seeded on day 0, and mice were i.v. injected on days 6 and 19. (B) Average weight of BxPC-3 tumor-bearing mice after different treatments. *p = 0.0007 (ANOVA on week 3).
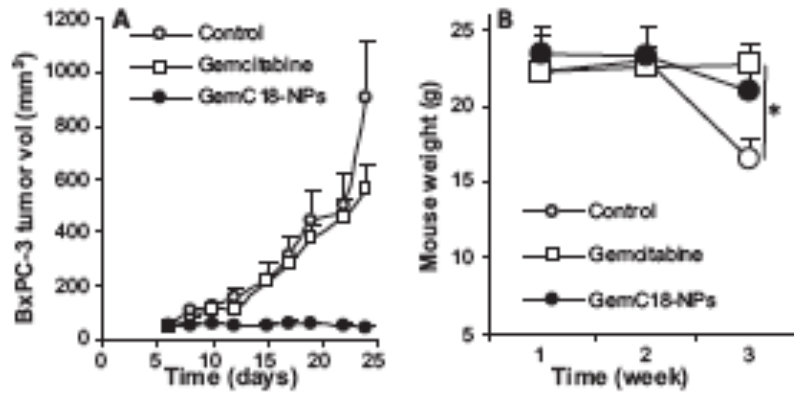
Figure 2.6:   Comparison of the *in vivo* anti-tumor activities of GemC18-NPs and PEGylated GemC18-NPs. (A) TC-1 tumors in C57Bl/6 mice. Mice (n = 5–7) were injected (i.v.) with GemC18-NPs or PEG-GemC18-NPs once (1 mg GemC18 per mouse). (B) BxPC-3 tumors in athymic mice. Mice (n = 5) were injected (i.v.) with GemC18-NPs or PEG-GemC18-NPs 3 times (days 0, 12, and 21). In A and B, tumor sizes were reported starting from the day of the injection of the nanoparticles. Data shown are mean ± S.E.M. Statistical analysis did not reveal any differences between the GemC18-NPs and PEG-GemC18-NPs in A–B.
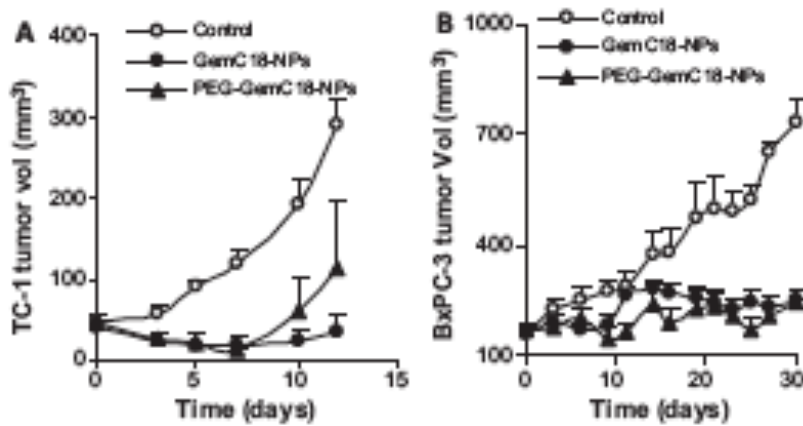
Figure 2.7:   Healthy C57Bl/6 mice (n = 3) were injected via the tail vein with
GemC18-NPs (1 mg of GemC18/mouse) or 0.566 mg of gemcitabine HCl
in sterile mannitol (5%). As controls, mice were either injected (i.v.) with
polyriboinosinic-polyribocytidylic acid (poly(I:C) or pI:C, 50 µg/mouse
(Sigma) as a positive control or sterile mannitol solution as a negative
control. Twenty-four h (A) or 7 days (B) later, mice were euthanized to
collect blood samples. Aspartate aminotransferase (AST) and alanine
aminotransferase (ALT) activities in the serum samples were determined
using AST and ALT kits from Teco Diagnostics (Anaheim, CA). Date
reported are mean ± S.D. in A, * $p < 0.0001$, ** $p = 0.008$, Control vs.
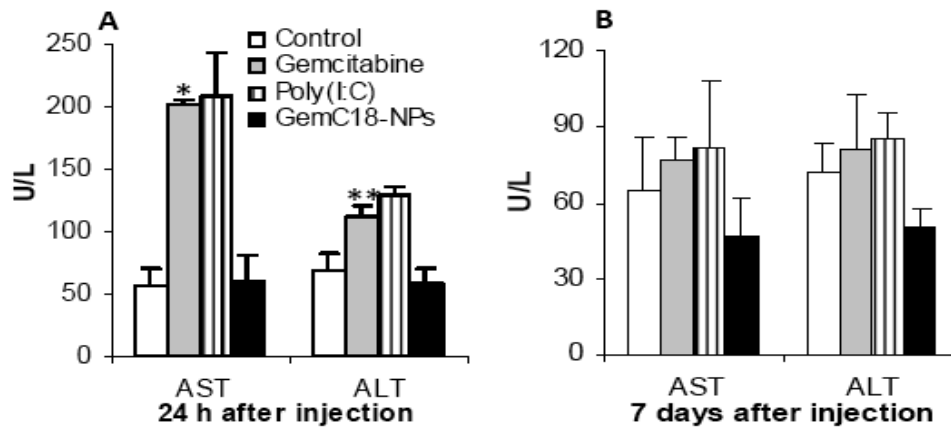Gemcitabine.

Figure 3.1: *In vitro* uptake of EGF-GemC18-NPs by tumor cells expressing different levels of EGFR. (A). MCF-7, MDA-MB-231, or MDA-MB-468 cells were incubated with fluorescein-labeled EGF-GemC18-NPs (EGF-NPs) or fluorescein-labeled OVA-GemC18-NPs (OVA-NPs) for 6 h, and the extent of nanoparticle uptake was determined by measuring the fluorescence intensity (*p = 0.0001; **p = 0.03). (B). The uptake of the EGF-GemC18-NPs or OVA-GemC18-NPs by MDA-MB-468 cells with (EGF+) or without pre-incubation of the cells with free EGF (***p = 0.009, EGF-NPs vs. EGF + EGF-NPs). The initial fluorescence intensity values of the EGF-NPs and the OVA-NPs were not different. Data shown are mean ± S.D. (n = 4 in A, and 3 in B).
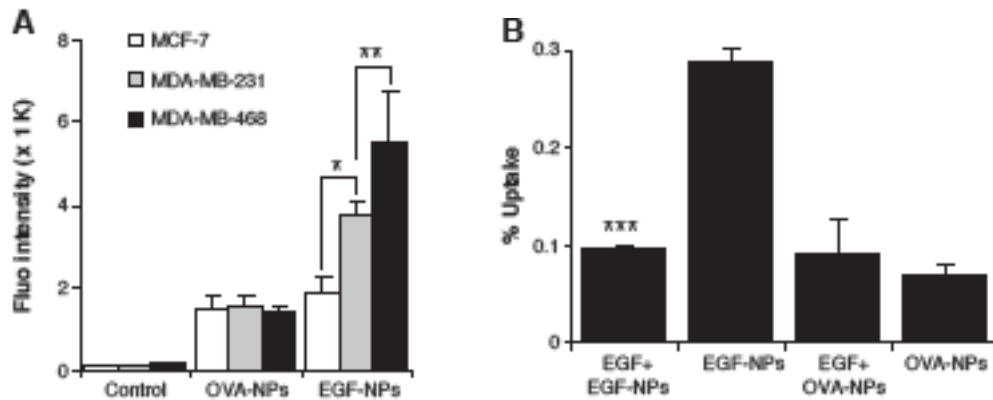
Figure 3.2: Flow cytometric and fluorescent microscopic analyses of the uptake of EGF-GemC18-NPs by tumor cells expressing different levels of EGFR. (A). Typical flow cytometric graphs of cells after 6 h of incubation with fluorescein-labeled EGF-GemC18-NPs (green, far right), fluorescein-labeled OVA-GemC18-NPs (gray, middle), or sterile PBS (solid gray area). Experiment was repeated three times with similar results. (B). Fluorescent microscopic images of MDA-MB-468 and MCF-7 cells after 6 h of incubation with EGF-GemC18-NPs, OVA-GemC18-NPs, or sterile PBS (control). Cell nucleus was stained with DAPI (blue). Nanoparticles were labeled with fluorescein and shown in green.
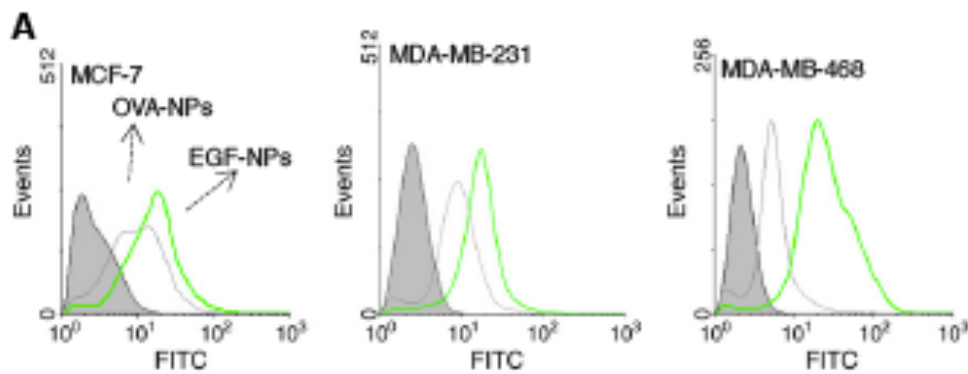
Figure 3.2:   continued (p. 84).
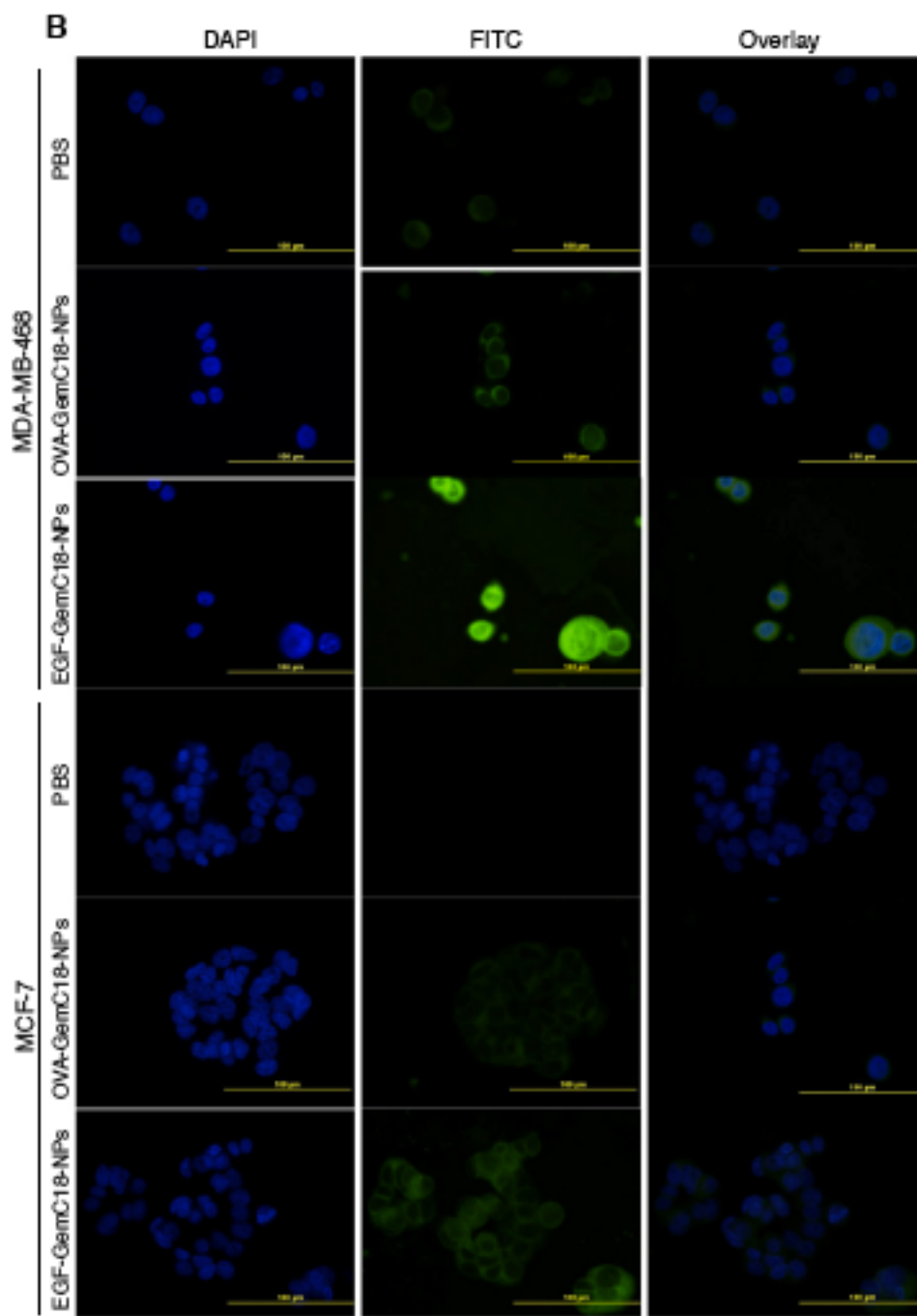
Figure 3.3: *In vitro* cytotoxicity of EGF-GemC18-NPs. (A). Percent of cells alive after 48 h of incubation with different concentration of GemC18 in EGF-GemC18-NPs or OVA-GemC18-NPs (n = 4). (B). Flow cytometric graphs of MDA-MB-468 cells after 24 h of incubation with EGF-GemC18-NPs or OVA-GemC18-NPs and stained with Annexin V and 7-AAD. Numbers in the quadrants are % of cells in early apoptosis (LR), late apoptosis (UR), and cell debris (UL). Experiment was repeated 3 times with similar results.
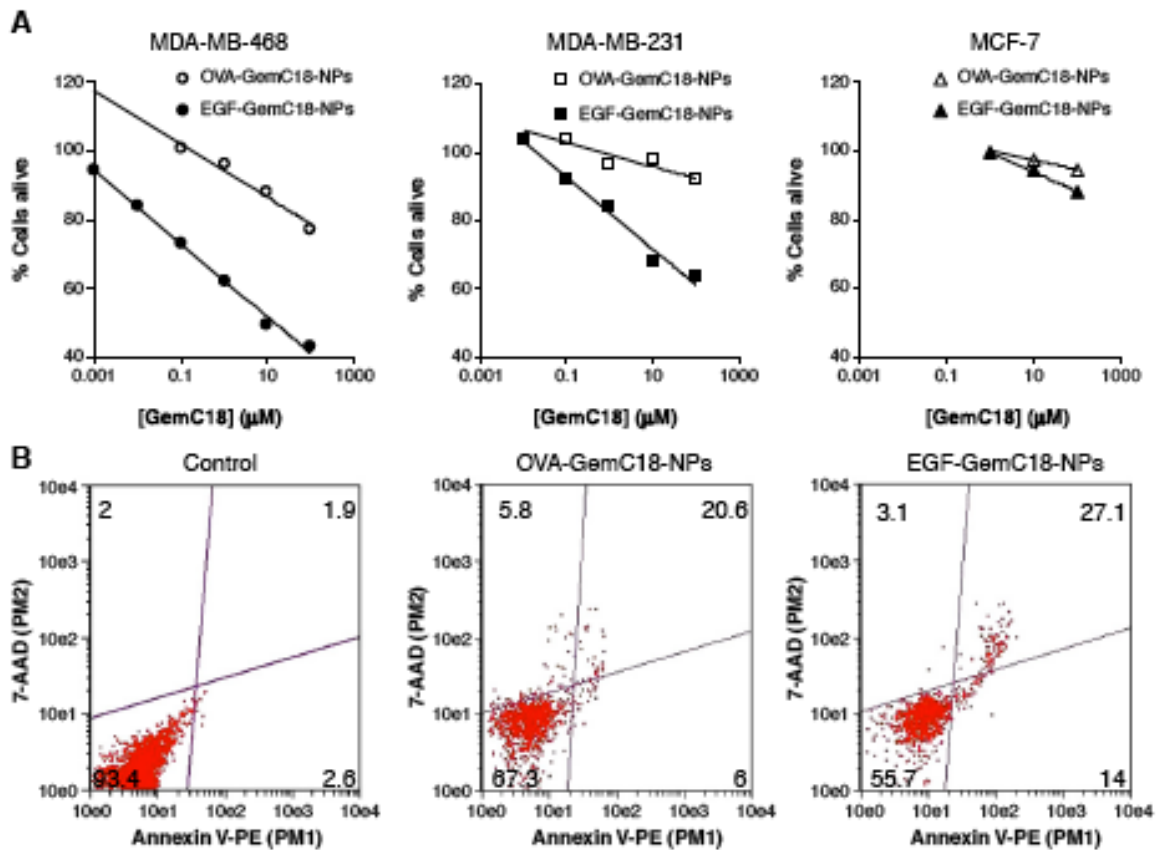
Figure 3.4: Anti-tumor activity of EGF-GemC18-NPs in nude mice with pre-established MDA-MB-468 tumors. (A). Tumor growth curves. (B). Mouse survival curves (p = 0.053, EGF-GemC18-NPs vs. OVA-GemC18-NPs). In A and B, mice were dosed 11, 17, 28, and 37 days after tumor cell injection. (C). Tumor growth curves in mice used for immunohistology analysis. In A and C, *p < 0.05, EGF-GemC18-NPs vs. OVA-GemC18-NPs.
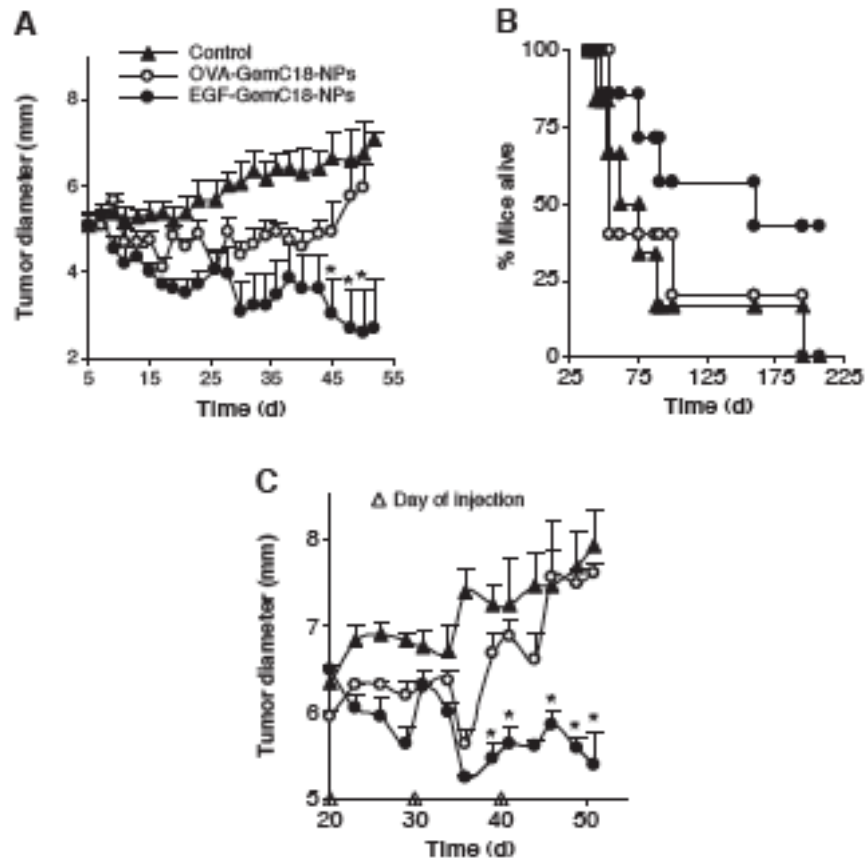
Figure 3.5:   Immunohistographs of MDA-MB-468 tumors after treatment with EGF-GemC18-NPs or OVA-GemC18-NPs. (A, slides prepared by M.D Anderson). Tumor tissues were staining with antibodies against BrdU, CD31, or caspase 3 (Cas 3). Scale bars = 100 μm. (B). The % of BrdU positive cells. (C). The % of caspase 3 positive cells.
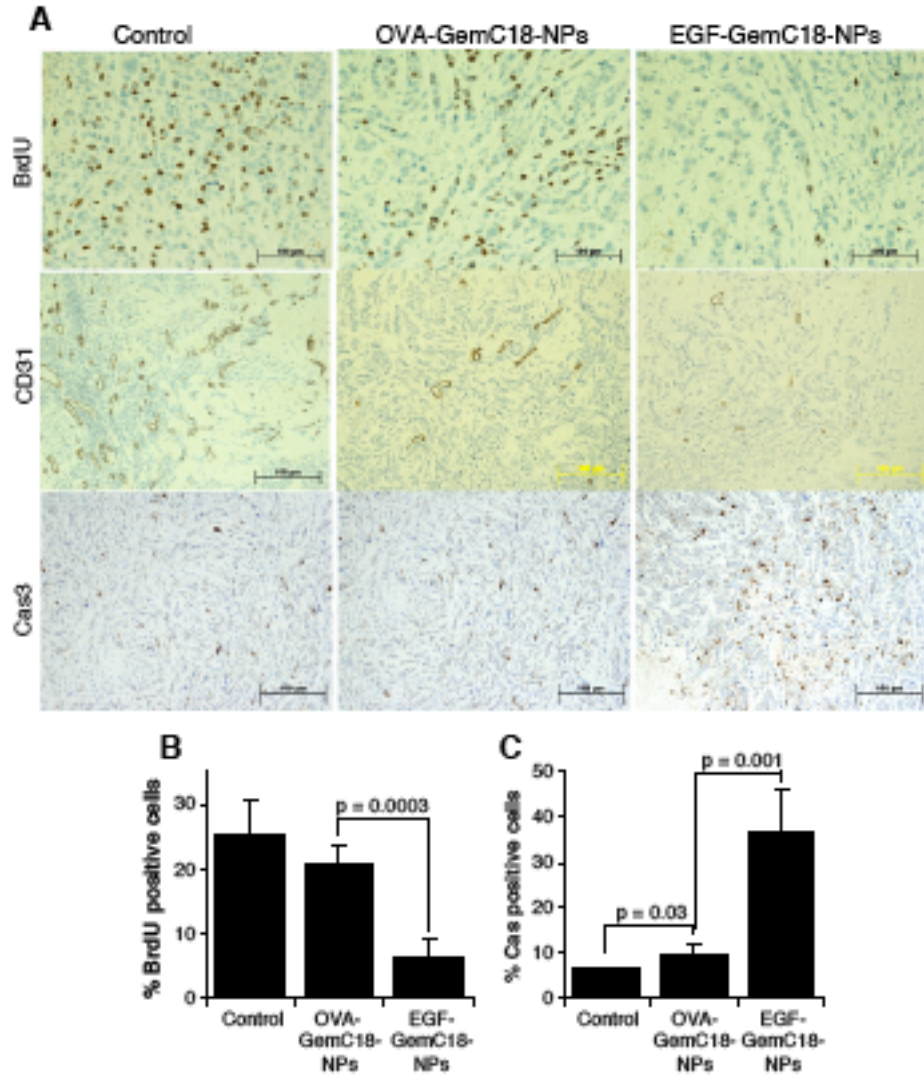
Figure 3.6: Biodistribution of EGF-GemC18-NPs. (A). *Ex vivo* fluorescence IVIS images of MDA-MB-468 tumors and organs 24 h after injection (T = tumor, K = kidney, H = heart, and S = spleen). (B). A comparison of the normalized fluorescence intensity of EGF-GemC18-NPs or OVA-GemC18-NPs in tumors and different organs 24 h after injection (*, $p = 0.0003$ in tumors). (C). Fluorescence intensity in the blood of healthy C57BL/6 mice at different time points after i.v. injection of fluorescein-labeled nanoparticles. Data shown in B and C are mean ± S.D. from three replicates.
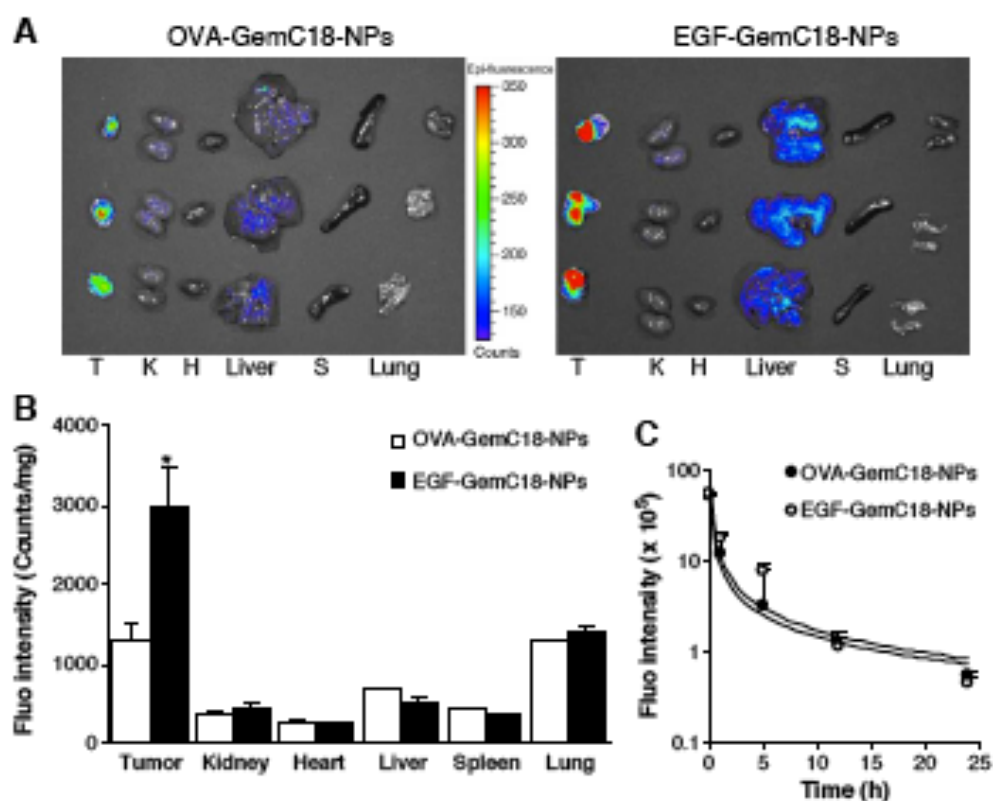
Figure 3.7:   At 28.3 mg/kg, gemcitabine hydrochloride was toxic to nude mice with MDA-MB-468 tumors. MDA-MB-468 tumor cells (1×10^7 cells/mouse) were mixed with BD MatrigelTM (50%:50%) and subcutaneously injected in the right flank of the mice on day 0. On day 11, mice were randomized and injected intravenously (i.v.) via the tail vein with 200 μL of gemcitabine hydrochloride (n = 5), OVA-GemC18-NPs in sterile mannitol (5%, w/v) (n = 7) or sterile mannitol alone as a negative control (n = 5). Injection was repeated on days 17, 28, and 37. The dose of the GemC18 was about 0.860 mg per mouse per injection; the dose of the gemcitabine hydrochloride was 0.566 mg per mouse per injection.
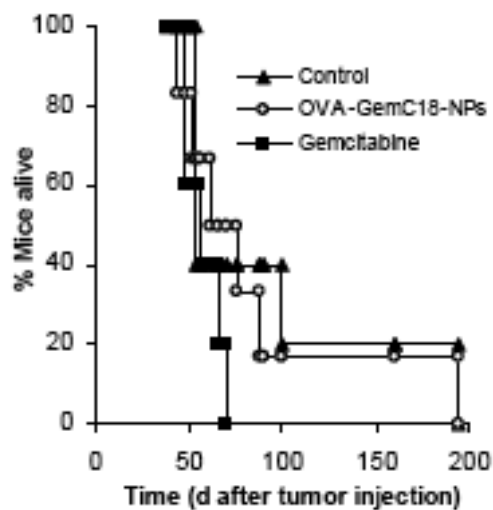
Figure 4.1: Stability of GemC18-NPs in Simulated Gastric Fluid (SGF, pH 1.2) or
Simulated Intestinal Fluid (SIF, pH 6.8) for up to 6 h at 37°C.
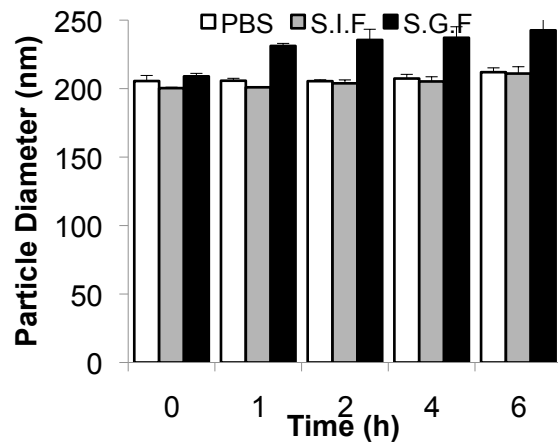
Figure 4.2: *In vitro* release of GemC18 from GemC18-NPs or GemC18-in Tween 20
micelles (GemC18-Micelles) in Simulated Gastric Fluid (SGF, pH 1.2)
or Simulated Intestinal Fluid (SIF, pH 6.8).
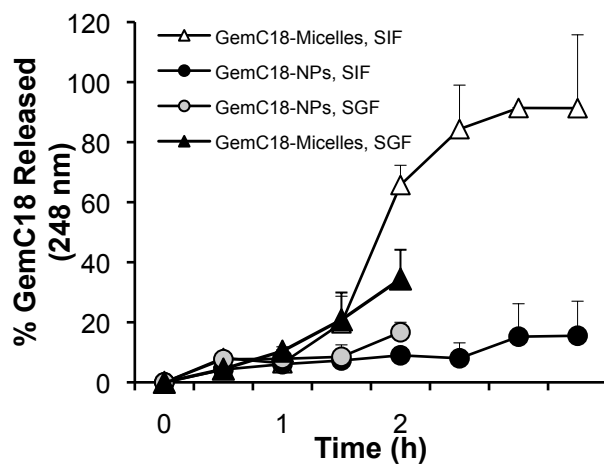
Figure 4.3: The anti-tumor activity of GemC18-NPs in mice with pre-established TC-1 tumors. (A) Tumor growth curves. TC-1 tumors were subcutanously implanted in C57BL/6 mice and when reached 4-5 mm (n = 5) the mice were orally gavaged with GemC18-NPs, GemC18-in-oil, or Blank-NPs. Mice were also intravenoulsy injected with GemC18-NPs as positive control. (B) Survival curves of mice is A.
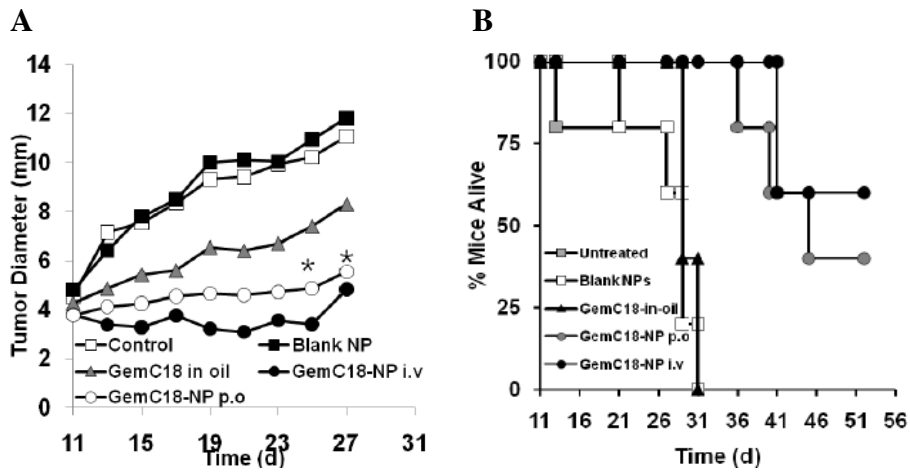
Figure 4.4: Plamsa gemcitabine concentration (ug/mL) versus time (h) curves after GemC18-NPs were (A) intravenously injected or (B) orally gavaged into BALB/c mice.
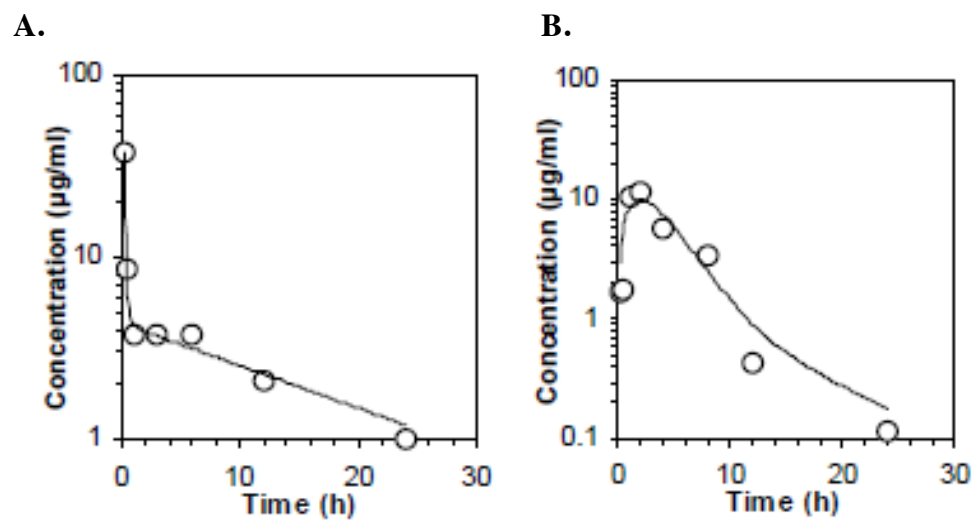
Bibliography

Abbruzzese, J. L., R. Grunewald, et al. (1991). "A phase I clinical, plasma, and cellular pharmacology study of gemcitabine." <u>J Clin Oncol</u> **9**(3): 491-498.

Allen, C., N. Dos Santos, et al. (2002). "Controlling the physical behavior and biological performance of liposome formulations through use of surface grafted poly(ethylene glycol)." <u>Biosci Rep</u> **22**(2): 225-250.

Arias, J. L., L. H. Reddy, et al. (2008). "Magnetoresponsive squalenoyl gemcitabine composite nanoparticles for cancer active targeting." <u>Langmuir</u> **24**(14): 7512-7519.

Arias, J. L., L. H. Reddy, et al. (2009). "Polymeric nanoparticulate system augmented the anticancer therapeutic efficacy of gemcitabine." <u>J Drug Target</u> **17**(8): 586-598.

Arias, J. L., L. H. Reddy, et al. (2011). "Superior preclinical efficacy of gemcitabine developed as chitosan nanoparticulate system." <u>Biomacromolecules</u> **12**(1): 97-104.

Arya, G., M. Vandana, et al. (2011). "Enhanced antiproliferative activity of Herceptin (HER2)-conjugated gemcitabine-loaded chitosan nanoparticle in pancreatic cancer therapy." <u>Nanomedicine</u>.

Bardelmeijer, H. A., O. van Tellingen, et al. (2000). "The oral route for the administration of cytotoxic drugs: strategies to increase the efficiency and consistency of drug delivery." <u>Invest New Drugs</u> **18**(3): 231-241.

Barton-Burke, M. (1999). "Gemcitabine: a pharmacologic and clinical overview." <u>Cancer Nurs</u> **22**(2): 176-183.

Baselga, J. (2000). "Monoclonal antibodies directed at growth factor receptors." <u>Ann Oncol</u> **11 Suppl 3**: 187-190.

Bazile, D., C. Prud'homme, et al. (1995). "Stealth Me.PEG-PLA nanoparticles avoid uptake by the mononuclear phagocytes system." <u>J Pharm Sci</u> **84**(4): 493-498.

Bergman, A. M., A. D. Adema, et al. (2010). "Antiproliferative activity, mechanism of action and oral antitumor activity of CP-4126, a fatty acid derivative of gemcitabine, in in vitro and in vivo tumor models." <u>Invest New Drugs</u>.

Bergman, A. M., A. D. Adema, et al. (2011). "Antiproliferative activity, mechanism of action and oral antitumor activity of CP-4126, a fatty acid derivative of gemcitabine, in in vitro and in vivo tumor models." <u>Invest New Drugs</u> **29**(3): 456-466.

Bergman, A. M., H. M. Pinedo, et al. (2002). "Determinants of resistance to 2',2'-difluorodeoxycytidine (gemcitabine)." <u>Drug Resist Updat</u> **5**(1): 19-33.

Bharali, D. J., M. Khalil, et al. (2009). "Nanoparticles and cancer therapy: a concise review with emphasis on dendrimers." <u>Int J Nanomedicine</u> **4**: 1-7.

Blessing, T., M. Kursa, et al. (2001). "Different strategies for formation of pegylated EGF-conjugated PEI/DNA complexes for targeted gene delivery." <u>Bioconjug Chem</u> **12**(4): 529-537.

Bouffard, D. Y., J. Laliberte, et al. (1993). "Kinetic studies on 2',2'-difluorodeoxycytidine (Gemcitabine) with purified human deoxycytidine kinase and cytidine deaminase." <u>Biochem Pharmacol</u> **45**(9): 1857-1861.

Brusa, P., M. L. Immordino, et al. (2007). "Antitumor activity and pharmacokinetics of liposomes containing lipophilic gemcitabine prodrugs." <u>Anticancer Res</u> **27**(1A): 195-199.

Burris, H. A., 3rd, M. J. Moore, et al. (1997). "Improvements in survival and clinical benefit with gemcitabine as first-line therapy for patients with advanced pancreas cancer: a randomized trial." <u>J Clin Oncol</u> **15**(6): 2403-2413.

Byrne, J. D., T. Betancourt, et al. (2008). "Active targeting schemes for nanoparticle systems in cancer therapeutics." <u>Adv Drug Deliv Rev</u> **60**(15): 1615-1626.

Carpenter, G. and S. Cohen (1979). "Epidermal growth factor." <u>Annu Rev Biochem</u> **48**: 193-216.

Castelli, F., M. G. Sarpietro, et al. (2007). "Interaction of lipophilic gemcitabine prodrugs with biomembrane models studied by Langmuir-Blodgett technique." <u>J Colloid Interface Sci</u> **313**(1): 363-368.

Celano, M., M. G. Calvagno, et al. (2004). "Cytotoxic effects of gemcitabine-loaded liposomes in human anaplastic thyroid carcinoma cells." <u>BMC Cancer</u> **4**: 63.

Chou, T. C. and P. Talalay (1984). "Quantitative analysis of dose-effect relationships: the combined effects of multiple drugs or enzyme inhibitors." <u>Adv Enzyme Regul</u> **22**: 27-55.

Chung, W. G., M. A. Sandoval, et al. (2012). "Stearoyl gemcitabine nanoparticles overcome resistance related to the over-expression of ribonucleotide reductase subunit M1." J Control Release **157**(1): 132-140.

Ciardiello, F. and G. Tortora (2003). "Epidermal growth factor receptor (EGFR) as a target in cancer therapy: understanding the role of receptor expression and other molecular determinants that could influence the response to anti-EGFR drugs." Eur J Cancer **39**(10): 1348-1354.

Collins, K., T. Jacks, et al. (1997). "The cell cycle and cancer." Proc Natl Acad Sci U S A **94**(7): 2776-2778.

Couvreur, P., B. Stella, et al. (2006). "Squalenoyl nanomedicines as potential therapeutics." Nano Lett **6**(11): 2544-2548.

Cuenca, A. G., H. Jiang, et al. (2006). "Emerging implications of nanotechnology on cancer diagnostics and therapeutics." Cancer **107**(3): 459-466.

Cui, Z., F. Qiu, et al. (2006). "Lecithin-based cationic nanoparticles as a potential DNA delivery system." Int J Pharm **313**(1-2): 206-213.

Danhier, F., N. Lecouturier, et al. (2009). "Paclitaxel-loaded PEGylated PLGA-based nanoparticles: in vitro and in vivo evaluation." J Control Release **133**(1): 11-17.

Davies, B. and T. Morris (1993). "Physiological parameters in laboratory animals and humans." Pharm Res **10**(7): 1093-1095.

De Jong, W. H. and P. J. A. Borm (2008). "Drug delivery and nanoparticles: Applications and hazards." International Journal of Nanomedicine **3**(2): 133-149.

Dellian, M., G. Helmlinger, et al. (1996). "Fluorescence ratio imaging of interstitial pH in solid tumours: effect of glucose on spatial and temporal gradients." Br J Cancer **74**(8): 1206-1215.

DeMario, M. D. and M. J. Ratain (1998). "Oral chemotherapy: rationale and future directions." J Clin Oncol **16**(7): 2557-2567.

Dienst, A., A. Grunow, et al. (2005). "Specific occlusion of murine and human tumor vasculature by VCAM-1-targeted recombinant fusion proteins." J Natl Cancer Inst **97**(10): 733-747.

Dinarvand, R., N. Sepehri, et al. (2011). "Polylactide-co-glycolide nanoparticles for controlled delivery of anticancer agents." Int J Nanomedicine **6**: 877-895.

DiPiro, J. T., R. L. Talbert, et al. (2008). Pharmacotherapy: A Pathophysiologic Approach. New York, McGraw-Hill Medical.

Francis, G. E., C. Delgado, et al. (1996). "Polyethylene glycol modification: relevance of improved methodology to tumour targeting." J Drug Target **3**(5): 321-340.

French, A. R., D. K. Tadaki, et al. (1995). "Intracellular trafficking of epidermal growth factor family ligands is directly influenced by the pH sensitivity of the receptor/ligand interaction." J Biol Chem **270**(9): 4334-4340.

Gang, J., S. B. Park, et al. (2007). "Magnetic poly epsilon-caprolactone nanoparticles containing Fe3O4 and gemcitabine enhance anti-tumor effect in pancreatic cancer xenograft mouse model." J Drug Target **15**(6): 445-453.

Gao, J., K. Chen, et al. (2010). "Ultrasmall near-infrared non-cadmium quantum dots for in vivo tumor imaging." Small **6**(2): 256-261.

Garcia-Manteiga, J., M. Molina-Arcas, et al. (2003). "Nucleoside transporter profiles in human pancreatic cancer cells: role of hCNT1 in 2',2'-difluorodeoxycytidine- induced cytotoxicity." Clin Cancer Res **9**(13): 5000-5008.

Gref, R., Y. Minamitake, et al. (1994). "Biodegradable long-circulating polymeric nanospheres." Science **263**(5153): 1600-1603.

Grunewald, R., H. Kantarjian, et al. (1992). "Gemcitabine in leukemia: a phase I clinical, plasma, and cellular pharmacology study." J Clin Oncol **10**(3): 406-413.

Guo Zw, Z. and J. M. Gallo (1999). "Selective Protection of 2',2'-Difluorodeoxycytidine (Gemcitabine)." J Org Chem **64**(22): 8319-8322.

Hammel, P., C. Louvet, et al. (1999). "Multicenter phase II study in advanced pancreatic adenocarcinoma patients treated with a combination of leucovorin, 5FU bolus and infusion, and emcitabine (FOLFUGEM regimen)." Gastroenterology **116**(4): A417-A417.

Herbst, R. S. and D. M. Shin (2002). "Monoclonal antibodies to target epidermal growth factor receptor-positive tumors: a new paradigm for cancer therapy." Cancer **94**(5): 1593-1611.

Hoff, P. M., R. Ansari, et al. (2001). "Comparison of oral capecitabine versus intravenous fluorouracil plus leucovorin as first-line treatment in 605 patients with metastatic

colorectal cancer: results of a randomized phase III study." <u>J Clin Oncol</u> **19**(8): 2282-2292.

Huang, P., S. Chubb, et al. (1991). "Action of 2',2'-difluorodeoxycytidine on DNA synthesis." <u>Cancer Res</u> **51**(22): 6110-6117.

Immordino, M. L., P. Brusa, et al. (2004). "Preparation, characterization, cytotoxicity and pharmacokinetics of liposomes containing lipophilic gemcitabine prodrugs." <u>J Control Release</u> **100**(3): 331-346.

Jain, R. K. (1996). "1995 Whitaker Lecture: delivery of molecules, particles, and cells to solid tumors." <u>Ann Biomed Eng</u> **24**(4): 457-473.

Jain, R. K. (1996). "Delivery of molecular medicine to solid tumors." <u>Science</u> **271**(5252): 1079-1080.

Jantscheff, P., V. Ziroli, et al. (2009). "Anti-metastatic effects of liposomal gemcitabine in a human orthotopic LNCaP prostate cancer xenograft model." <u>Clin Exp Metastasis</u> **26**(8): 981-992.

Jemal, A., E. Ward, et al. (2007). "Recent trends in breast cancer incidence rates by age and tumor characteristics among U.S. women." <u>Breast Cancer Res</u> **9**(3): R28.

Jin, C., L. Bai, et al. (2009). "Cytotoxicity of paclitaxel incorporated in PLGA nanoparticles on hypoxic human tumor cells." <u>Pharm Res</u> **26**(7): 1776-1784.

Kalantarian, P., I. Haririan, et al. (2011). "Entrapment of 5-fluorouracil into PLGA matrices using supercritical antisolvent processes." <u>J Pharm Pharmacol</u> **63**(4): 500-506.

Kim, I. Y., Y. S. Kang, et al. (2009). "Antitumor activity of EGFR targeted pH-sensitive immunoliposomes encapsulating gemcitabine in A549 xenograft nude mice." <u>J Control Release</u> **140**(1): 55-60.

Kirpotin, D. B., D. C. Drummond, et al. (2006). "Antibody targeting of long-circulating lipidic nanoparticles does not increase tumor localization but does increase internalization in animal models." <u>Cancer Res</u> **66**(13): 6732-6740.

Kleeff, J., C. Michalski, et al. (2006). "Pancreatic cancer: from bench to 5-year survival." <u>Pancreas</u> **33**(2): 111-118.

Klijn, J. G., P. M. Berns, et al. (1992). "The clinical significance of epidermal growth factor receptor (EGF-R) in human breast cancer: a review on 5232 patients." <u>Endocr Rev</u> **13**(1): 3-17.

Klose, D., F. Siepmann, et al. (2008). "PLGA-based drug delivery systems: importance of the type of drug and device geometry." Int J Pharm **354**(1-2): 95-103.

Kullberg, E. B., M. Nestor, et al. (2003). "Tumor-cell targeted epiderimal growth factor liposomes loaded with boronated acridine: uptake and processing." Pharm Res **20**(2): 229-236.

Kurihara, K., S. Miyashita, et al. (1999). "Incorporation of impurity to a tetragonal lysozyme crystal." Journal of Crystal Growth **196**(2-4): 285-290.

Le, U. M., N. Yanasarn, et al. (2008). "Tumor chemo-immunotherapy using gemcitabine and a synthetic dsRNA." Cancer Biol Ther **7**(3): 440-447.

Lemaire, V., J. Belair, et al. (2003). "Structural modeling of drug release from biodegradable porous matrices based on a combined diffusion/erosion process." Int J Pharm **258**(1-2): 95-107.

LeMaistre, C. F., C. Meneghetti, et al. (1994). "Targeting the EGF receptor in breast cancer treatment." Breast Cancer Res Treat **32**(1): 97-103.

Li, X., Y. Xu, et al. (2008). "PLGA nanoparticles for the oral delivery of 5-Fluorouracil using high pressure homogenization-emulsification as the preparation method and in vitro/in vivo studies." Drug Dev Ind Pharm **34**(1): 107-115.

Lillemoe, K. D. (1995). "Current management of pancreatic carcinoma." Ann Surg **221**(2): 133-148.

Lin, R., L. Shi Ng, et al. (2005). "In vitro study of anticancer drug doxorubicin in PLGA-based microparticles." Biomaterials **26**(21): 4476-4485.

Liu, G., E. Franssen, et al. (1997). "Patient preferences for oral versus intravenous palliative chemotherapy." J Clin Oncol **15**(1): 110-115.

Lu, J. M., X. W. Wang, et al. (2009). "Current advances in research and clinical applications of PLGA-based nanotechnology." Expert Review of Molecular Diagnostics **9**(4): 325-341.

Mamot, C., D. C. Drummond, et al. (2003). "Epidermal growth factor receptor (EGFR)-targeted immunoliposomes mediate specific and efficient drug delivery to EGFR- and EGFRvIII-overexpressing tumor cells." Cancer Res **63**(12): 3154-3161.

Milas, L., K. A. Mason, et al. (2004). "CpG oligodeoxynucleotide enhances tumor response to radiation." Cancer Res **64**(15): 5074-5077.

Mini, E., S. Nobili, et al. (2006). "Cellular pharmacology of gemcitabine." Ann Oncol **17 Suppl 5**: v7-12.

Muller, R. H., C. Jacobs, et al. (2001). "Nanosuspensions as particulate drug formulations in therapy. Rationale for development and what we can expect for the future." Adv Drug Deliv Rev **47**(1): 3-19.

O'Shaughnessy, J. A., R. E. Wittes, et al. (1991). "Commentary concerning demonstration of safety and efficacy of investigational anticancer agents in clinical trials." J Clin Oncol **9**(12): 2225-2232.

Owens, D. E., 3rd and N. A. Peppas (2006). "Opsonization, biodistribution, and pharmacokinetics of polymeric nanoparticles." Int J Pharm **307**(1): 93-102.

Paolino, D., D. Cosco, et al. (2010). "Gemcitabine-loaded PEGylated unilamellar liposomes vs GEMZAR: biodistribution, pharmacokinetic features and in vivo antitumor activity." J Control Release **144**(2): 144-150.

Pappas, P., D. Mavroudis, et al. (2006). "Coadministration of oxaliplatin does not influence the pharmacokinetics of gemcitabine." Anticancer Drugs **17**(10): 1185-1191.

Parveen, S. and S. K. Sahoo (2011). "Long circulating chitosan/PEG blended PLGA nanoparticle for tumor drug delivery." Eur J Pharmacol **670**(2-3): 372-383.

Philip, P. A. (2010). "Novel targets for pancreatic cancer therapy." Surg Oncol Clin N Am **19**(2): 419-429.

Pratesi, G., G. Petrangolini, et al. (2005). "Therapeutic synergism of gemcitabine and CpG-oligodeoxynucleotides in an orthotopic human pancreatic carcinoma xenograft." Cancer Res **65**(14): 6388-6393.

Priestman, T. (2008). Cancer therapy in clinical practice. London, Springer-Verlag.

Ramesh, H. (2010). "Management of pancreatic cancer: current status and future directions." Indian J Surg **72**(4): 285-289.

Ranson, M., L. A. Hammond, et al. (2002). "ZD1839, a selective oral epidermal growth factor receptor-tyrosine kinase inhibitor, is well tolerated and active in patients with solid, malignant tumors: results of a phase I trial." J Clin Oncol **20**(9): 2240-2250.

Reddy, L. H., C. Dubernet, et al. (2007). "A new nanomedicine of gemcitabine displays enhanced anticancer activity in sensitive and resistant leukemia types." J Control Release **124**(1-2): 20-27.

Reid, J. M., W. Qu, et al. (2004). "Phase I trial and pharmacokinetics of gemcitabine in children with advanced solid tumors." J Clin Oncol **22**(12): 2445-2451.

Reilly, R. M., R. Kiarash, et al. (2000). "111In-labeled EGF is selectively radiotoxic to human breast cancer cells overexpressing EGFR." J Nucl Med **41**(3): 429-438.

Romberg, B., W. E. Hennink, et al. (2008). "Sheddable coatings for long-circulating nanoparticles." Pharm Res **25**(1): 55-71.

Rubin, R. and D. Strayer (2008). Rubin's Patholoty: Clinicopathologic Foundations of Medicine. Philadelphia, Lippincott Williams & Wilkins.

Sandoval, M. A., B. R. Sloat, et al. (2011). "EGFR-targeted stearoyl gemcitabine nanoparticles show enhanced anti-tumor activity." J Control Release.

Schellens, J. H., M. M. Malingre, et al. (2000). "Modulation of oral bioavailability of anticancer drugs: from mouse to man." Eur J Pharm Sci **12**(2): 103-110.

Semete, B., L. Booysen, et al. (2010). "In vivo evaluation of the biodistribution and safety of PLGA nanoparticles as drug delivery systems." Nanomedicine **6**(5): 662-671.

Shive, M. S. and J. M. Anderson (1997). "Biodegradation and biocompatibility of PLA and PLGA microspheres." Adv Drug Deliv Rev **28**(1): 5-24.

Singh, M. (1999). "Transferrin As A targeting ligand for liposomes and anticancer drugs." Curr Pharm Des **5**(6): 443-451.

Sinko, P. J. and A. N. Martin (2006). Martin's physical pharmacy and pharmaceutical sciences: physical chemical and biopharmaceutical principles in the pharmaceutical sciences. . Philadelphia, Lippincott Williams & Wilkins.

Sloat, B. R., M. A. Sandoval, et al. (2010). "Strong antibody responses induced by protein antigens conjugated onto the surface of lecithin-based nanoparticles." J Control Release **141**(1): 93-100.

Sloat, B. R., M. A. Sandoval, et al. (2011). "In vitro and in vivo anti-tumor activities of a gemcitabine derivative carried by nanoparticles." Int J Pharm.

Society, A. C. (2012). Cancer Facts & Figures, American Cancer Society.

Sparreboom, A., M. J. de Jonge, et al. (2002). "The use of oral cytotoxic and cytostatic drugs in cancer treatment." Eur J Cancer **38**(1): 18-22.

Spitzer, E., M. de Los Angeles, et al. (1989). "Binding properties of biotinylated epidermal growth factor to its receptor on cultured cells and tissue sections." J Cell Biochem **41**(2): 47-56.

Stella, B., S. Arpicco, et al. (2007). "Encapsulation of gemcitabine lipophilic derivatives into polycyanoacrylate nanospheres and nanocapsules." Int J Pharm **344**(1-2): 71-77.

Sugrue, S. (1992). "Predicting and Controlling Colloid Suspension Stability Using Electrophoretic Mobility and Particle-Size Measurements." American Laboratory **24**(6): 64-&.

Tsai, Y. H., Y. H. Hsieh, et al. (2010). "Microemulsions for intravesical delivery of gemcitabine." Chem Pharm Bull (Tokyo) **58**(11): 1461-1465.

Veltkamp, S. A., R. S. Jansen, et al. (2008). "Oral administration of gemcitabine in patients with refractory tumors: a clinical and pharmacologic study." Clin Cancer Res **14**(11): 3477-3486.

Veltkamp, S. A., D. Pluim, et al. (2008). "New insights into the pharmacology and cytotoxicity of gemcitabine and 2',2'-difluorodeoxyuridine." Mol Cancer Ther **7**(8): 2415-2425.

Veltkamp, S. A., D. Pluim, et al. (2008). "Extensive metabolism and hepatic accumulation of gemcitabine after multiple oral and intravenous administration in mice." Drug Metab Dispos **36**(8): 1606-1615.

Vertzoni, M., N. Fotaki, et al. (2004). "Dissolution media simulating the intralumenal composition of the small intestine: physiological issues and practical aspects." J Pharm Pharmacol **56**(4): 453-462.

Vicari, L., T. Musumeci, et al. (2008). "Paclitaxel loading in PLGA nanospheres affected the in vitro drug cell accumulation and antiproliferative activity." BMC Cancer **8**: 212.

Vij, N., T. Min, et al. (2010). "Development of PEGylated PLGA nanoparticle for controlled and sustained drug delivery in cystic fibrosis." J Nanobiotechnology **8**: 22.
von Pawel, J., U. Gatzemeier, et al. (2001). "Phase ii comparator study of oral versus intravenous topotecan in patients with chemosensitive small-cell lung cancer." J Clin Oncol **19**(6): 1743-1749.

Wade A, W. P. J. (1994). <u>Handbook of Pharmaceutical Excipients (2nd Ed)</u>: 392-399.

Walker, R. A. and S. J. Dearing (1999). "Expression of epidermal growth factor receptor mRNA and protein in primary breast carcinomas." <u>Breast Cancer Res Treat</u> **53**(2): 167-176.

Wang, A. Z., R. Langer, et al. (2012). "Nanoparticle delivery of cancer drugs." <u>Annu Rev Med</u> **63**: 185-198.

Wang, C. X., L. S. Huang, et al. (2009). "Antitumor effects of polysorbate-80 coated gemcitabine polybutylcyanoacrylate nanoparticles in vitro and its pharmacodynamics in vivo on C6 glioma cells of a brain tumor model." <u>Brain Res</u> **1261**: 91-99.

Wang, H., Y. Zhao, et al. (2011). "Enhanced anti-tumor efficacy by co-delivery of doxorubicin and paclitaxel with amphiphilic methoxy PEG-PLGA copolymer nanoparticles." <u>Biomaterials</u> **32**(32): 8281-8290.

Wang, N., X. S. Wu, et al. (2000). "Synthesis, characterization, biodegradation, and drug delivery application of biodegradable lactic/glycolic acid polymers: I. Synthesis and characterization." <u>J Biomater Sci Polym Ed</u> **11**(3): 301-318.

Yanasarn, N., B. R. Sloat, et al. (2009). "Nanoparticles engineered from lecithin-in-water emulsions as a potential delivery system for docetaxel." <u>Int J Pharm</u> **379**(1): 174-180.

Zhang, L., F. X. Gu, et al. (2008). "Nanoparticles in medicine: therapeutic applications and developments." <u>Clin Pharmacol Ther</u> **83**(5): 761-769.

Zhang, Y., M. Huo, et al. (2010). "PKSolver: An add-in program for pharmacokinetic and pharmacodynamic data analysis in Microsoft Excel." <u>Comput Methods Programs Biomed</u> **99**(3): 306-314.

Zhang, Y. and J. Zhang (2005). "Surface modification of monodisperse magnetite nanoparticles for improved intracellular uptake to breast cancer cells." <u>J Colloid Interface Sci</u> **283**(2): 352-357.

Zhu, S., P. D. Lansakara, et al. (2012). "Lysosomal Delivery of a Lipophilic Gemcitabine Prodrug Using Novel Acid-Sensitive Micelles Improved Its Antitumor Activity." <u>Bioconjug Che.</u>